



AFRL-RI-RS-TR-2011-050

**COGNITIVE AIRBORNE NETWORKING:  
SELF-AWARE COMMUNICATIONS VIA SENSING, ADAPTATION, AND  
CROSS-LAYER OPTIMIZATION**

---

STATE UNIVERSITY OF NEW YORK AT BUFFALO

*MARCH 2011*

FINAL TECHNICAL REPORT

*APPROVED FOR PUBLIC RELEASE; DISTRIBUTION UNLIMITED.*

STINFO COPY

**AIR FORCE RESEARCH LABORATORY  
INFORMATION DIRECTORATE**

## NOTICE AND SIGNATURE PAGE

Using Government drawings, specifications, or other data included in this document for any purpose other than Government procurement does not in any way obligate the U.S. Government. The fact that the Government formulated or supplied the drawings, specifications, or other data does not license the holder or any other person or corporation; or convey any rights or permission to manufacture, use, or sell any patented invention that may relate to them.

This report is the result of contracted fundamental research deemed exempt from public affairs security and policy review in accordance with SAF/AQR memorandum dated 10 Dec 08 and AFRL/CA policy clarification memorandum dated 16 Jan 09. This report is available to the general public, including foreign nationals. Copies may be obtained from the Defense Technical Information Center (DTIC) (<http://www.dtic.mil>).

AFRL-RI-RS-TR-2011-050 HAS BEEN REVIEWED AND IS APPROVED FOR PUBLICATION IN ACCORDANCE WITH ASSIGNED DISTRIBUTION STATEMENT.

FOR THE DIRECTOR:

/s/

MICHAEL MEDLEY  
Work Unit Manager

/s/

WARREN H. DEBANY JR., Technical Advisor  
Information Grid Division  
Information Directorate

This report is published in the interest of scientific and technical information exchange, and its publication does not constitute the Government's approval or disapproval of its ideas or findings.

**REPORT DOCUMENTATION PAGE***Form Approved*  
**OMB No. 0704-0188**

Public reporting burden for this collection of information is estimated to average 1 hour per response, including the time for reviewing instructions, searching data sources, gathering and maintaining the data needed, and completing and reviewing the collection of information. Send comments regarding this burden estimate or any other aspect of this collection of information, including suggestions for reducing this burden to Washington Headquarters Service, Directorate for Information Operations and Reports, 1215 Jefferson Davis Highway, Suite 1204, Arlington, VA 22202-4302, and to the Office of Management and Budget, Paperwork Reduction Project (0704-0188) Washington, DC 20503.

**PLEASE DO NOT RETURN YOUR FORM TO THE ABOVE ADDRESS.**

<b>1. REPORT DATE (DD-MM-YYYY)</b> March 2011		<b>2. REPORT TYPE</b> Final Technical Report		<b>3. DATES COVERED (From - To)</b> January 2008 – October 2010	
<b>4. TITLE AND SUBTITLE</b>  COGNITIVE AIRBORNE NETWORKING: SELF-AWARE COMMUNICATIONS VIA SENSING, ADAPTION, AND CROSS-LAYER OPTIMIZATION				<b>5a. CONTRACT NUMBER</b> N/A	
				<b>5b. GRANT NUMBER</b> FA8750-08-1-0063	
				<b>5c. PROGRAM ELEMENT NUMBER</b> 62702F	
<b>6. AUTHOR(S)</b>  Dimitris Pados Stella Batalama Weifeng Su Tornmaso Melodia				<b>5d. PROJECT NUMBER</b> AN08	
				<b>5e. TASK NUMBER</b> UB	
				<b>5f. WORK UNIT NUMBER</b> DP	
<b>7. PERFORMING ORGANIZATION NAME(S) AND ADDRESS(ES)</b> University at Buffalo State Univeristy of New York (SUNY) 501 Capen Hall Buffalo NY 14260				<b>8. PERFORMING ORGANIZATION REPORT NUMBER</b>	
<b>9. SPONSORING/MONITORING AGENCY NAME(S) AND ADDRESS(ES)</b> Air Force Research Laboratory/Information Directorate Rome Research Site/RIGF 525 Brooks Road Rome NY 13441				<b>10. SPONSOR/MONITOR'S ACRONYM(S)</b> AFRL/RI	
				<b>11. SPONSORING/MONITORING AGENCY REPORT NUMBER</b> AFRL-RI-RS-TR-2011-050	
<b>12. DISTRIBUTION AVAILABILITY STATEMENT</b> Approved for Public Release; Distribution Unlimited. This report is the result of contracted fundamental research deemed exempt from public affairs security and policy review in accordance with SAF/AQR memorandum dated 10 Dec 08 and AFRL/CA policy clarification memorandum dated 16 Jan 09.					
<b>13. SUPPLEMENTARY NOTES</b>					
<b>14. ABSTRACT</b> We cover five general areas in this report: (1) design and optimize cooperative automatic-repeat-request (ARQ) relaying protocol for airborne networks; (2) optimize power assignment for hybrid ARQ protocols in airborne networks; (3) design and optimize differential cooperative relaying protocols for airborne networks; (4) design and optimize multi-source multi destination relaying schemes for airborne networks; and (5) design and optimize cognitive code-division channelization for airborne networks.					
<b>15. SUBJECT TERMS</b> Airborne networks, cooperative communications, cognitive radios, hybrid automatic-repeat-request protocols, code-division channelization, cross-layer optimization.					
<b>16. SECURITY CLASSIFICATION OF:</b>			<b>17. LIMITATION OF ABSTRACT</b>  UU	<b>18. NUMBER OF PAGES</b>  91	<b>19a. NAME OF RESPONSIBLE PERSON</b> MICHAEL MEDLEY
<b>a. REPORT</b> U	<b>b. ABSTRACT</b> U	<b>c. THIS PAGE</b> U			<b>19b. TELEPHONE NUMBER (Include area code)</b> N/A

# Contents

<b>1</b>	<b>Executive Summary</b>	<b>1</b>
1.1	Overview and Main Results . . . . .	1
1.2	List of People Involved . . . . .	2
1.3	List of Publications . . . . .	2
<b>2</b>	<b>Introduction to the Project</b>	<b>4</b>
2.1	Overview of Cooperative ARQ Relaying . . . . .	4
2.2	Overview of Optimal Power Assignment for Hybrid-ARQ Protocols . . . . .	5
2.3	Overview of Differential Amplify-and-Forward Relaying . . . . .	6
2.4	Overview of Joint Power Optimization for Multi-Source Multi-Destination Relay Networks . . . . .	6
2.5	Overview of Cognitive Code-Division Channelization . . . . .	8
<b>3</b>	<b>Models, Assumptions, Methods and Procedures</b>	<b>8</b>
3.1	Cooperative Decode-and-Forward ARQ Relaying . . . . .	8
3.1.1	System Model . . . . .	9
3.1.2	Outage Probability Analysis . . . . .	10
3.1.3	Optimum Power Allocation for the DF Cooperative ARQ Relay Scheme . . . . .	17
3.1.4	Simulation Results and Discussion . . . . .	18
3.2	Optimal Power Assignment for Hybrid-ARQ Rayleigh Fading Links . . . . .	22
3.2.1	System Model and Problem Formulation . . . . .	23
3.2.2	Optimal Transmission Power Assignment . . . . .	24
3.2.3	Approximation of the Optimal Power Sequence . . . . .	29
3.2.4	Performance Comparisons between the Equal and Optimal Power Assignments . . . . .	34
3.3	Differential Amplify-and-Forward Relaying: Performance Analysis and Power Optimization . . . . .	38
3.3.1	System Model . . . . .	38
3.3.2	Outage Analysis for The DAF Relaying . . . . .	40
3.3.3	Optimum Power Assignment . . . . .	43
3.3.4	Simulation Results and Discussions . . . . .	44
3.4	Joint Power Optimization for Multi-Source and Multi-Destination Relay Network . . . . .	48
3.4.1	System Model . . . . .	49
3.4.2	System Performance Analysis . . . . .	51
3.4.3	Optimum Power Assignment Under SINR Constraints for All Source-Destination Pairs . . . . .	53
3.4.4	Optimum Power Assignment Under a Total Power Budget Constraint . . . . .	58
3.4.5	Numerical Results and Discussions . . . . .	60
3.5	Cognitive Code-Division Channelization . . . . .	65
3.5.1	System Model and Problem Formulation . . . . .	65
3.5.2	Proposed Cognitive Secondary Channel Design . . . . .	67
3.5.3	Simulation Studies and Discussions . . . . .	73
<b>4</b>	<b>Conclusions</b>	<b>75</b>
	<b>Bibliography</b>	<b>78</b>
	<b>Acronyms</b>	<b>84</b>

## List of Figures

1	Illustration of the cooperative ARQ relay scheme with one source, one relay and one destination.	9
2	Outage probability of the direct and DF cooperative ARQ schemes (L=2).	19
3	Outage probability of the direct and DF cooperative ARQ schemes (L=3).	19
4	Outage probability of the direct and DF cooperative ARQ schemes (L=4).	20
5	Optimum power ratio $\lambda$ for the DF cooperative ARQ scheme. When L=2, 3 and 4, the asymptotic power allocation is $\lambda = 0.8203$ , $\lambda = 0.7969$ and $\lambda = 0.7838$ , respectively.	20
6	Outage probability of the DF cooperative ARQ scheme with equal and optimum power allocations (L=2).	21
7	Outage probability of the DF cooperative ARQ scheme with equal and optimum power allocations (L=3).	21
8	Outage probability of the DF cooperative ARQ scheme with equal and optimum power allocations (L=4).	22
9	Illustration of a hybrid-ARQ protocol with transmission power $P_l$ in the $l$ th (re-)transmission round, $1 \leq l \leq L$ .	23
10	Transmission power sequence of the optimal power assignment strategy with $L = 3$ , $\gamma_0 = 10$ dB, $p_0 = 10^{-3}$ .	32
11	Transmission power sequence of the optimal power assignment strategy with $L = 5$ , $\gamma_0 = 10$ dB, $p_0 = 10^{-3}$ .	32
12	Transmission power sequence of the optimal assignment strategy with $L = 10$ , $\gamma_0 = 10$ dB, $p_0 = 10^{-1}$ .	33
13	Comparisons of the average total transmission power between the equal and optimal power assignment strategies with different targeted SNRs. $L = 2$ , $p_0 = 10^{-3}$ .	35
14	Comparisons of the average total transmission power of the equal and optimal power assignment strategies with different targeted SNRs. $L = 3$ , $p_0 = 10^{-3}$ .	35
15	Comparisons of the average total transmission power of the equal and optimal power assignment strategies with different targeted SNRs. $L = 5$ , $p_0 = 10^{-3}$ .	36
16	Comparisons of the average total transmission power of the equal and optimal power assignment strategies with different targeted outage probabilities. $L = 2$ , $\gamma_0 = 10$ dB.	36
17	Comparisons of the average total transmission power of the equal and optimal power assignment strategies with different targeted outage probabilities. $L = 3$ , $\gamma_0 = 10$ dB.	37
18	Comparisons of the average total transmission power of the equal and optimal power assignment strategies with different targeted outage probabilities. $L = 5$ , $\gamma_0 = 10$ dB.	37
19	An illustrative cooperative system model.	39
20	Outage probability of the DAF relaying with variances $\{\delta_{s,d}^2, \delta_{s,r}^2, \delta_{r,d}^2\} = \{1, 1, 1\}$ .	45
21	Outage probability of the DAF relaying with variances $\{\delta_{s,d}^2, \delta_{s,r}^2, \delta_{r,d}^2\} = \{1, 1, 100\}$ .	45
22	Outage probability of the DAF relaying with variances $\{\delta_{s,d}^2, \delta_{s,r}^2, \delta_{r,d}^2\} = \{1, 100, 1\}$ .	46
23	Numerical search of the optimum power ratio $r$ for the DAF relaying with variances $\{\delta_{s,d}^2, \delta_{s,r}^2, \delta_{r,d}^2\} = \{1, 1, 1\}$ , and different transmit power $P=20$ dB, 30dB and 40dB.	46
24	Performance comparison of the DAF relaying with the equal and the optimum power allocation, with variances $\{\delta_{s,d}^2, \delta_{s,r}^2, \delta_{r,d}^2\} = \{1, 1, 1\}$ .	47
25	Numerical search of the optimum power ratio $r$ for the DAF relaying with variances $\{\delta_{s,d}^2, \delta_{s,r}^2, \delta_{r,d}^2\} = \{1, 1, 100\}$ , and different transmit power $P=20$ dB, 30dB and 40dB.	47
26	Performance comparison of the DAF relaying with the equal and the optimum power allocation, with variances $\{\delta_{s,d}^2, \delta_{s,r}^2, \delta_{r,d}^2\} = \{1, 1, 100\}$ .	48
27	Multi-source multi-destination relay network.	49
28	Minimization of the total power consumption under varying parameter $x$ for an <i>asymmetric</i> multi-source multi-destination relay network with given SINR constraints ( $K = 2$ ).	62

29	Minimization of the total power consumption with varying parameter $x$ for a <i>symmetric</i> multi-source multi-destination relay network under given SINR constraints ( $K = 2$ ). . . . .	62
30	Minimization of the total power consumption with varying parameter $x$ for an <i>asymmetric</i> multi-source multi-destination relay network under given SINR constraints ( $K = 3$ ). . . . .	63
31	Minimization of the total power consumption with varying parameter $x$ for a <i>symmetric</i> multi-source multi-destination relay network under given SINR constraints ( $K = 3$ ). . . . .	63
32	Maximization of the minimum SINR among all source-destination pairs under given total power budget $P_{total} = 30\text{dB}$ ( $K = 2$ ). . . . .	64
33	Comparison of the minimum SINR resulting from the proposed optimum power assignment scheme and the equal power assignment scheme with any given total power budget ( $K = 2$ ). . . . .	64
34	Primary/secondary CDMA system model of $K$ primary transmitters $PT_i, i = 1, 2, \dots, K$ , a primary receiver $PR$ , and a secondary transmitter-receiver pair $ST, SR$ . All paths $h_1, \dots, h_K, q_1, \dots, q_K, h_s, q_s$ exhibit independent (quasi-static) Rayleigh fading. . . . .	66
35	Proposed interior-point algorithm for solving (225). . . . .	70
36	Flow-chart of proposed power and code allocation algorithm for secondary link. . . . .	71
37	Secondary transmission percentage as a function of the number of primary users under Cases $rank(\mathbf{X}'') = 1$ and $> 1$ (the study includes also the code assignment scheme in [86]). . . . .	74
38	Secondary receiver SINR as a function of the iteration step of the linearized optimizer in (237) initialized at the best feasible sample out of $P = 50$ drawings from the $\mathcal{N}(\mathbf{0}, \mathbf{X}'')$ pdf. . . . .	74
39	Instantaneous output SINR of a primary signal against SINR-QoS threshold $\alpha$ (thick line) and instantaneous output SINR of secondary signal. . . . .	75

## List of Tables

1	Algorithm to determine the optimal power assignment sequence $P_k (1 \leq k \leq L)$ . . . . .	27
2	Algorithm to determine the approximation of the optimal power sequence $P_k (1 \leq k \leq L)$ . .	30
3	Comparing the optimum power ratio by exhaustive search and approximation, assuming $\{\delta_{s,d}^2, \delta_{s,r}^2, \delta_{r,d}^2\} = \{1, 1, 1\}$ . . . . .	44
4	Comparing the optimum power ratio by exhaustive search and approximation, assuming $\{\delta_{s,d}^2, \delta_{s,r}^2, \delta_{r,d}^2\} = \{1, 1, 100\}$ . . . . .	44
5	Optimum power assignment that minimizes the total power under given SINR constraints using the proposed method and the exhaustive search method for an <i>asymmetric</i> setting ( $K = 2$ ) . .	60
6	Optimum power assignment that minimizes the total power under given SINR constraints using the proposed method and the exhaustive search method for a <i>symmetric</i> setting ( $K = 2$ ) . . .	60
7	Comparison of the total power consumption resulting from the optimum power assignment scheme and the equal power assignment scheme ( $K = 3$ ) . . . . .	65
8	Optimum power assignment that maximizes the minimum SINR among two source-destination pairs under given total power budget $P_{total} = 30\text{dB}$ , by using the proposed method and the exhaustive search method ( $K = 2$ ) . . . . .	65

# 1 Executive Summary

## 1.1 Overview and Main Results

This report describes work performed from 1 December 2007 to 15 January 2011 under AFRL grant number FA8750-08-1-0063 entitled “Cognitive Airborne Networking: Self-Aware Communications via Sensing, Adaptation, and Cross-Layer Optimization”. We cover five general areas: (1) cooperative automatic-repeat-request (ARQ) relaying in airborne networks; (2) power assignment for hybrid ARQ protocols in airborne networks; (3) differential cooperative relaying in airborne networks; (4) joint power optimization for multi-source multi-destination relay networks; and (5) cognitive code-division channelization in airborne networks. Some main results are summarized in the following:

- A new analytical methodology was developed to evaluate the outage probability of cooperative decode-and-forward (DF) automatic-repeat-request (ARQ) relaying under packet-rate fading (fast fading or block fading) channels. Specifically, (i) we derived a closed-form asymptotically tight (as  $\text{SNR} \rightarrow \infty$ ) approximation of the outage probability; (ii) we showed that the diversity order of the DF cooperative ARQ relay scheme is equal to  $2L - 1$ , where  $L$  is the maximum number of ARQ (re)transmissions; and (iii) we developed an optimum power allocation for the DF cooperative ARQ relay scheme.
- We addressed the fundamental problem of identifying the optimal power assignment sequence for hybrid automatic-repeat-request (H-ARQ) communications over quasi-static Rayleigh fading channels. For any targeted H-ARQ link outage probability, we determined the sequence of power values that minimizes the average total expended transmission power. We first derived a set of equations that describe the optimal transmission power assignment and enable its exact recursive calculation. To reduce calculation complexity, we also developed an approximation to the optimal power sequence that is close to the numerically calculated exact result. The newly founded power allocation solution reveals that conventional equal-power H-ARQ assignment is far from optimal. Interestingly, we found that the optimal transmission power assignment sequence is neither increasing nor decreasing; its form depends on given total power budget and targeted outage performance levels.
- Differential Amplify-and-Forward (DAF) relaying is an attractive cooperative communication strategy for airborne networks where channel estimation is not feasible or it is rather avoided. We found a new exact outage probability expression for DAF relaying that involves only a single integral, which is much simpler than an existing result available in literature that involves a triple integral. To get further insight understanding of the DAF relaying scheme, we obtained an asymptotically tight closed-form approximation at high signal-to-noise ratio (SNR) scenario. Based on the tight approximation of the outage probability, we were able to determine an asymptotically optimum power assignment for the DAF relaying scheme.
- We developed a low-complexity joint power assignment algorithm for multi-source and multi-destination relay networks where multiple sources share a common relay that forwards all received signals simultaneously to destinations. We considered two power optimization strategies: (i) Minimization of the total transmission power of the sources and the relay under the constraint that the signal to interference plus noise ratio (SINR) requirement of each source-destination pair is satisfied, and (ii) Maximization of the minimum SINR among all source-destination pairs subject to any given total power budget. Both optimization problems involve  $K$  power variables, where  $K$  is the number of source-destination pairs in the network, and an exhaustive search is prohibitive for large  $K$ . In this project, we developed a methodology that allows us to obtain an asymptotically tight approximation of the SINR and reformulate the original optimization problems to single-variable optimization problems, which can be easily solved by numerical search of the single variable. Then, the corresponding optimal transmission power at each source and relay can be calculated directly. The proposed optimization schemes are scalable and lead to power assignment algorithms that exhibit the same optimization complexity for any number ( $K$ ) of source-destination pairs in the network. Moreover, we also applied the methodology that we developed

to solve a related max-min SINR based optimization problem in which we determined power assignment for the sources and the relay to maximize the minimum SINR among all source-destination pairs subject to any given total power budget.

- We solved the problem of cognitive code-division channelization for cognitive airborne networks. The goal is to improve the efficiency of spectrum utilization and coexisting of primary and secondary users in heterogeneous cognitive airborne networks, by jointly assigning power and code-channel allocation for a secondary transmitter/receiver pair coexisting with a primary code-division multiple-access (CDMA) system. In pursuit of a computationally manageable and performance-wise appealing suboptimal solution, we first converted the amplitude/code-vector optimization problem to an equivalent matrix optimization problem under a rank-1 constraint. Disregarding (relaxing in formal language) the rank-1 constraint makes the problem amenable to an easy polynomial-cost semidefinite programming solution. When luckily, a rank-1 matrix happens to be returned, optimal secondary-line design is achieved. For the common case of a higher rank, we developed an iterative linearized polynomial-cost convex optimizer with much appealing (yet suboptimal) amplitude/code-vector design solutions after a few iterations. Extensive numerical studies have validated our theoretical developments and the proposed iterative algorithm. The proposed scheme almost doubled the occurrences of secondary transmission compared to some early work. The joint power and sequence optimization executed by the proposed scheme results in superior SINR performance for the secondary receiver compared to prior work. The proposed scheme has great potential to improve the efficiency of coexisting of primary and secondary users in heterogeneous cognitive airborne networks.

The introduction to the project and an overview of each area is given in Section 2. Then in Section 3 we present specifically models, assumptions, methods, and main results for each area. Section 4 contains the conclusions and bibliography is included at the end.

## 1.2 List of People Involved

There are four faculty members involved in the project, which are listed in the following:

- Prof. Dimitris Pados; University at Buffalo, State University of New York (SUNY); PI
- Prof. Stella Batalama; University at Buffalo, State University of New York (SUNY); Co-PI
- Prof. Weifeng Su; University at Buffalo, State University of New York (SUNY); Co-PI
- Prof. Tommaso Melodia; University at Buffalo, State University of New York (SUNY); Co-PI

Additionally, the project supported four Ph.D students, working in the project toward their Ph.D degrees.

## 1.3 List of Publications

The project has resulted in the following peer-reviewed journal articles and conference proceeding papers. One work received the 2010 IEEE International Conference on Communications (ICC) Best Paper Award.

### Peer-Reviewed Journal Articles:

- S. Lee, W. Su, S. N. Batalama, and J. D. Matyjas, "Cooperative decode-and-forward ARQ relaying: performance analysis and power optimization," IEEE Transactions on Wireless Communications, vol. 9, no. 8, pp.2632-2642, August 2010.
- L. Ding, T. Melodia, S. Batalama, J. Matyjas and M. Medley, "Cross-layer Routing and Dynamic Spectrum Allocation in Cognitive Radio Ad Hoc Networks," IEEE Transactions on Vehicular Technology - Special Issue on "Ten Years of Cognitive Radio: Achievements and the Road Ahead," Eds. J. Mitola and al., Vol. 59 No. 4, pp. 1969 - 1979, May 2010.

- M. Li, S. N. Batalama, D. A. Pados, and J. D. Matyjas, "Minimum total-squared-correlation quaternary signature sets: New bounds and optimal designs," *IEEE Transactions on Communications*, vol. 57, pp. 3662-3671, Dec. 2009.
- K. Gao, S. N. Batalama, D. A. Pados, and J. D. Matyjas, "Cognitive code-division channelization," *IEEE Transactions on Wireless Communications*, to appear.
- F. Chen, W. Su, S. N. Batalama, and J. D. Matyjas, "Joint power optimization for multi-source and multi-destination relay networks," *IEEE Transactions on Signal Processing*, to appear.
- K. Gao, S. N. Batalama, D. A. Pados, "Bounds on the maximum SINR of binary and quaternary code division," submitted to *IEEE Transactions on Communications*, 2010.
- W. Su, S. Lee, D. A. Pados, and J. D. Matyjas, "Optimal power assignment for minimizing the average total transmission power in hybrid-ARQ Rayleigh fading links," submitted to *IEEE Transactions on Communications*, review feedback with minor revision, 2010.
- S. Kundu, W. Su, D. A. Pados, and M. Medley, "Fast maximum-likelihood decoding of quasi-orthogonal STBCs with QAM signals," submitted to *IEEE Transactions on Wireless Communications*, 2010.

#### **Peer-Reviewed Conference Proceeding Papers:**

- F. Chen, W. Su, S. N. Batalama, and J. D. Matyjas, "Jointly optimal power assignment for multi-source multi-destination relay networks," in *Proceedings of IEEE Global Telecommunications Conference (GLOBECOM)*, Miami, FL, Dec. 6-10, 2010.
- S. Lee, W. Su, D. A. Pados, and J. D. Matyjas, "The average total power consumption of cooperative hybrid-ARQ on quasi-static Rayleigh fading links," in *Proceedings of IEEE Global Telecommunications Conference (GLOBECOM)*, Miami, FL, Dec. 6-10, 2010.
- S. Kundu, W. Su, D. A. Pados, and M. Medley, "Fast maximum-likelihood decoding of 4x4 full-diversity quasi-orthogonal STBCs with QAM signals," in *Proceedings of IEEE Global Telecommunications Conference (GLOBECOM)*, Miami, FL, Dec. 6-10, 2010.
- W. Su, F. Chen, D. A. Pados, and J. D. Matyjas, "The outage probability and optimum power assignment for differential amplify-and-forward relaying," in *Proceedings of IEEE International Conference on Communications (ICC)*, pp.1-5, Cape Town, South Africa, May 23-27, 2010. (This paper received the 2010 IEEE ICC Best Paper Award)
- W. Su, S. Lee, D. A. Pados, and J. D. Matyjas, "The optimal transmission power per round for hybrid-ARQ Rayleigh fading links," in *Proceedings of IEEE International Conference on Communications (ICC)*, pp.1-5, Cape Town, South Africa, May 23-27, 2010.
- S. Lee, W. Su, S. N. Batalama, and J. D. Matyjas, "Performance analysis and optimization for ARQ decode-and-forward relaying protocol in fast fading channels," in *Proceedings of IEEE International Conference on Acoustics, Speech, and Signal Processing (ICASSP)*, pp.3442-3445, Dallas, Texas, March 14-19, 2010.
- W. Su, J. D. Matyjas, and S. N. Batalama, "Active cooperation between primary users and cognitive users in cognitive ad hoc networks," in *Proceedings of IEEE International Conference on Acoustics, Speech, and Signal Processing (ICASSP)*, Dallas, Texas, March 14-19, 2010.
- S. Lee, W. Su, S. N. Batalama, and J. D. Matyjas, "Outage probability for ARQ decode-and-forward relaying under packet-rate fading," in *Proceedings of International Workshop on Cross-Layer Design in Wireless Mobile Ad-Hoc Networks*, Niagara Fall, Ontario, Canada, September 22-24, 2009.

- L. Ding, T. Melodia, S. Batalama, J. Matyjas, “Joint Routing, Relay Selection, and Spectrum Allocation in Cognitive and Cooperative Ad Hoc Networks,” in Proc. of IEEE Intl. Conf. on Sensor, Mesh and Ad Hoc Communications and Networks (SECON), Boston, MA, June 2010.
- M. Li, S. N. Batalama, D. A. Pados, T. Melodia, M. J. Medley, and J. D. Matyjas, Cognitive code-division channelization with blind primary-system identification, in Proceedings IEEE MILCOM 2010 (Conf. on Military Communication), San Jose, CA, Oct. 31 - Nov. 3, 2010.
- L. Ding, P. B. Nagaraju, T. Melodia, S. N. Batalama, D. A. Pados, and J. D. Matyjas, Software-defined joint routing and waveform selection for cognitive ad hoc networks, in Proceedings IEEE MILCOM 2010 (Conf. on Military Communication), San Jose, CA, Oct. 31 - Nov. 3, 2010.
- P. B. Nagaraju, L. Ding, T. Melodia, S. N. Batalama, D. A. Pados, and J. D. Matyjas, Implementation of a distributed joint routing and dynamic spectrum allocation algorithm on USRP2 radios, in Proceedings 2010 IEEE Comm. Society Conf. on Sensor, Mesh and Ad Hoc Comm. and Networks (SECON), Boston, MA, June 21 - 25, 2010, pp. 1-2.
- K. Gao; Batalama, S.N.; Pados, D.A.; Matyjas, J.D.; “Cognitive CDMA channelization,” in Proceedings 43rd Asilomar Conf. on Signals, Syst. and Comp., Pacific Grove, CA, Nov. 2009, pp. 672 - 676.

## 2 Introduction to the Project

### 2.1 Overview of Cooperative ARQ Relaying

Conventional wireless networks involve point-to-point communication links and for that reason do not guarantee reliable transmissions over severe fading channels. On the other hand, cooperative wireless networks exhibit increased network reliability due to the fact that information can be delivered with the cooperation of other users in networks [1]–[13]. In particular, in cooperative systems each user utilizes other cooperative users to create a virtual antenna array and exploit spatial diversity that minimizes the effects of fading and improves overall system performance. Cooperative communications, also known as relay channels, was first introduced in [9] in which a three-way channel was analyzed based on the capacity region. More information-theoretic analysis of the relay channels was developed in [10] and recently in [11, 12]. Various practical cooperative communication protocols were proposed for wireless networks [1]–[6] and performance analysis has been extensively developed (see [7, 13] and the references therein).

Automatic-repeat-request (ARQ) protocols for wireless communications have been studied extensively in the past and proved themselves as efficient control mechanisms for reliable data packet transmissions at the data link layer [15]–[21]. The basic idea of ARQ protocols is that a receiver requests retransmission when a packet is not correctly received. Recently, in an effort to increase network reliability over poor quality channels, ARQ protocols were studied in the context of cooperative relay networks [22]–[25]. In particular, [22] was among the first such studies to present a general framework of cooperative ARQ relay networks. It was shown that cooperative ARQ relay networks have great advantages in terms of throughput, delay, and energy consumption compared with the conventional multihop ARQ approach in which point-to-point ARQ links are concatenated in network routes. In [23], information-theoretic analysis was developed and upper bounds for the diversity order of a decode-and-forward (DF) cooperative ARQ relay scheme were characterized for both slow and fast fading channels as a means to study the diversity-multiplexing-delay tradeoff for the cooperative ARQ relay scheme. In [25], a closed-form expression of the outage probability of the DF cooperative ARQ relay scheme was obtained for slow fading channels, but unfortunately the introduced approach cannot be extended to fast fading channels.

Outage probability is arguably a fundamental performance metric for wireless ARQ relay schemes and so is the diversity order. In this project, we developed a new analytical methodology for the treatment of DF cooperative ARQ relay networks in fast fading (packet-rate fading) channels, which leads, for the first time, to a closed-form asymptotically tight (as  $\text{SNR} \rightarrow \infty$ ) approximation of the outage probability. The closed-form

expression shows that the overall diversity order of the DF cooperative ARQ relay scheme is equal to  $2L - 1$ , where  $L$  is the maximum number of ARQ retransmissions. The achieved diversity is partially due to the DF cooperative relaying and partially due to the fast fading nature of the channels (temporal diversity due to retransmissions over independent fading channels). We note that the diversity of the direct ARQ scheme (without relaying) is only  $L$  and it is due to the fast fading channels. Based on the asymptotically tight approximation of the outage probability, we are able to determine an optimum resource allocation for the DF cooperative ARQ relay scheme. For any given total transmission power budget, optimum power allocated at the source and at the relay can be determined which depends on the variances of the channels and the maximum number of retransmissions allowed in the protocol. It turns out that the conventional equal-power allocation strategy is not optimum in general and the optimum power allocation relies heavily on the link quality of the channels related to the relay. We have conducted extensive numerical and simulation results to illustrate and validate the theoretical developments.

## 2.2 Overview of Optimal Power Assignment for Hybrid-ARQ Protocols

ARQ communication protocols, in which a receiver requests retransmission when a packet is not correctly received, are commonly used in data link control to enable reliable data packet transmissions as shown in [15]–[21]. In a basic/simplest ARQ protocol, a receiver decodes an information packet based only on the received signal in each transmission round [15, 16]. Advanced ARQ schemes, in which a receiver may decode an information packet by combining received signals from all previous transmission rounds, have been known as hybrid ARQ (H-ARQ) protocols [17]–[21]. Since the receiver needs to save previously received signals, H-ARQ communication protocols require more memory at the receiver side compared to the basic ARQ protocols. However, the performance of the H-ARQ protocols is substantially better than that of the basic ARQ protocols and the performance improvement is worth of the memory increase at the receiver side [16, 20, 21], especially in nowadays memory chips are cheaper and their sizes become smaller.

In wireless links formed by wireless devices with limited power resources, power efficiency is a key research matter in the optimization of ARQ retransmission protocols [31]–[35]. In [31], a power control scheme was proposed for ARQ retransmissions in down-link cellular systems in order to minimize the total transmission power of multiple users where each user uses constant transmission power. In [32], the power efficiency of various ARQ protocols was discussed by taking into account the energy consumed by the transmitting and receiving electronic circuitry in ARQ retransmissions. Note that in both [31] and [32], the power efficiency of ARQ protocols was examined under the assumption of the same transmission power level in each retransmission round. In [33], the transmission power in each retransmission round was optimized for a variety of ARQ protocols by assuming that channel state information (CSI) is available at the transmitter side and CSI takes values from a prescribed finite set of values. In [34], by assuming that partial CSI is available, optimal transmission power in each retransmission round was determined for an H-ARQ protocol by a linear programming method that selects a power value from a set of discrete power levels. Recently in [35], without assuming CSI available at the transmitter side, an optimal power transmission strategy was identified for a basic ARQ protocol where the receiver decodes based only on the received signal in each transmission round. It was assumed that the channel changes independently in each retransmission round. A necessary and sufficient condition for the optimal transmission power sequence was found which indicates that power must be increasing in every retransmission. We note that this result is not valid to slowly fading channels. More recently in [36], without a priori CSI at the transmitter, the authors maximized the average transmission rate for an incremental redundancy H-ARQ protocol where the transmitter sends out different encoded redundant parity symbols in each retransmission round. The average transmission rate maximization under optimal power assignment was also formulated and numerical results were presented for an incremental redundancy H-ARQ protocol with one maximum retransmission.

In this project, we considered advanced H-ARQ transmission protocols for airborne networks in which a destination node may decode an information packet by combining all received signals from previous transmission rounds to increase detection reliability. We assume that the source-destination channel experiences *quasi-static* Rayleigh fading, i.e. the channel does not change during retransmissions of the same information packet and it may change independently when transmitting a new information packet. Our goal is to find the

optimal power assignment strategy that minimizes the average total transmission power for any given targeted outage probability. First, we derived a set of equations that describe the optimal transmission power values in H-ARQ retransmission rounds. Then, a simple recursive algorithm was developed to exactly calculate the optimal transmission power level for each retransmission round. Interestingly, it turns out that the optimal transmission power assignment sequence is neither increasing nor decreasing; its form depends on given total power budget and targeted outage performance levels. This is fundamentally different from the case in [35] that the optimal transmission power must be increasing in retransmissions in the fast fading scenario (i.e. the channel changes independently in each retransmission round). To reduce calculation complexity and obtain more insight understanding of the optimal power assignment strategy, we also developed an approximation to the optimal power sequence that is close to the numerically calculated exact result. The tight approximation shows that the optimal transmission power in each retransmission round is a function of  $P_1$  (the transmission power in the first round) in a polynomial form. The optimal power assignment values also reveal that the conventional equal-power assignment (using the same transmission power in all retransmission rounds) is far from optimal. As an example, for a targeted outage probability of  $10^{-3}$  and maximum number of transmissions  $L = 2$ , the average total transmission power based on the optimal power assignment is 9 dB less than that of using the common equal-power scheme. We also observed that the larger the maximum number of retransmissions allowed in the H-ARQ protocol or the lower the required outage probabilities, the more power savings the optimal power assignment strategy offers.

### 2.3 Overview of Differential Amplify-and-Forward Relaying

The concept of cooperative relaying has been attracting much attention recently with the promise of increased wireless network capacity and throughput/delay performance ([39, 53] and references therein). In cooperative relaying, a source node involves nearby nodes to jointly/cooperatively send information to a destination. To reduce implementation complexity and system requirements, differential cooperative relaying is particularly attractive in wireless networks due to its advantage that information can be differentially modulated/demodulated and channel estimation can be avoided (at the cost of an arguably tolerable error rate loss). In [41], Differential Decode-and-Forward (DDF) relaying was proposed and optimized in which each relay differentially decodes the information from a source node and forwards it to a destination. Since relays may decode information incorrectly, some reliability control mechanism has to be deployed at relays in the DDF relaying scheme to avoid error propagation from relays to destination. In [42], Differential Amplify-and-Forward (DAF) relaying was proposed in which a signal from a source is simply amplified by the relays and forwarded to the destination. In the DAF relaying scheme, implementation at each relay is quite simplified since no decoding and detection is needed in this case. The outage performance of the DAF relay has been studied [43], however, the presented outage probability result involves a triple integral, which therefore offers little insight in the problem of DAF protocol optimization.

In this project, we applied and optimized the DAF relaying scheme for airborne networks. Specifically, we devised a new exact outage probability expression for DAF relaying which involves only a single integral. Furthermore, to provide further insight in the process of DAF relaying, we developed a simple closed-form approximation of the outage probability which is tight at high signal-to-noise ratio (SNR) and reveals the asymptotic performance of the DAF relaying scheme. Then, based on the tight outage probability approximation, we were able to determine an asymptotically optimum power allocation scheme for DAF relaying. Numerical calculations and simulation results have been carried out to validate and illustrate our theoretical findings.

### 2.4 Overview of Joint Power Optimization for Multi-Source Multi-Destination Relay Networks

Recent work on information-theoretic aspects of cooperative relaying as well as recent proposals of practical cooperative relaying protocols ([50]–[57] and references therein) suggest that cooperative relaying may lead to significant improvements in detection reliability at destinations and overall system performance. In cooperative relaying, a user/node may serve as a relay and assist others by forwarding their signals to destinations, thus

enhancing detection reliability at the destination. Various relaying strategies have been studied in the literature for relay to forward signals. For example, relay may decode the received signal and forward the decoded information to a destination, or it may simply amplify the received signal and forward it to the destination.

More recently, there is increasing interest in investigating the advantages of relaying in multi-source multi-destination networks [58]–[65], [71]–[73]. The simplest multi-source multi-destination relay network is modeled as an interference relay channel (IRC) [58] where a relay helps two independent source-destination pairs by using different relaying strategies such as decode-and-forward, amplify-and-forward, or compress-and-forward. Past literature on multi-source multi-destination relay networks focused primarily on information-theoretic studies including achievable rate regions or bounds of capacity region [58]–[65]. For example, in [58] a rate splitting technique is used to study the problem of achievable rate region for a Gaussian IRC channel, where each message is split into a common message which is decodable at all destinations and a private message which is decodable only at the intended destination [61]. Since the receivers are able to decode part of the interference messages, the effect of interference is reduced and the overall communication rate is therefore increased. The achievable rate region of [58] was further improved in [59] by considering both intended message and interference forwarding at the relay (optimal relay strategies were studied under the assumption that the relay is connected to each source and each destination via orthogonal and finite capacity links). The capacity region of the interference channel with a single-relay was investigated in [62, 63], where it was shown that forwarding the intended message of just one source, the achievable rates for both source-destination pairs can be improved. By assuming that the relay knows the source message a priori, a relaying strategy was proposed in [64, 65] where generalized beamforming with dirty paper coding was considered for a two-source two-destination relay network to further improve the capacity region of the network.

Power control is an important technique to improve the performance of multi-source multi-destination relay networks. While past literature offers a significant amount of work on power allocation for single-source single-destination relay networks (see, for example [67]–[70] and references therein), there are rather limited studies on power optimization for multi-source multi-destination relay networks. In [71], power allocation was optimized by exhaustive search for a two-source two-destination relay network where a half-duplex decode-and-forward relay was considered. Unfortunately the exhaustive search is not scalable and leads to prohibitive optimization complexity for networks with larger number of source-destination pairs. In [72, 73], a power allocation scheme was proposed for a multi-source multi-destination relay network based on geometric programming (the scheme assumes that signals from different sources are sent through orthogonal channels and the direct transmission link is not involved in detection at destinations).

In this project, we designed and optimized a general multi-source multi-destination relay scheme with  $K$  sources ( $K$  can be large) for cognitive airborne networks. The network allows simultaneous multi-source transmissions through non-orthogonal, in general, channels. We considered two power optimization strategies: (i) Minimization of the total power consumption of all sources and relay under the constraint that the signal to interference plus noise ratio (SINR) requirement of each source-destination pair is satisfied, and (ii) Maximization of the minimum SINR among all source-destination pairs subject to any given total power budget. Thanks to an asymptotically tight approximation of the SINR that we developed, we were able to reformulate the original optimization problems, which involve  $K$  power variables, to single-variable optimization problems. Then, the resulting optimization problems can be easily solved by a simple numerical search of the single variable. The proposed optimization schemes are scalable and lead to power assignment algorithms that exhibit the same optimization complexity for any number ( $K$ ) of source-destination pairs in the network. Moreover, for the special case of transmission over orthogonal channels, we were able to further simplify the single-variable optimizations and obtain analytical solutions for a symmetric system. Extensive numerical studies show that the proposed power assignment is almost identical to the exhaustive search method, and the optimum power assignment schemes can significantly improve the performance of multi-source multi-destination relay networks with equal power assignment.

## 2.5 Overview of Cognitive Code-Division Channelization

Recent experimental studies [77] demonstrated that much of the licensed radio spectrum experiences low utilization. Cognitive radio (CR) [78] emerges as a promising technology to improve spectrum utilization by allowing secondary users/networks to share spectrum licensed by primary users. As licensees, the primary users are to have guaranteed access to the spectrum [79]. Therefore, the underlying challenge of CR technology is to ensure the Quality-of-Service (QoS) requirements of the primary users and, simultaneously, maximize in a best-effort context the QoS of the secondary users [80]-[83].

Herein, we are particularly interested in cognitive radio built around a code-division multiple-access (CDMA) primary system. In contrast to frequency or time division operation where cognitive secondary users may transmit opportunistically in sensed spectrum holes/void only, cognitive code-division users may in principle operate in parallel in frequency and time to a primary system as long as the induced spread-spectrum interference remains below a pre-defined acceptable threshold<sup>1</sup>. Power control for cognitive code-division systems was considered in [85] under an “interference temperature” constraint (total secondary user disturbance power over primary band). No optimization was carried out with respect to the code channels (signatures) of the secondary users in [85]. In contrast, in [86] a secondary code assignment scheme was presented to minimize the mean-square crosscorrelation of the secondary code with the primary received signal. Extension to multiple secondary users was also considered in the form of iterative secondary code set construction. Under interference minimizing code assignments, bit rate and spreading factor adjustments for a secondary CDMA system were considered in [87]. Interesting work outside the framework of CDMA CR in the form of joint beamforming and power allocation algorithms was reported in [88], [89], while auction mechanisms for power control were presented in [90].

In this project, we considered the problem of cognitive code-division channelization for cognitive airborne networks. The goal is to improve the efficiency of spectrum utilization and coexisting of primary and secondary users in heterogeneous cognitive airborne networks, by jointly assigning power and code-channel allocation for a secondary transmitter/receiver pair coexisting with a primary code-division multiple-access (CDMA) system. In pursuit of a computationally manageable and performance-wise appealing suboptimal solution, we first converted the amplitude/code-vector optimization problem to an equivalent matrix optimization problem under a rank-1 constraint. Disregarding (relaxing in formal language) the rank-1 constraint makes the problem amenable to an easy polynomial-cost semidefinite programming solution. When luckily, a rank-1 matrix happens to be returned, optimal secondary-line design is achieved. For the common case of a higher rank, we developed an iterative linearized polynomial-cost convex optimizer with much appealing (yet suboptimal) amplitude/code-vector design solutions after a few iterations. Extensive numerical studies have validated our theoretical developments and the proposed iterative algorithm. The proposed scheme almost doubled the occurrences of secondary transmission compared to some early work. The joint power and sequence optimization executed by the proposed scheme results in superior SINR performance for the secondary receiver compared to prior work. The proposed scheme has great potential to improve the efficiency of coexisting of primary and secondary users in heterogeneous cognitive airborne networks.

## 3 Models, Assumptions, Methods and Procedures

### 3.1 Cooperative Decode-and-Forward ARQ Relaying

In this subsection, first we describe briefly the DF cooperative ARQ relay scheme and model the fast (packet-rate) fading channels. Second, we develop two useful lemmas which are the bases of our analytical approach, and calculate the outage probability and derive the asymptotically tight outage probability for the DF cooperative ARQ relay scheme. Third, based on the tight approximation of the outage probability, we determine the asymptotically optimum power allocation for the DF cooperative ARQ relay scheme. Numerical and simulation studies are presented and some conclusions are drawn at the end of this subsection.

---

<sup>1</sup>While early standardization and regulation discussions have begun [84], no conclusive “interference temperature” rules and agreements have been reached yet.

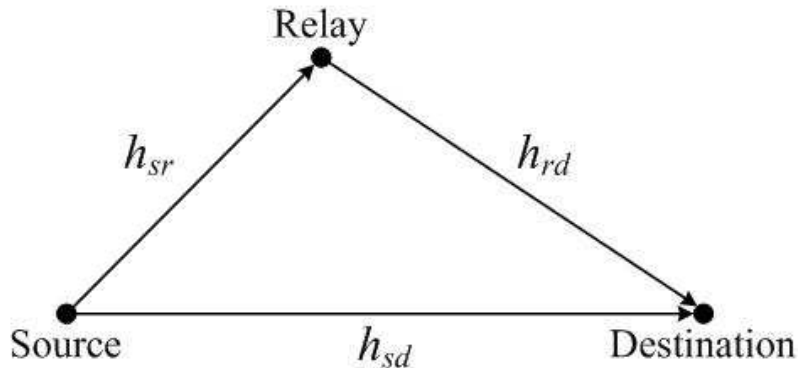


Figure 1: Illustration of the cooperative ARQ relay scheme with one source, one relay and one destination.

### 3.1.1 System Model

We consider a cooperative ARQ relay scheme with one source, one relay and one destination as illustrated in Fig. 1. The DF cooperative ARQ relay scheme works as follows. First, a data packet of  $b$  bits are encoded into a codeword of length  $LT$ , where  $L$  is the maximum number of ARQ retransmission rounds allowed in the protocol and  $T$  is the number of channel uses in a single ARQ retransmission round. Then, the codeword is divided into  $L$  different blocks each of length  $T$ . In each ARQ retransmission round a block of the message is sent, so the transmission rate is  $R = b/T$ . When the source transmits a block of the message to the destination, it is also received by the relay. The destination indicates success or failure of receiving the message by feeding back a single bit of acknowledgement (ACK) or negative-acknowledgement (NACK). The feedback is assumed to be detected reliably at the source and at the relay. If an ACK is received or the retransmission reaches the maximum number of rounds, the source stops transmitting the current message and starts transmitting a new message. If a NACK is received and the retransmission has not reached the maximum number of rounds, the source sends another block of the same message. If the relay decodes successfully before the destination is able to, the relay starts cooperating with the source by transmitting corresponding blocks of the message to the destination by using a space-time transmission [23], for example, using the Alamouti scheme [28]. The destination combines the received signal in current round and those in previous rounds to jointly decode the data packet. After  $L$  ARQ retransmission rounds, if the destination still cannot decode the data packet, an outage is declared which means that the mutual information of the DF cooperative ARQ relay channel is below the transmission rate.

The DF cooperative ARQ relay scheme can be modeled as follows. The received signal  $y_{r,m}$  at the relay at the  $m$ -th ( $1 \leq m \leq L$ ) ARQ retransmission round can be modeled as

$$y_{r,m} = \sqrt{P_s} h_{sr,m} x_s + \eta_{r,m}, \quad (1)$$

where  $P_s$  is the transmitted power of the source signal  $x_s$ ,  $h_{sr,m}$  is the coefficient of the source-relay channel at the  $m$ -th ARQ retransmission round, and  $\eta_{r,m}$  is the additive noise. If the relay is not involved in forwarding, the received signal  $y_{d,m}$  at the destination at the  $m$ -th ARQ retransmission round is

$$y_{d,m} = \sqrt{P_s} h_{sd,m} x_s + \eta_{d,m}, \quad (2)$$

where  $h_{sd,m}$  is the source-destination channel coefficient at the  $m$ -th ARQ retransmission round. If the relay receives the data packet from the source successfully, it helps in forwarding the packet to the destination using the Alamouti scheme. Specifically, each block of the data packet can be partitioned into two parts as  $x_s = [x_{s,1} \ x_{s,2}]$ , then the relay forwards a corresponding block  $x_r = [-x_{s,2}^* \ x_{s,1}^*]$ . The received signal  $y_{d,m}$  at the destination at the  $m$ -th ARQ retransmission round can be written as

$$y_{d,m} = \sqrt{P_s} h_{sd,m} x_s + \sqrt{P_r} h_{rd,m} x_r + \eta_{d,m}, \quad (3)$$

where  $P_r$  is the transmitted power at the relay and  $h_{rd,m}$  is the channel coefficient from the relay to the destination at the  $m$ -th ARQ retransmission round. At the destination, the message block  $x_s$  can be recovered based on the orthogonal structure of the Alamouti code [23, 28]. The channel coefficients  $h_{sd,m}$ ,  $h_{sr,m}$  and  $h_{rd,m}$  are modeled as independent, zero-mean complex Gaussian random variables with variances  $\sigma_{sd}^2$ ,  $\sigma_{sr}^2$  and  $\sigma_{rd}^2$ , respectively. We consider a fast fading scenario, i.e. the channels remain fixed within one ARQ retransmission round, but change independently from one round to another (packet-rate fading). The channel state information is assumed to be known at the receiver and unknown at the transmitter. The noise  $\eta_{r,m}$  and  $\eta_{d,m}$  are modeled as zero-mean complex Gaussian random variables with variance  $\mathcal{N}_0$ .

### 3.1.2 Outage Probability Analysis

In this subsection, first we develop two lemmas which play key roles in our outage probability analysis. Second, we derive the outage probability of the direct ARQ transmission scheme. Finally, we derive the outage probability of the DF cooperative ARQ relay scheme under packet-rate fading conditions.

First we develop two lemmas and some notations. The two lemmas will play key roles in analyzing the outage probability of the DF cooperative ARQ relay scheme.

**Lemma 1** *If  $\mathbf{u}_{s_1, \dots, s_M}$  and  $\mathbf{v}_{s_1, \dots, s_M}$  are two independent random variables satisfying the following properties*

$$\begin{aligned} \lim_{\substack{s_i \rightarrow \infty \\ 1 \leq i \leq M}} \prod_{i=1}^M s_i^{d_1} \cdot \Pr[\mathbf{u}_{s_1, \dots, s_M} < t] &= a \cdot f(t), \\ \lim_{\substack{s_i \rightarrow \infty \\ 1 \leq i \leq M}} \prod_{i=1}^M s_i^{d_2} \cdot \Pr[\mathbf{v}_{s_1, \dots, s_M} < t] &= b \cdot g(t), \end{aligned}$$

where  $d_1, d_2, a$  and  $b$  are constants,  $f(t)$  and  $g(t)$  are monotonically increasing functions, and  $f'(t)$  is integrable, then

$$\lim_{\substack{s_i \rightarrow \infty \\ 1 \leq i \leq M}} \prod_{i=1}^M s_i^{d_1+d_2} \cdot \Pr[\mathbf{u}_{s_1, \dots, s_M} + \mathbf{v}_{s_1, \dots, s_M} < t] = ab \cdot \int_0^t g(x) f'(t-x) dx. \quad (4)$$

*Proof* : For any partition of the interval  $[0, t]$ , denoted as  $\mathbf{U} = \{u_0, u_1, \dots, u_J\}$  with  $u_0 = 0$  and  $u_J = t$ , we can obtain upper and lower bounds of the event  $\{\mathbf{u}_{s_1, \dots, s_M} + \mathbf{v}_{s_1, \dots, s_M} < t\}$  as follows:

$$\begin{aligned} \{\mathbf{u}_{s_1, \dots, s_M} + \mathbf{v}_{s_1, \dots, s_M} < t\} &\subseteq \bigcup_{j=1}^J \{u_{j-1} \leq \mathbf{u}_{s_1, \dots, s_M} < u_j\} \cap \{\mathbf{v}_{s_1, \dots, s_M} < t - u_{j-1}\}, \\ \{\mathbf{u}_{s_1, \dots, s_M} + \mathbf{v}_{s_1, \dots, s_M} < t\} &\supseteq \bigcup_{j=1}^J \{u_{j-1} \leq \mathbf{u}_{s_1, \dots, s_M} < u_j\} \cap \{\mathbf{v}_{s_1, \dots, s_M} < t - u_j\}. \end{aligned}$$

The upper and lower bounds are considered as a union of rectangles between  $u_{j-1}$  and  $u_j$  for  $0 \leq j \leq J$ . First, let us focus on the upper bound. The probability of the subset  $\{u_{j-1} \leq \mathbf{u}_{s_1, \dots, s_M} < u_j\} \cap \{\mathbf{v}_{s_1, \dots, s_M} < t - u_{j-1}\}$  can be calculated as

$$\begin{aligned} \Pr[u_{j-1} \leq \mathbf{u}_{s_1, \dots, s_M} < u_j, \mathbf{v}_{s_1, \dots, s_M} < t - u_{j-1}] \\ = \{\Pr[\mathbf{u}_{s_1, \dots, s_M} < u_j] - \Pr[\mathbf{u}_{s_1, \dots, s_M} < u_{j-1}]\} \Pr[\mathbf{v}_{s_1, \dots, s_M} < t - u_{j-1}]. \end{aligned} \quad (5)$$

Let  $s_i \rightarrow \infty$  for  $1 \leq i \leq M$ , according to the assumption in the lemma, we have

$$\lim_{\substack{s_i \rightarrow \infty \\ 1 \leq i \leq M}} \prod_{i=1}^M s_i^{d_1+d_2} \cdot \Pr[u_{j-1} \leq \mathbf{u}_{s_1, \dots, s_M} < u_j, \mathbf{v}_{s_1, \dots, s_M} < t - u_{j-1}] = ab \cdot \{f(u_j) - f(u_{j-1})\} g(t - u_{j-1}). \quad (6)$$

Since  $f(t)$  and  $g(t)$  are monotonically increasing functions, we obtain an upper bound of (4) as follows

$$\sup_{\mathcal{U}} \lim_{s_i \rightarrow \infty} \prod_{1 \leq i \leq M} s_i^{d_1+d_2} \cdot \Pr[\mathbf{u}_{s_1, \dots, s_M} + \mathbf{v}_{s_1, \dots, s_M} < t] \leq ab \cdot \sum_{j=1}^J g(t - u_{j-1}) \{f(u_j) - f(u_{j-1})\}. \quad (7)$$

Similarly, we can obtain a lower bound as

$$\inf_{\mathcal{U}} \lim_{s_i \rightarrow \infty} \prod_{1 \leq i \leq M} s_i^{d_1+d_2} \cdot \Pr[\mathbf{u}_{s_1, \dots, s_M} + \mathbf{v}_{s_1, \dots, s_M} < t] \geq ab \cdot \sum_{j=1}^L g(t - u_j) \{f(u_j) - f(u_{j-1})\}. \quad (8)$$

The above upper and lower bounds are good for any partition  $\mathcal{U} = \{u_0, u_1, \dots, u_J\}$  over the interval  $[0, t]$ . Since  $f'(t)$  is integrable, so let  $J \rightarrow \infty$ , the summations in (7) and (8) converge to the same integral  $\int_0^t g(x) f'(t-x) dx$ . Therefore we have the result in (4).  $\square$

We note that the special case of Lemma 1 with  $M = 1$  was presented in [29]. Lemma 1 will be used to approximate the outage probability of the ARQ schemes at high SNR scenario. In the following, we would like to define a special function  $F_n(\beta_1, \dots, \beta_n; t)$  which will be used to characterize the outage probability of the DF cooperative ARQ relay scheme. For any integer  $n \geq 2$  and non-zero constants  $\beta_1, \beta_2, \dots, \beta_n$ , define

$$F_n(\beta_1, \dots, \beta_n; t) \triangleq \int_0^t \int_0^{x_1} \dots \int_0^{x_{n-1}} 2^{\beta_1 x_1 + \beta_2 x_2 + \dots + \beta_n x_n} dx_1 dx_2 \dots dx_n.$$

A closed-form expression for calculating the special function  $F_n(\beta_1, \dots, \beta_n; t)$  can be obtained. We have the following result.

**Lemma 2** For any integer  $n \geq 2$  and non-zero constants  $\beta_1, \beta_2, \dots, \beta_n$ , the function  $F_n(\beta_1, \dots, \beta_n; t)$  can be calculated as follows

$$F_n(\beta_1, \dots, \beta_n; t) = \sum_{\substack{\delta_1, \dots, \delta_{n-1} \\ \in \{0,1\}}} \frac{(-1)^{n+\delta_1+\dots+\delta_{n-1}} (\ln 2)^{-n}}{\prod_{m=1}^n [\sum_{l=1}^m i_{m,l}(\boldsymbol{\delta}) \beta_l]} \left( 2^{[\sum_{l=1}^n i_{n,l}(\boldsymbol{\delta}) \beta_l] t} - 1 \right), \quad (9)$$

where the variables  $\delta_1, \delta_2, \dots, \delta_{n-1} \in \{0, 1\}$ ,  $\boldsymbol{\delta} \triangleq \{\delta_1, \delta_2, \dots, \delta_{n-1}\}$ , and the coefficients  $\{i_{m,l}(\boldsymbol{\delta}) : 1 \leq m \leq n, 1 \leq l \leq m\}$  are specified as

$$i_{1,1}(\boldsymbol{\delta}) = i_{2,2}(\boldsymbol{\delta}) = \dots = i_{n,n}(\boldsymbol{\delta}) = 1,$$

and, for any  $m = 2, 3, \dots, n$ ,

$$i_{m,l}(\boldsymbol{\delta}) = \delta_{m-1} \cdot i_{m-1,l}(\boldsymbol{\delta}), \quad l = 1, 2, \dots, m-1.$$

*Proof* : We use induction to prove the result for any integer  $n \geq 2$ . When  $n = 2$ , it is easy to see that

$$\begin{aligned} F_2(\beta_1, \beta_2; t) &= \int_0^t \int_0^{x_2} 2^{\beta_1 x_1 + \beta_2 x_2} dx_1 dx_2 \\ &= \frac{(\ln 2)^{-1}}{\beta_1} \left\{ \frac{(\ln 2)^{-1}}{\beta_1 + \beta_2} \left( 2^{(\beta_1 + \beta_2)t} - 1 \right) - \frac{(\ln 2)^{-1}}{\beta_2} \left( 2^{\beta_2 t} - 1 \right) \right\} \\ &= \sum_{\delta_1 \in \{0,1\}} \frac{(-1)^{2+\delta_1} (\ln 2)^{-2}}{\prod_{m=1}^2 [\sum_{l=1}^m i_{m,l}(\boldsymbol{\delta}) \beta_l]} \left( 2^{[\sum_{l=1}^2 i_{2,l}(\boldsymbol{\delta}) \beta_l] t} - 1 \right), \end{aligned} \quad (10)$$

i.e. the closed-form expression in (9) is valid for  $n = 2$ . Next, we assume that the result in (9) is good for any  $k \geq 2$ . Then, for  $n = k + 1$ ,

$$\begin{aligned}
F_{k+1}(\beta_1, \dots, \beta_{k+1}; t) &= \int_0^t \int_0^{x_{k+1}} \dots \int_0^{x_2} 2^{\beta_1 x_1 + \beta_2 x_2 + \dots + \beta_{k+1} x_{k+1}} \mathbf{d}x_1 \mathbf{d}x_2 \dots \mathbf{d}x_{k+1} \\
&= \int_0^t \underbrace{\int_0^{x_{k+1}} \dots \int_0^{x_2} 2^{\beta_1 x_1 + \beta_2 x_2 + \dots + \beta_k x_k} \mathbf{d}x_1 \mathbf{d}x_2 \dots \mathbf{d}x_k}_{F_k(\beta_1, \dots, \beta_k; x_{k+1})} 2^{\beta_{k+1} x_{k+1}} \mathbf{d}x_{k+1} \\
&= \int_0^t F_k(\beta_1, \dots, \beta_k; x_{k+1}) 2^{\beta_{k+1} x_{k+1}} \mathbf{d}x_{k+1}. \tag{11}
\end{aligned}$$

According to the induction assumption that the result in (9) is good for any  $k \geq 2$ , we have

$$\begin{aligned}
F_k(\beta_1, \dots, \beta_k; x_{k+1}) &= \int_0^{x_{k+1}} \int_0^{x_k} \dots \int_0^{x_2} 2^{\beta_1 x_1 + \beta_2 x_2 + \dots + \beta_k x_k} \mathbf{d}x_1 \mathbf{d}x_2 \dots \mathbf{d}x_k \\
&= \sum_{\substack{\delta_1, \dots, \delta_{k-1} \\ \in \{0,1\}}} \frac{(-1)^{k+\delta_1+\dots+\delta_{k-1}} (\ln 2)^{-k}}{\prod_{m=1}^k [\sum_{l=1}^m i_{m,l}(\boldsymbol{\delta}) \beta_l]} \left( 2^{[\sum_{l=1}^k i_{k,l}(\boldsymbol{\delta}) \beta_l] x_{k+1}} - 1 \right). \tag{12}
\end{aligned}$$

Substituting (12) into (11), we have

$$\begin{aligned}
&F_{k+1}(\beta_1, \dots, \beta_{k+1}; t) \\
&= \sum_{\substack{\delta_1, \dots, \delta_{k-1} \\ \in \{0,1\}}} \frac{(-1)^{k+\delta_1+\dots+\delta_{k-1}} (\ln 2)^{-k}}{\prod_{m=1}^k [\sum_{l=1}^m i_{m,l}(\boldsymbol{\delta}) \beta_l]} \int_0^t \left( 2^{[\sum_{l=1}^k i_{k,l}(\boldsymbol{\delta}) \beta_l + \beta_{k+1}] x_{k+1}} - 2^{\beta_{k+1} x_{k+1}} \right) \mathbf{d}x_{k+1} \\
&= \sum_{\substack{\delta_1, \dots, \delta_{k-1} \\ \in \{0,1\}}} \frac{(-1)^{k+\delta_1+\dots+\delta_{k-1}} (\ln 2)^{-(k+1)}}{\prod_{m=1}^k [\sum_{l=1}^m i_{m,l}(\boldsymbol{\delta}) \beta_l] \cdot [\sum_{l=1}^k i_{k,l}(\boldsymbol{\delta}) \beta_l + \beta_{k+1}]} \left( 2^{[\sum_{l=1}^k i_{k,l}(\boldsymbol{\delta}) \beta_l + \beta_{k+1}] t} - 1 \right) \\
&\quad - \sum_{\substack{\delta_1, \dots, \delta_{k-1} \\ \in \{0,1\}}} \frac{(-1)^{k+\delta_1+\dots+\delta_{k-1}} (\ln 2)^{-(k+1)}}{\prod_{m=1}^k [\sum_{l=1}^m i_{m,l}(\boldsymbol{\delta}) \beta_l] \cdot \beta_{k+1}} \left( 2^{\beta_{k+1} t} - 1 \right) \\
&= \sum_{\substack{\delta_1, \dots, \delta_k \\ \in \{0,1\}}} \frac{(-1)^{k+1+\delta_1+\dots+\delta_k} (\ln 2)^{-(k+1)}}{\prod_{m=1}^{k+1} [\sum_{l=1}^m i_{m,l}(\boldsymbol{\delta}) \beta_l]} \left( 2^{[\sum_{l=1}^{k+1} i_{k+1,l}(\boldsymbol{\delta}) \beta_l] t} - 1 \right), \tag{13}
\end{aligned}$$

where  $\delta_k \in \{0, 1\}$ ,  $i_{k+1,k+1}(\boldsymbol{\delta}) = 1$  and  $i_{k+1,l}(\boldsymbol{\delta}) = \delta_k \cdot i_{k,l}(\boldsymbol{\delta})$ ,  $l = 1, 2, \dots, k$ . Also, we have

$$\sum_{l=1}^{k+1} i_{k+1,l}(\boldsymbol{\delta}) \beta_l = \begin{cases} \sum_{l=1}^k i_{k,l}(\boldsymbol{\delta}) \beta_l + \beta_{k+1}, & \text{if } \delta_k = 1; \\ \beta_{k+1}, & \text{if } \delta_k = 0. \end{cases} \tag{14}$$

Therefore, the closed-form expression in (9) is valid for  $n = k + 1$ . By induction, we conclude that the result in (9) is true for all  $n \geq 2$ .  $\square$

For comparison purpose we specify the outage probability for the direct ARQ transmission scheme. In the direct ARQ transmission scheme, the destination receives information from the source directly, without involving the relay. The mutual information between the source and the destination in the  $m$ -th round of the direct ARQ transmission scheme is

$$I_{sd,m} = \log_2 \left( 1 + \frac{P_s}{\mathcal{N}_0} |h_{sd,m}|^2 \right). \tag{15}$$

The total mutual information after  $L$  ARQ rounds is  $I_{sd}^{tot} = \sum_{m=1}^L I_{sd,m}$ . Thus, the outage probability of the direct ARQ scheme after  $L$  ARQ rounds is

$$P^{out,L} = \Pr [I_{sd}^{tot} < R]. \quad (16)$$

A closed-form expression of (16) is not tractable. An approximation of the outage probability can be obtained for high-SNR scenario as follows [29]

$$P^{out,L} \sim g_L(R) \left( \frac{\mathcal{N}_0}{\sigma_{sd}^2 P_s} \right)^L, \quad (17)$$

where  $g_L(\cdot)$  is defined as

$$g_n(t) = \int_0^t g_{n-1}(x) f'(t-x) dx, \quad n \geq 1, \quad (18)$$

with  $g_0(t) = 1$  and  $f(t) = 2^t - 1$ . Note that (17) is a direct result of Lemma 1 with  $M = 1$ .

The calculation of the coefficient  $g_L(R)$  involves  $L$  recursive integrals. In the following, we develop a closed-form expression for the function  $g_n(t)$  for any  $n \geq 1$ . Since  $g_n(t) = \int_0^t g_{n-1}(x) f'(t-x) dx$  and  $f'(t) = 2^t \ln 2$ , we have

$$\begin{aligned} g_n(t) &= \int_0^t \int_0^{x_{n-1}} \cdots \int_0^{x_2} g_1(x_1) f'(x_2 - x_1) f'(x_3 - x_2) \cdots f'(x_{n-1} - x_{n-2}) \\ &\quad f'(t - x_{n-1}) dx_1 dx_2 \cdots dx_{n-1} \\ &= \int_0^t \int_0^{x_{n-1}} \cdots \int_0^{x_2} (2^{x_1} - 1) (\ln 2)^{n-1} 2^{x_2 - x_1} 2^{x_3 - x_2} \cdots 2^{x_{n-1} - x_{n-2}} 2^{t - x_{n-1}} dx_1 dx_2 \cdots dx_{n-1} \\ &= 2^t (\ln 2)^{n-1} \int_0^t \int_0^{x_{n-1}} \cdots \int_0^{x_2} (1 - 2^{-x_1}) dx_1 dx_2 \cdots dx_{n-1} \\ &= 2^t \frac{(\ln 2)^{n-1}}{(n-2)!} \int_0^t x^{n-2} (1 - 2^{-t+x}) dx. \end{aligned}$$

Since  $\int_0^t x^{n-2} dx = \frac{1}{n-1} t^{n-1}$  and ([30])

$$\int_0^t x^{n-2} 2^x dx = -2^t \sum_{m=1}^{n-1} \frac{(n-2)!}{(-\ln 2)^m (n-m-1)!} t^{n-m-1} + \frac{(n-2)!}{(-\ln 2)^{n-1}},$$

therefore, a closed-form expression of  $g_n(t)$  can be obtained as follows

$$\begin{aligned} g_n(t) &= 2^t \frac{(t \cdot \ln 2)^{n-1}}{(n-1)!} + 2^t \sum_{m=1}^{n-1} \frac{(-1)^m (t \cdot \ln 2)^{n-m-1}}{(n-m-1)!} + (-1)^n \\ &= 2^t \sum_{m=1}^n \frac{(-1)^{n-m}}{(m-1)!} (t \cdot \ln 2)^{m-1} + (-1)^n, \end{aligned} \quad (19)$$

which can be calculated efficiently.

In the following, we derive the outage probability of the DF cooperative ARQ relay scheme under packet-rate fading conditions. In the DF cooperative ARQ relay scheme, if the relay decodes the message from the source correctly, say, at the  $k$ -th round, then at the  $(k+1)$ -th round, the relay starts forwarding appropriate ARQ blocks to the destination. Let  $\{T_r = k\}$  denote the event of successful message decoding by the relay at the  $k$ -th round and subsequent ARQ block forwarding at the  $(k+1)$ -th round. Let  $P_{T_r=k}^{out}$  denote the probability that the destination decodes the message unsuccessfully after  $L$  ARQ retransmission rounds if the event  $\{T_r = k\}$  occurs. Then, the outage probability of the DF cooperative ARQ relay scheme after  $L$  ARQ retransmission rounds can be written as

$$P^{out,L} = \sum_{k=1}^L P_{T_r=k}^{out} \cdot \Pr [T_r = k]. \quad (20)$$

Note that the channels change independently over each ARQ retransmission round in a fast fading scenario, so the mutual information of fading channels can be viewed as a sum of independent random variables.

First, we calculate the probability of the event  $\{T_r = k\}$ , i.e.  $\Pr[T_r = k]$ . We note that the mutual information between the source and the relay in the  $m$ -th ARQ round is

$$I_{sr,m} = \log_2 \left( 1 + \frac{P_s}{\mathcal{N}_0} |h_{sr,m}|^2 \right). \quad (21)$$

The probability that the relay decodes the message successfully at the first round ( $T_r = 1$ ) is

$$\Pr[T_r = 1] = \Pr[I_{sr,1} \geq R] = \exp \left( -\frac{2^R - 1}{\sigma_{sr}^2} \cdot \frac{\mathcal{N}_0}{P_s} \right). \quad (22)$$

For any  $T_r = k$ ,  $k = 2, 3, \dots, L - 1$ , we have

$$\begin{aligned} \Pr[T_r = k] &= \Pr \left[ \sum_{m=1}^{k-1} I_{sr,m} < R, \sum_{m=1}^k I_{sr,m} \geq R \right] \\ &= \Pr \left[ \sum_{m=1}^{k-1} I_{sr,m} < R \right] - \Pr \left[ \sum_{m=1}^k I_{sr,m} < R \right] \\ &\sim g_{k-1}(R) \left( \frac{\mathcal{N}_0}{\sigma_{sr}^2 P_s} \right)^{k-1} - g_k(R) \left( \frac{\mathcal{N}_0}{\sigma_{sr}^2 P_s} \right)^k, \end{aligned} \quad (23)$$

where  $g_{k-1}(\cdot)$  and  $g_k(\cdot)$  are specified in (19) in the previous subsection. The approximation in (23) is obtained by applying Lemma 1 with  $M = 1$ . Finally, if  $T_r = L$ , we have

$$\Pr[T_r = L] = \Pr \left[ \sum_{m=1}^{L-1} I_{sr,m} < R \right] \sim g_{L-1}(R) \left( \frac{\mathcal{N}_0}{\sigma_{sr}^2 P_s} \right)^{L-1}. \quad (24)$$

Next, we calculate the conditional outage probability  $P_{T_r=k}^{out}$  when the relay decodes correctly at the  $k$ -th round and starts forwarding at the  $(k + 1)$ -th round. When the relay cooperates with the source by jointly sending a message block via the Alamouti scheme, the mutual information of the cooperative channels in the  $m$ -th ARQ round is given by [23]

$$I_{srd,m} = \log_2 \left( 1 + \frac{P_s}{\mathcal{N}_0} |h_{sd,m}|^2 + \frac{P_r}{\mathcal{N}_0} |h_{rd,m}|^2 \right). \quad (25)$$

Thus, with  $L$  ARQ rounds, the total mutual information is

$$I_{d,T_r=k}^{tot} = \begin{cases} \sum_{m=1}^k I_{sd,m} + \sum_{m=k+1}^L I_{srd,m}, & 1 \leq k < L; \\ \sum_{m=1}^L I_{sd,m}, & k = L. \end{cases} \quad (26)$$

We note that if  $T_r = L$ , the relay has no chance to cooperate since the source starts sending a new packet. The conditional outage probability can be evaluated as

$$P_{T_r=k}^{out} = \Pr [I_{d,T_r=k}^{tot} < R]. \quad (27)$$

When  $T_r = L$ , the conditional outage probability is reduced to the direct ARQ scenario and it is given by

$$P_{T_r=L}^{out} = \Pr [I_{d,T_r=L}^{tot} < R] \sim g_L(R) \left( \frac{\mathcal{N}_0}{\sigma_{sd}^2 P_s} \right)^L. \quad (28)$$

In the following, we calculate the conditional outage probability (27) for any  $T_r = k$ ,  $k = 1, 2, \dots, L - 1$ . For simplicity in presentation, we introduce the following notation

$$u_m = \begin{cases} \log_2 (1 + s_1 |h_{sd,m}|^2), & 1 \leq m \leq k; \\ \log_2 (1 + s_1 |h_{sd,m}|^2 + s_2 |h_{rd,m}|^2), & k + 1 \leq m \leq L, \end{cases} \quad (29)$$

where  $s_1 = P_s/\mathcal{N}_0$  and  $s_2 = P_r/\mathcal{N}_0$ . Then, the total mutual information can be written as

$$I_{d,T_r=k}^{tot} = \sum_{m=1}^L u_m. \quad (30)$$

Note that for any  $1 \leq m \leq k$ ,  $|h_{sd,m}|^2$  is an exponential random variable with parameter  $\sigma_{sd}^{-2}$ , so

$$\lim_{s_1 \rightarrow \infty} s_1 \cdot \Pr[u_m < t] = \lim_{s_1 \rightarrow \infty} s_1 \cdot \Pr\left[|h_{sd,m}|^2 < \frac{2^t - 1}{s_1}\right] = \frac{1}{\sigma_{sd}^2} (2^t - 1), \quad m = 1, 2, \dots, k. \quad (31)$$

Since  $u_m$ ,  $1 \leq m \leq k$ , are independent random variables, by applying Lemma 1 with  $M = 1$  recursively, we have

$$\lim_{s_1 \rightarrow \infty} s_1^k \cdot \Pr\left[\sum_{m=1}^k u_m < t\right] = \left(\frac{1}{\sigma_{sd}^2}\right)^k g_k(t), \quad (32)$$

where  $g_k(t)$  is given in (19). For any  $m$ ,  $k+1 \leq m \leq L$ ,  $u_m$  involves the sum of two independent exponential random variables  $|h_{sd,m}|^2$  and  $|h_{rd,m}|^2$  with parameters  $\sigma_{sd}^{-2}$  and  $\sigma_{rd}^{-2}$ , respectively, and the distribution of  $u_m$  can be specified as

$$\begin{aligned} \Pr[u_m < t] &= \Pr[s_1|h_{sd,m}|^2 + s_2|h_{rd,m}|^2 < 2^t - 1] \\ &= \begin{cases} 1 - \left(1 + \frac{1}{\sigma_{sd}^2} \frac{2^t - 1}{s_1}\right) \exp\left(-\frac{1}{\sigma_{sd}^2} \frac{2^t - 1}{s_1}\right), & \text{if } \frac{s_1}{\sigma_{rd}^2} = \frac{s_2}{\sigma_{sd}^2}; \\ 1 - \frac{s_1 \sigma_{sd}^2}{s_1 \sigma_{sd}^2 - s_2 \sigma_{rd}^2} \exp\left(-\frac{1}{\sigma_{sd}^2} \frac{2^t - 1}{s_1}\right) - \frac{s_2 \sigma_{rd}^2}{s_2 \sigma_{rd}^2 - s_1 \sigma_{sd}^2} \exp\left(-\frac{1}{\sigma_{rd}^2} \frac{2^t - 1}{s_2}\right), & \text{if } \frac{s_1}{\sigma_{rd}^2} \neq \frac{s_2}{\sigma_{sd}^2}, \end{cases} \end{aligned} \quad (33)$$

for any  $m = k+1, \dots, L$ . Thus, for any  $m = k+1, \dots, L$ , we have

$$\lim_{\substack{s_i \rightarrow \infty \\ 1 \leq i \leq 2}} s_1 s_2 \cdot \Pr[u_m < t] = \frac{1}{2\sigma_{sd}^2 \sigma_{rd}^2} (2^t - 1)^2. \quad (34)$$

Let  $q_0(t) = 1$  and  $p(t) = (2^t - 1)^2$ , then  $p'(t) = 2(2^{2t} - 2^t) \ln 2$ . Since  $u_m$ ,  $k+1 \leq m \leq L$ , are independent to each other, by applying Lemma 1 with  $M = 2$  recursively, we can show that for any  $n = 1, 2, \dots, L - k$ ,

$$\lim_{\substack{s_i \rightarrow \infty \\ 1 \leq i \leq 2}} (s_1 s_2)^n \cdot \Pr\left[\sum_{m=k+1}^{k+n} u_m < t\right] = \left(\frac{1}{2\sigma_{sd}^2 \sigma_{rd}^2}\right)^n q_n(t), \quad (35)$$

in which

$$q_n(t) = \int_0^t q_{n-1}(x) p'(t-x) dx, \quad n = 1, 2, \dots, L - k. \quad (36)$$

Based on Lemma 2, a closed-form expression for  $q_n(t)$  can be obtained as follows:

$$\begin{aligned} q_n(t) &= \int_0^t \int_0^{x_{n-1}} \dots \int_0^{x_2} q_1(x_1) p'(x_2 - x_1) p'(x_3 - x_2) \dots p'(x_{n-1} - x_{n-2}) \\ &\quad \times p'(t - x_{n-1}) dx_1 dx_2 \dots dx_{n-1} \\ &= \int_0^t \int_0^{x_{n-1}} \dots \int_0^{x_2} (2^{x_1} - 1)^2 (2 \ln 2)^{n-1} \prod_{m=1}^{n-2} (2^{x_{m+1} - x_m} - 1) \\ &\quad \times (2^{t-x_{n-1}} - 1) 2^{t-x_1} dx_1 dx_2 \dots dx_{n-1} \\ &= (-2 \ln 2)^{n-1} \sum_{\substack{\alpha_1, \dots, \alpha_{n-1} \\ \in \{0,1\}}} (-1)^{\alpha_1 + \dots + \alpha_{n-1}} 2^{(1+\alpha_{n-1})t} \\ &\quad \times \int_0^t \int_0^{x_{n-1}} \dots \int_0^{x_2} (2^{x_1} - 1)^2 \cdot 2^{-\alpha_1 x_1} \prod_{m=2}^{n-1} 2^{(\alpha_{m-1} - \alpha_m) x_m} dx_1 dx_2 \dots dx_{n-1} \\ &= (-2 \ln 2)^{n-1} \sum_{\substack{\alpha_1, \dots, \alpha_{n-1} \\ \in \{0,1\}}} (-1)^{\alpha_1 + \dots + \alpha_{n-1}} 2^{(1+\alpha_{n-1})t} \{F_{n-1}(1 - \alpha_1, \beta_2, \dots, \beta_{n-1}; t) \\ &\quad - 2F_{n-1}(-\alpha_1, \beta_2, \dots, \beta_{n-1}; t) + F_{n-1}(-1 - \alpha_1, \beta_2, \dots, \beta_{n-1}; t)\}, \end{aligned} \quad (37)$$

where  $\beta_2 = \alpha_1 - \alpha_2$ ,  $\beta_3 = \alpha_2 - \alpha_3$ , ...,  $\beta_{n-1} = \alpha_{n-2} - \alpha_{n-1}$ , and the function  $F_{n-1}(\cdot; t)$  is defined in (9) and it has a closed-form expression specified in Lemma 2. Note that in case for some  $i$ ,  $\beta_i$  is zero which does not satisfied the non-zero condition in Lemma 2, we may calculate  $F_{n-1}(\cdot; t)$  as follows. Since the function  $F_n(\beta_1, \dots, \beta_n; t)$  defined in (9) is continuous in terms of each variable  $\beta_i$  and the closed-form expression in Lemma 2 is also continuous in terms of  $\beta_i$ , so we can apply Lemma 2 with  $\beta_i = \varepsilon_i$  where  $\varepsilon_i$  is sufficiently small (i.e.  $\varepsilon_i \rightarrow 0$ ) to accommodate the calculation of  $F_{n-1}(\cdot; t)$ .

According to the result in (35) with  $n = L - k$ , we have

$$\lim_{\substack{s_i \rightarrow \infty \\ 1 \leq i \leq 2}} (s_1 s_2)^{L-k} \cdot \Pr \left[ \sum_{m=k+1}^L u_m < t \right] = \left( \frac{1}{2\sigma_{sd}^2 \sigma_{rd}^2} \right)^{L-k} q_{L-k}(t), \quad (38)$$

where  $q_{L-k}(t)$  can be calculated specifically based on (37). Combining (32) and (38), and applying Lemma 1, we obtain

$$\lim_{\substack{s_i \rightarrow \infty \\ 1 \leq i \leq 2}} s_1^L s_2^{L-k} \cdot \Pr \left[ \sum_{m=1}^k I_{sd,m} + \sum_{m=k+1}^L I_{srd,m} < R \right] = b_k(R) \left( \frac{1}{\sigma_{sd}^2} \right)^L \left( \frac{1}{2\sigma_{rd}^2} \right)^{L-k}, \quad (39)$$

where

$$b_k(t) = \int_0^t g_k(x) q'_{L-k}(t-x) dx. \quad (40)$$

Since  $s_1 = P_s/\mathcal{N}_0$  and  $s_2 = P_r/\mathcal{N}_0$ , so for any  $T_r = k$ ,  $k = 1, 2, \dots, L-1$ , the conditional probability (27) can be asymptotically approximated as

$$P_{T_r=k}^{out} = \Pr \left[ \sum_{m=1}^k I_{sd,m} + \sum_{m=k+1}^L I_{srd,m} < R \right] \sim \frac{b_k(R)}{2^{L-k}} \left( \frac{\mathcal{N}_0}{\sigma_{sd}^2 P_s} \right)^L \left( \frac{\mathcal{N}_0}{\sigma_{rd}^2 P_r} \right)^{L-k}. \quad (41)$$

Finally, combining (22)–(24) and (41), we can obtain the outage probability for the DF cooperative ARQ relay scheme as follows

$$\begin{aligned} P^{out,L} &\sim \sum_{k=1}^{L-1} \frac{b_k(R)}{2^{L-k}} \left[ g_{k-1}(R) - g_k(R) \frac{\mathcal{N}_0}{\sigma_{sr}^2 P_s} \right] \left( \frac{\mathcal{N}_0}{\sigma_{sd}^2 P_s} \right)^L \left( \frac{\mathcal{N}_0}{\sigma_{rd}^2 P_r} \right)^{L-k} \left( \frac{\mathcal{N}_0}{\sigma_{sr}^2 P_s} \right)^{k-1} \\ &\quad + g_L(R) g_{L-1}(R) \left( \frac{\mathcal{N}_0}{\sigma_{sd}^2 P_s} \right)^L \left( \frac{\mathcal{N}_0}{\sigma_{sr}^2 P_s} \right)^{L-1}, \end{aligned} \quad (42)$$

where  $g_k(R)$  and  $b_k(R)$  are specified in (19) and (40), respectively. Furthermore, we note that the term  $g_k(R) \frac{\mathcal{N}_0}{\sigma_{sr}^2 P_s}$  would be much smaller than  $g_{k-1}(R)$  at high SNR  $\frac{P_s}{\mathcal{N}_0}$ , so the asymptotic outage probability in (42) can be further simplified as

$$P^{out,L} \sim \sum_{k=1}^L \frac{b_k(R) g_{k-1}(R)}{2^{L-k}} \left( \frac{\mathcal{N}_0}{\sigma_{sd}^2 P_s} \right)^L \left( \frac{\mathcal{N}_0}{\sigma_{rd}^2 P_r} \right)^{L-k} \left( \frac{\mathcal{N}_0}{\sigma_{sr}^2 P_s} \right)^{k-1}, \quad (43)$$

where  $b_L(R) = g_L(R)$ . The asymptotic outage probability is tight at high SNR which will be shown in simulation results.

Based on the above asymptotic outage probability, we observe that the term  $\left( \frac{\mathcal{N}_0}{\sigma_{sd}^2 P_s} \right)^L$  in (43) contributes a diversity order  $L$  in the asymptotic outage performance, which is due to the fast fading nature of the channels. The term  $\left( \frac{\mathcal{N}_0}{\sigma_{rd}^2 P_r} \right)^{L-k} \left( \frac{\mathcal{N}_0}{\sigma_{sr}^2 P_s} \right)^{k-1}$  contributes an overall diversity order  $(L-k) + (k-1) = L-1$  which is due to the cooperative relaying. Thus, the asymptotic outage probability of the DF cooperative ARQ relay scheme has an overall diversity order  $2L-1$ . The observation is more obvious in case of an equal power allocation scenario, i.e.,  $P_s = P_r = P$ . As a comparison, we recall that the diversity order of the direct ARQ transmission scheme is only  $L$ , which is much less than that of the DF cooperative ARQ relay scheme. The diversity order of the direct ARQ scheme comes from the fast fading nature of the source-destination channel.

### 3.1.3 Optimum Power Allocation for the DF Cooperative ARQ Relay Scheme

In this subsection, we derive an asymptotic optimum power allocation for the DF cooperative ARQ relay scheme based on the tight approximation of the outage probability we presented in the previous section. Without loss of generality, we denote the total transmission power  $P_s + P_r \triangleq 2P$ . For any given total transmission power  $2P$ , we try to determine optimum power  $P_s$  used at the source and power  $P_r$  at the relay in order to minimize the asymptotic outage probability.

Let us denote  $\lambda$  as the ratio of the transmit power  $P_s$  to the total transmission power, i.e.  $\lambda = \frac{P_s}{2P}$ , then  $0 \leq \lambda \leq 1$  and  $P_r = (1 - \lambda)2P$ . The asymptotic outage probability of the DF cooperative ARQ relay scheme can be written as

$$P^{out,L} \sim \frac{\sigma_{sr}^2}{(2\sigma_{sd}^2\sigma_{rd}^2)^L} \left(\frac{\mathcal{N}_0}{2P}\right)^{2L-1} \sum_{k=1}^L b_k(R)g_{k-1}(R) \left(\frac{2\sigma_{rd}^2}{\sigma_{sr}^2}\right)^k \frac{1}{\lambda^{L+k-1}(1-\lambda)^{L-k}}. \quad (44)$$

We try to find the optimum power ratio  $\lambda$  ( $0 \leq \lambda \leq 1$ ) such that the asymptotic outage probability is minimized. Let  $A_k(R) \triangleq b_k(R)g_{k-1}(R) \left(\frac{2\sigma_{rd}^2}{\sigma_{sr}^2}\right)^k$  and

$$G(\lambda) \triangleq \sum_{k=1}^L \frac{A_k(R)}{\lambda^{L+k-1}(1-\lambda)^{L-k}}, \quad (45)$$

then the optimization problem can be formulated as follows

$$\begin{aligned} & \min_{\lambda} G(\lambda) \\ & s.t. \quad 0 < \lambda < 1. \end{aligned} \quad (46)$$

By taking derivative of  $G(\lambda)$  with respect to  $\lambda$ , we have

$$\frac{\partial G(\lambda)}{\partial \lambda} = \sum_{k=1}^L A_k(R) \left\{ \frac{-(L+k-1)}{\lambda^{L+k}(1-\lambda)^{L-k}} + \frac{L-k}{\lambda^{L+k-1}(1-\lambda)^{L-k+1}} \right\}. \quad (47)$$

Let  $\frac{\partial G(\lambda)}{\partial \lambda} = 0$ , an optimum power ratio can be found by solving the following equation

$$\sum_{k=1}^L A_k(R) \left\{ -(L+k-1) \left(\frac{1-\lambda}{\lambda}\right)^k + (L-k) \left(\frac{1-\lambda}{\lambda}\right)^{k-1} \right\} = 0. \quad (48)$$

The equation can be easily solved by using the Newton method. Based on the equation, we have two observations. First, since  $A_k(R)$  is positive, so  $\frac{1-\lambda}{\lambda}$  in the equation must be less than 1, otherwise the left-hand side of (48) is negative. It implies that  $\lambda > \frac{1}{2}$ , i.e.  $P_s > P$  and  $P_r < P$ , which means we should allocate more power at the source and less power at the relay. It also shows that the equal power allocation scheme assigning power equally between the source and the relay is not optimum in general. Second, we observe that for a given transmission rate  $R$ , the parameters  $A_k(R)$  in the equation (48) depend only on  $\sigma_{sr}^2$  and  $\sigma_{rd}^2$  which are the variances of the source-relay and relay-destination channel links, respectively. Thus, the asymptotic optimum power ratio  $\lambda$  depends only on the the variances of the source-relay and relay-destination channels, not on the source-destination channel link. A similar observation was reported in [7] where the optimum power allocation between the source and the relay was determined based on the analysis of the symbol-error-rate performance.

When  $L = 2$ , a closed-form expression of the optimum power ratio can be obtained as follows. In this case, the equation (48) is reduced as

$$3A_2(R) \left(\frac{1-\lambda}{\lambda}\right)^2 + 2A_1(R) \left(\frac{1-\lambda}{\lambda}\right) - A_1(R) = 0, \quad (49)$$

so the optimum power ratio is

$$\lambda = \frac{1 + \sqrt{1 + 3 \frac{A_2(R)}{A_1(R)}}}{2 + \sqrt{1 + 3 \frac{A_2(R)}{A_1(R)}}}. \quad (50)$$

Thus the corresponding optimum power allocation at the source and at the relay is given by

$$P_s = \frac{1 + \sqrt{1 + 3 \frac{A_2(R)}{A_1(R)}}}{1 + \frac{1}{2} \sqrt{1 + 3 \frac{A_2(R)}{A_1(R)}}} P, \quad (51)$$

$$P_r = \frac{1}{1 + \frac{1}{2} \sqrt{1 + 3 \frac{A_2(R)}{A_1(R)}}} P. \quad (52)$$

In (51) and (52), the parameter  $\frac{A_2(R)}{A_1(R)} = \frac{2b_2(R)g_1(R)}{b_1(R)} \frac{\sigma_{rd}^2}{\sigma_{sr}^2}$ . So the optimum power allocation depends only on the ratio of the variances of the source-relay and relay-destination channels. This result is consistent with the observation based on the general optimization equation in (48). Also, from (51) and (52), we can see that  $P < P_s < 2P$  and  $0 < P_r < P$ , i.e. we should put more power at the source and less power at the relay to optimize the overall performance at the destination. Furthermore, from (51) and (52) we observe that if the relay is located close to the source, i.e.,  $\sigma_{sr}^2 \gg \sigma_{rd}^2$ ,  $P_s$  goes to  $\frac{4}{3}P$  and  $P_r$  goes to  $\frac{2}{3}P$ . On the contrary, if the relay is located close to the destination, i.e.,  $\sigma_{sr}^2 \ll \sigma_{rd}^2$ ,  $P_s$  goes to  $2P$  and  $P_r$  goes to 0, which means we should allocate most power at the source in this case. It is reasonable to allocate most of the total power  $2P$  to the source since the role of the relay helping in forwarding is minor in this case.

### 3.1.4 Simulation Results and Discussion

In this section, we present numerical and simulation studies for the DF cooperative ARQ relay scheme to validate our theoretical analysis in the previous sections. We also compare the performance of the DF cooperative ARQ scheme with that of the direct ARQ scheme. In all studies, the variance of the channel  $h_{ij} \{(i, j) \in (s, d), (s, r), (r, d)\}$  is assumed to be  $\sigma_{ij}^2 = d_{ij}^{-\mu}$ , where  $d_{ij}$  is the distance between two nodes and  $\mu$  is the path loss exponent which is assumed to be  $\mu = 3$  in a typical fading environment. We assume that the source-destination distance is  $d_{sd} = 10$  m and the relay is located in the midpoint between the source and the destination. We consider a target transmission rate of  $R = 2$  bits/s/Hz.

Figs. 2, 3 and 4 present the simulation studies for the DF cooperative ARQ relay scheme when the maximum number of ARQ retransmission rounds is  $L = 2, 3$  and 4, respectively. In these simulations, we allocated power equally at the source and at the relay, i.e.,  $P_s = P_r = P$ . The simulation results show that the theoretical approximation of the outage probability of the DF cooperative ARQ relay scheme is loose at low SNR and tight at high SNR. For example, in case of  $L = 2$  in Fig. 2, the analytical approximation matches with the simulated curve at an outage performance of around  $10^{-3}$ . Moreover, the larger the number of ARQ retransmission rounds, the higher the diversity order of the DF cooperative ARQ relay scheme. This observation is consistent with the theoretical result that the diversity order of the DF cooperative ARQ relay scheme increases in terms of the number of ARQ retransmission rounds.

For comparison, Figs. 2–4 also include the performance of the direct ARQ scheme. We can see that the DF cooperative ARQ relay scheme significantly outperforms the direct ARQ scheme. At an outage performance of  $10^{-4}$ , the performance of the DF cooperative ARQ relay scheme is about 8dB better than that of the direct ARQ scheme. For the same maximum number of retransmission rounds  $L$ , the performance of the DF cooperative ARQ relay scheme shows a higher diversity order than that of the direct ARQ scheme. This observation is consistent with our theoretical developments showing that the DF cooperative ARQ relay scheme has diversity order  $2L - 1$ , while the direct ARQ scheme has diversity order only  $L$ .

In Fig. 5, we show the optimum power ratio  $\lambda$  for the DF cooperative ARQ relay scheme with  $L = 2, 3$  and 4, respectively. We plot the optimization function  $G(\lambda)$  in terms of  $\lambda$  ( $0 \leq \lambda \leq 1$ ). We assume that the quality of the source-relay link is the same as that of the relay-destination link, i.e.,  $\sigma_{sr}^2 = \sigma_{rd}^2$ . We observe

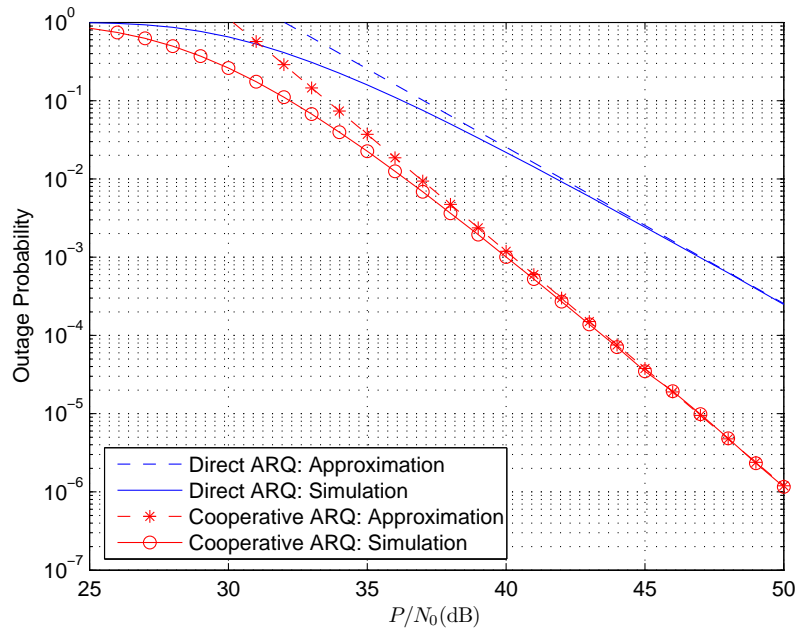


Figure 2: Outage probability of the direct and DF cooperative ARQ schemes ( $L=2$ ).

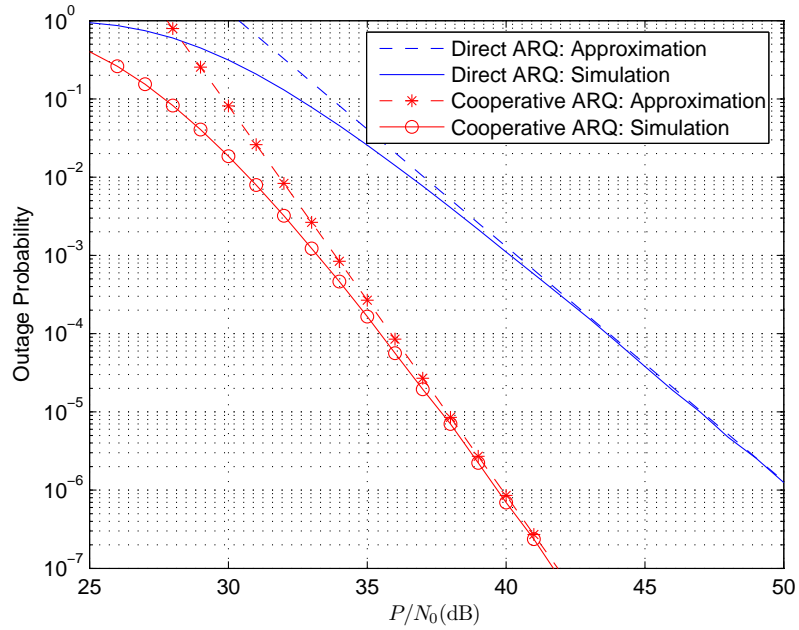


Figure 3: Outage probability of the direct and DF cooperative ARQ schemes ( $L=3$ ).

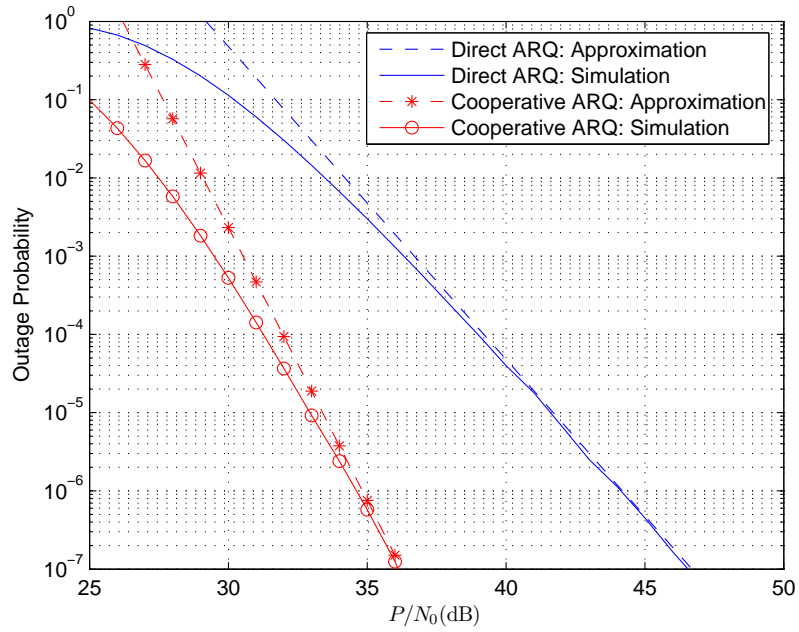


Figure 4: Outage probability of the direct and DF cooperative ARQ schemes (L=4).

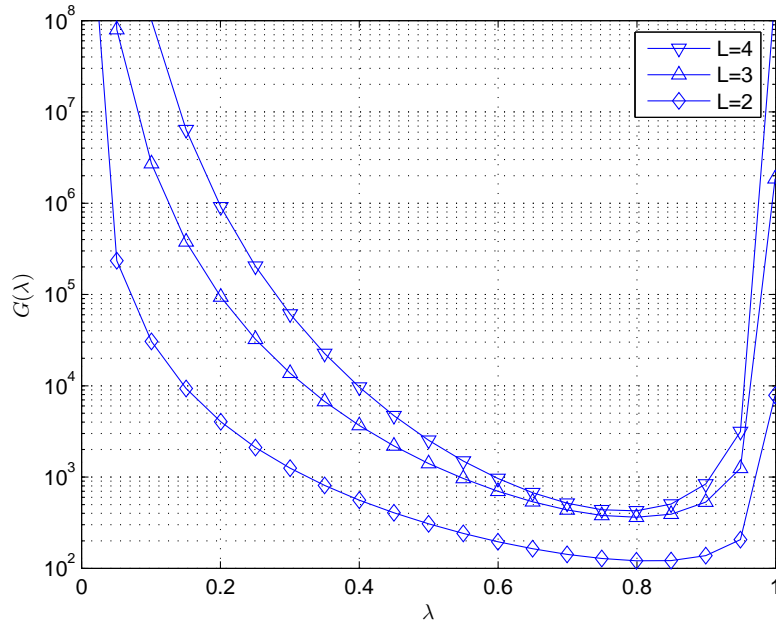


Figure 5: Optimum power ratio  $\lambda$  for the DF cooperative ARQ scheme. When L=2, 3 and 4, the asymptotic power allocation is  $\lambda = 0.8203$ ,  $\lambda = 0.7969$  and  $\lambda = 0.7838$ , respectively.

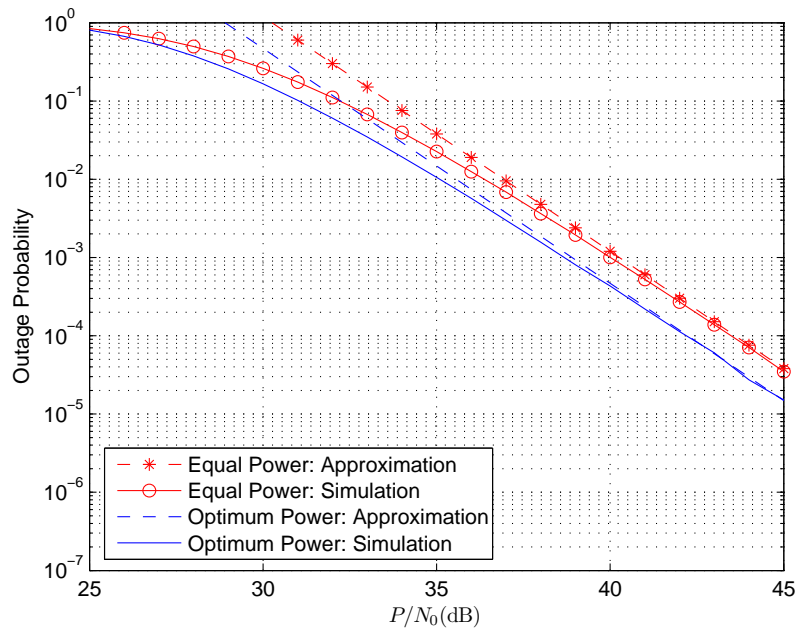


Figure 6: Outage probability of the DF cooperative ARQ scheme with equal and optimum power allocations ( $L=2$ ).

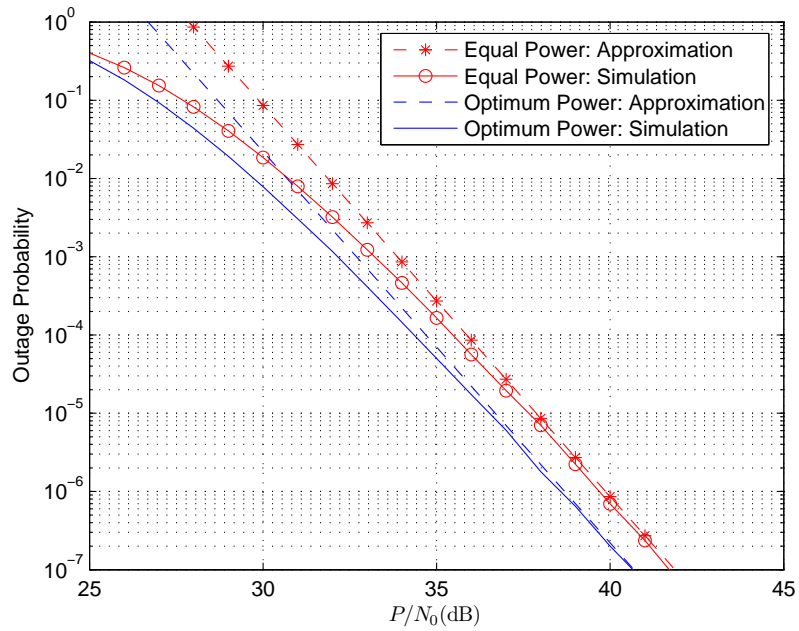


Figure 7: Outage probability of the DF cooperative ARQ scheme with equal and optimum power allocations ( $L=3$ ).

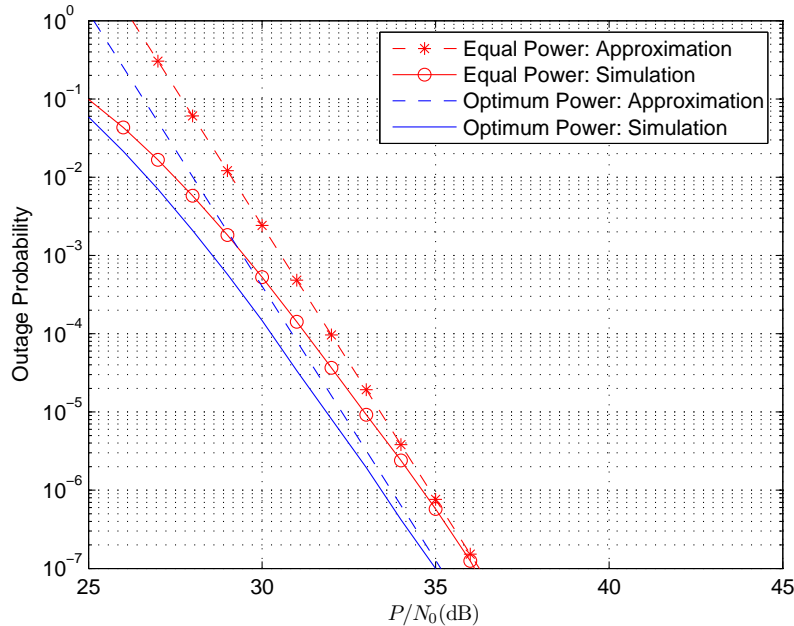


Figure 8: Outage probability of the DF cooperative ARQ scheme with equal and optimum power allocations ( $L=4$ ).

that the optimum power ratio  $\lambda$  is around 0.8 for the three cases. More precisely, from the numerical results, the optimum power ratios are  $\lambda = 0.8203$ ,  $\lambda = 0.7969$  and  $\lambda = 0.7838$  for  $L = 2, 3$  and  $4$ , respectively. It appears that the optimum power ratio decreases gradually when the maximum number of retransmission rounds is increased. Furthermore, the optimum power ratio is much larger than  $1/2$  which is consistent with our analysis that we should allocate more power at the source and less at the relay.

We compare the performances of the the DF cooperative ARQ relay scheme with the optimum power allocation as well as the equal power allocation in Figs. 6–8  $L = 2, 3$  and  $4$ , respectively. In case of  $L = 2$  in Fig. 6, the optimum power allocation is  $P_s/2P = 0.8203$  and  $P_r/2P = 0.1797$  according to the numerical results in Fig. 5. From the figure, we observe that the performance of the DF cooperative ARQ relay scheme with the optimum power allocation is about 1.5dB better than that of the scheme with the equal power allocation. In cases of  $L = 3$  in Fig. 7, the optimum power allocation is  $P_s/2P = 0.7969$  and  $P_r/2P = 0.2031$ , and the optimum power allocation shows a performance improvement of 1.25dB compare to the equal power allocation. In case of  $L = 4$  in Fig. 8, the optimum power allocations is  $P_s/2P = 0.7838$  and  $P_r/2P = 0.2162$ . We can see that the DF cooperative ARQ relay scheme with the optimum power allocation also shows a 1.25dB gain compared to that with the equal power allocation. In Figs. 6–8, we also plot the approximation of the outage probability for the DF cooperative ARQ relay scheme with the optimum power allocation as well as the equal power allocation. We can see that the approximation of the outage probability matches with the simulation curves at high SNR in all scenarios, which further validate our theoretical analysis.

### 3.2 Optimal Power Assignment for Hybrid-ARQ Rayleigh Fading Links

In this subsection, first we review briefly the H-ARQ transmission scheme and formulate the power assignment optimization problem. Second, we find the optimal power assignment strategy for the H-ARQ protocol and present an exact recursive calculation algorithm. Third, we develop a simple approximation of the optimal power assignment sequence and compare it with the exact calculation result. By the end of this subsection, numerical and simulation studies are carried out to compare the performance of the equal and optimal power assignment strategies.

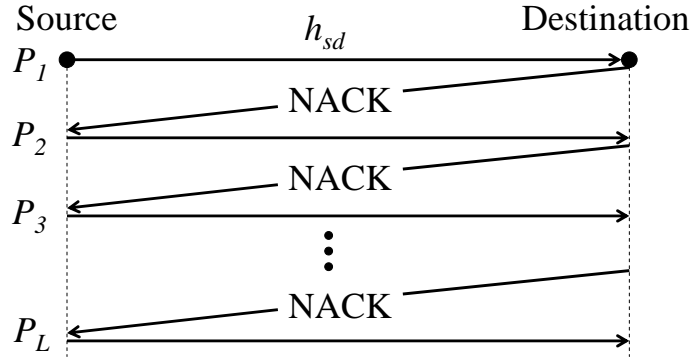


Figure 9: Illustration of a hybrid-ARQ protocol with transmission power  $P_l$  in the  $l$ th (re-)transmission round,  $1 \leq l \leq L$ .

### 3.2.1 System Model and Problem Formulation

We consider an H-ARQ transmission protocol implemented between a source node and a destination node as illustrated in Fig. 9. Assume that  $L$  is the number of retransmission rounds allowed in the H-ARQ protocol. The H-ARQ transmission scheme operates as follows. First, the source transmits an information packet to the destination and the destination indicates success or failure of receiving the packet by feeding back a single bit of acknowledge (ACK) or negative-acknowledgement (NACK), respectively. The feedback channel is assumed error-free. Then, if a NACK is received by the source and the maximum number of retransmissions  $L$  is not reached, the source retransmits the packet at a potentially different transmission power to be determined/optimized. If an ACK is received by the source or the maximum retransmission number  $L$  is reached, the source begins transmission of a new information packet. In each retransmission round, the destination attempts to decode an information packet by combining received signals from all previous transmission rounds by the standard maximal-ratio-combining (MRC) technique [37]. If the destination still cannot decode an information packet after  $L$  (re)transmission rounds, then an outage is declared which means that the signal-to-noise ratio (SNR) of the combined received signals at the destination is below a required SNR.

The H-ARQ transmission scheme can be modeled as follows. With  $L$  maximum retransmission rounds allowed in the H-ARQ protocol, the based-band received signal  $y_{sd,l}$  at the destination at the  $l$ th transmission round can be written as

$$y_{sd,l} = \sqrt{P_l} h_{sd} x_s + \eta_{sd,l}, \quad l = 1, 2, \dots, L, \quad (53)$$

where  $x_s$  is the transmitted information symbol from the source,  $P_l$  is the transmission power used by the source at the  $l$ th transmission round,  $h_{sd}$  is the source-destination channel coefficient, and  $\eta_{sd,l}$  is additive noise at the  $l$ th round. The channel coefficient  $h_{sd}$  is modeled as zero-mean complex Gaussian random variable with variance  $\sigma_{sd}^2$ . The channel is assumed to be *quasi-static*, i.e. the channel does not change during retransmissions of the same information packet and it may change independently when a new information packet is transmitted. The source-destination channel coefficient is assumed to be known at the receiver side, but unknown at the transmitter side. The additive noise contribution  $\eta_{sd,l}$  is modeled as a zero-mean complex Gaussian random variable with variance  $\mathcal{N}_0$ .

At the destination side, the receiving node combines the received signals from all previous retransmission rounds and jointly decodes the information packet based on the MRC combining technique [37]. Note that the MRC combining is applied over base-band symbol-level signals in (53) before decoding an entire information packet. With the assumption that the channel does not change in retransmissions of the same information packet, the SNR of the combined signal at the destination at the  $l$ th ( $1 \leq l \leq L$ ) retransmission round can be given as [37], [38]

$$\gamma_{sd,l} = \frac{\sum_{i=1}^l P_i |h_{sd}|^2 |x_s|^2}{\mathcal{N}_0}. \quad (54)$$

Without loss of generality, let us assume the average power of the transmitted information symbol is 1, then

we have  $\gamma_{sd,l} = \frac{\sum_{i=1}^l P_i |h_{sd}|^2}{N_0}$ . Since  $|h_{sd}|$  follows a Rayleigh distribution with mean zero and variance  $\sigma_{sd}^2$ , so for any targeted SNR  $\gamma_0$ , the probability of the event that the destination cannot decode correctly after  $l$  transmission rounds can be calculated as

$$p^{out,l} = \Pr[\gamma_{sd,l} < \gamma_0] = 1 - e^{-\frac{\gamma_0 N_0}{\sigma_{sd}^2 \sum_{i=1}^l P_i}}. \quad (55)$$

Set  $p^{out,0} = 1$ . Then, the probability that the H-ARQ protocol stops successfully at the  $l$ th,  $1 \leq l < L$ , transmission round is  $p^{out,l-1} - p^{out,l}$ , which means the destination cannot decode correctly at the  $(l-1)$ th round, but succeeds at the  $l$ th round.

Our goal is to find an optimal power assignment sequence  $\mathbf{P} = [P_1, P_2, \dots, P_L]$  for the H-ARQ protocol such that under a targeted outage probability  $p_0$ , the average total transmission power for the protocol to deliver an information packet is minimized. Since the probability that the protocol succeeds exactly at the  $l$ th ( $1 \leq l \leq L-1$ ) round is  $p^{out,l-1} - p^{out,l}$  and the corresponding total transmission power is  $P_1 + P_2 + \dots + P_l$ , so the average total transmission power of the H-ARQ protocol can be expressed as

$$\bar{P} = \sum_{l=1}^{L-1} (p^{out,l-1} - p^{out,l}) \sum_{i=1}^l P_i + p^{out,L-1} \sum_{i=1}^L P_i. \quad (56)$$

Note that the last term in (56) is due to the fact that the protocol stops retransmissions after the  $L$ th round no matter whether decoding at the  $L$ th round is successful or not. For the H-ARQ protocol with a targeted outage probability  $p_0$ , the problem of finding optimal power assignment can be formulated as follows:

$$\begin{aligned} & \min \quad \bar{P} \quad \text{with respect to } P_1, P_2, \dots, P_L \geq 0 \\ & \text{subject to} \quad p^{out,L} \leq p_0 \end{aligned} \quad (57)$$

where  $\bar{P}$  is specified in (56).

### 3.2.2 Optimal Transmission Power Assignment

In this section, we investigate the optimal power assignment strategy for the H-ARQ protocol to minimize the average total transmission power. We obtain a set of equations that describe the optimal transmission power values, and then develop a recursive algorithm to exactly calculate the optimal transmission power level for each retransmission round.

The average total transmission power in (56) can be rewritten by switching the summation order (between the indices  $l$  and  $i$ ) as follows

$$\bar{P} = \sum_{i=1}^L P_i \left[ \sum_{l=i}^{L-1} (p^{out,l-1} - p^{out,l}) + p^{out,L-1} \right] \quad (58)$$

where we first consider the summation by enumerating the index  $i$  from 1 to  $L$ , then consider the summation index  $l$  ( $i \leq l \leq L-1$ ). Since for each  $i$ ,  $\sum_{l=i}^{L-1} (p^{out,l-1} - p^{out,l}) = p^{out,i-1} - p^{out,L-1}$ , so the average total transmission power can be represented as

$$\bar{P} = P_1 + \sum_{l=2}^L P_l p^{out,l-1}. \quad (59)$$

Moreover, the constraint in (57) means that with a targeted SNR  $\gamma_0$ , the outage probability of the H-ARQ protocol with  $L$  retransmissions should not be larger than the specified outage probability value  $p_0$ , i.e.

$$p^{out,L} = 1 - e^{-\frac{\gamma_0 N_0}{\sigma_{sd}^2 \sum_{i=1}^L P_i}} \leq p_0. \quad (60)$$

Denote  $P_0 \triangleq \frac{\gamma_0 \mathcal{N}_0}{\sigma_{sd}^2 \ln \frac{1}{1-p_0}}$ , then the constraint is equivalent to

$$\sum_{l=1}^L P_l \geq P_0 \quad (61)$$

and the optimization problem in (57) can be further specified as

$$\begin{aligned} \min_{P_1, \dots, P_L \geq 0} \quad & \bar{P} = P_1 + \sum_{l=2}^L P_l \left[ 1 - e^{-\frac{\gamma_0 \mathcal{N}_0}{\sigma_{sd}^2 \sum_{i=1}^{l-1} P_i}} \right] \\ \text{subject to} \quad & \sum_{l=1}^L P_l \geq P_0. \end{aligned} \quad (62)$$

Next, we relax temporarily the non-negative condition on  $P_l$ ,  $l = 1, 2, \dots, L$ , and consider the sum-power constraint in (62) with equality in order to consider a Lagrange multiplier method to solve the optimization problem. We will prove later that the obtained solution is indeed optimal under the constraint in (62) and it satisfies the non-negative condition. Let us form a Lagrangian objective function as

$$\mathcal{L}(\mathbf{P}, \lambda) = P_1 + \sum_{l=2}^L P_l \left[ 1 - e^{-\frac{\gamma_0 \mathcal{N}_0}{\sigma_{sd}^2 \sum_{i=1}^{l-1} P_i}} \right] + \lambda \left[ \sum_{l=1}^L P_l - P_0 \right]. \quad (63)$$

Taking the derivative of  $\mathcal{L}(\mathbf{P}, \lambda)$  with respect to  $\lambda$  and setting it equal to zero, we have the power constraint as  $\sum_{l=1}^L P_l - P_0 = 0$ . The derivatives of  $\mathcal{L}(\mathbf{P}, \lambda)$  with respect to  $P_k$  are

$$\frac{\partial \mathcal{L}}{\partial P_1} = 1 - \sum_{l=2}^L \frac{P_l \gamma_0 \mathcal{N}_0}{\sigma_{sd}^2 (\sum_{i=1}^{l-1} P_i)^2} e^{-\frac{\gamma_0 \mathcal{N}_0}{\sigma_{sd}^2 \sum_{i=1}^{l-1} P_i}} + \lambda, \quad (64)$$

$$\frac{\partial \mathcal{L}}{\partial P_k} = \left[ 1 - e^{-\frac{\gamma_0 \mathcal{N}_0}{\sigma_{sd}^2 \sum_{i=1}^{k-1} P_i}} \right] - \sum_{l=k+1}^L \frac{P_l \gamma_0 \mathcal{N}_0}{\sigma_{sd}^2 (\sum_{i=1}^{l-1} P_i)^2} e^{-\frac{\gamma_0 \mathcal{N}_0}{\sigma_{sd}^2 \sum_{i=1}^{l-1} P_i}} + \lambda, \quad (65)$$

$$k = 2, 3, \dots, L,$$

$$\frac{\partial \mathcal{L}}{\partial P_L} = 1 - e^{-\frac{\gamma_0 \mathcal{N}_0}{\sigma_{sd}^2 \sum_{i=1}^{L-1} P_i}} + \lambda. \quad (66)$$

Based on  $\frac{\partial \mathcal{L}}{\partial P_1} = 0$  and  $\frac{\partial \mathcal{L}}{\partial P_2} = 0$ , we have

$$\frac{\partial \mathcal{L}}{\partial P_1} - \frac{\partial \mathcal{L}}{\partial P_2} = \left[ 1 - \frac{P_2 \gamma_0 \mathcal{N}_0}{\sigma_{sd}^2 P_1^2} \right] e^{-\frac{\gamma_0 \mathcal{N}_0}{\sigma_{sd}^2 P_1}} = 0, \quad (67)$$

which implies

$$P_2 = \frac{\sigma_{sd}^2 P_1^2}{\gamma_0 \mathcal{N}_0}. \quad (68)$$

For any  $k = 3, 4, \dots, L$ , according to  $\frac{\partial \mathcal{L}}{\partial P_{k-1}} = 0$  and  $\frac{\partial \mathcal{L}}{\partial P_k} = 0$ , we have

$$\frac{\partial \mathcal{L}}{\partial P_{k-1}} - \frac{\partial \mathcal{L}}{\partial P_k} = -e^{-\frac{\gamma_0 \mathcal{N}_0}{\sigma_{sd}^2 \sum_{i=1}^{k-2} P_i}} + \left[ 1 - \frac{P_k \gamma_0 \mathcal{N}_0}{\sigma_{sd}^2 (\sum_{i=1}^{k-1} P_i)^2} \right] e^{-\frac{\gamma_0 \mathcal{N}_0}{\sigma_{sd}^2 \sum_{i=1}^{k-1} P_i}} = 0, \quad (69)$$

which means

$$P_k = \frac{\sigma_{sd}^2 (\sum_{i=1}^{k-1} P_i)^2}{\gamma_0 \mathcal{N}_0} \left[ 1 - e^{-\frac{P_{k-1} \gamma_0 \mathcal{N}_0}{\sigma_{sd}^2 (\sum_{i=1}^{k-1} P_i) (\sum_{i=1}^{k-2} P_i)}} \right], \quad (70)$$

for any  $k = 3, 4, \dots, L$ . We can easily verify that the Lagrangian solutions  $P_2, P_3, \dots, P_L$  in (68) and (70) are positive.

In the following, we would like to show that the average total transmission power  $\bar{P}$  cannot be further minimized with strict inequality in (62). If there exists a power sequence  $P_1^*, P_2^*, \dots, P_L^*$  such that  $P_1^* + P_2^* + \dots + P_L^* > P_0$  and the average total transmission power  $\bar{P}$  is minimized, then let us consider another power sequence

$$\tilde{P}_k = rP_k^*, \quad k = 1, 2, \dots, L, \quad (71)$$

in which  $r$  is an arbitrary number satisfying

$$r \geq \frac{P_0}{P_1^* + P_2^* + \dots + P_L^*}. \quad (72)$$

We can see that the new power sequence  $\tilde{P}_1, \tilde{P}_2, \dots, \tilde{P}_L$  satisfies the power constraint in (62). With the new power sequence, the resulting average total transmission power is

$$\begin{aligned} f(r) &\triangleq \tilde{P}_1 + \sum_{l=2}^L \tilde{P}_l \left[ 1 - e^{-\frac{\gamma_0 \mathcal{N}_0}{\sigma_{sd}^2 \sum_{i=1}^{l-1} \tilde{P}_i}} \right] \\ &= rP_1^* + \sum_{l=2}^L rP_l^* \left[ 1 - e^{-\frac{\gamma_0 \mathcal{N}_0}{\sigma_{sd}^2 \sum_{i=1}^{l-1} rP_i^*}} \right], \end{aligned} \quad (73)$$

which is a function of  $r$ . Taking derivative of  $f(r)$  with respect to  $r$ , we have

$$\frac{\partial f(r)}{\partial r} = \sum_{l=1}^L P_l^* - \sum_{l=2}^L P_l^* \left[ 1 + \frac{\gamma_0 \mathcal{N}_0}{\sigma_{sd}^2 \sum_{i=1}^{l-1} rP_i^*} \right] e^{-\frac{\gamma_0 \mathcal{N}_0}{\sigma_{sd}^2 \sum_{i=1}^{l-1} rP_i^*}}. \quad (74)$$

Since  $e^{-x}(1+x) < 1$  for any positive  $x$ , so in (74),

$$\left[ 1 + \frac{\gamma_0 \mathcal{N}_0}{\sigma_{sd}^2 \sum_{i=1}^{l-1} rP_i^*} \right] e^{-\frac{\gamma_0 \mathcal{N}_0}{\sigma_{sd}^2 \sum_{i=1}^{l-1} rP_i^*}} < 1. \quad (75)$$

Thus, we have

$$\frac{\partial f(r)}{\partial r} > \sum_{l=1}^L P_l^* - \sum_{l=2}^L P_l^* = P_1^* > 0, \quad (76)$$

which means that  $f(r)$  is an increasing function for any  $r \geq \frac{P_0}{P_1^* + P_2^* + \dots + P_L^*}$ , and the minimum of  $f(r)$  is achieved when  $r = \frac{P_0}{P_1^* + P_2^* + \dots + P_L^*}$ . It implies that the average total transmission power resulting from the new power sequence with  $r = \frac{P_0}{P_1^* + P_2^* + \dots + P_L^*} (< 1)$  is less than that based on the power sequence  $P_1^*, P_2^*, \dots, P_L^*$ . This is contradictory to the assumption that the power sequence  $P_1^*, P_2^*, \dots, P_L^*$  minimizes the average total transmission power  $\bar{P}$ . Therefore, the minimum average total transmission power  $\bar{P}$  can be achieved at the boundary of the constraint (with equality) in (62). We note that with  $r = \frac{P_0}{P_1^* + P_2^* + \dots + P_L^*}$ , the new power sequence satisfies

$$\tilde{P}_1 + \tilde{P}_2 + \dots + \tilde{P}_L = P_0, \quad (77)$$

which is the boundary of the constraint in (62).

We note that in general a Lagrangian solution may not guarantee global optimality, i.e. it may lead to a local minima or maxima. Fortunately, the Lagrangian solution in (68) and (70) leads to a global minima as explained as follows. From the Lagrangian solution in (68) and (70) and the total power constraint  $P_1 + P_2 + \dots + P_L = P_0$ , we can see that there is only one unique power sequence  $P_1, P_2, \dots, P_L$  that results from the Lagrangian solution. So, the unique power sequence guarantees the global optimality which, however, can be either global minima or maxima. We further exam that with a trivial power assignment  $P_1 = P_0, P_2 = P_3 = \dots = P_L,$

Table 1: Algorithm to determine the optimal power assignment sequence  $P_k$  ( $1 \leq k \leq L$ )

<p>Step 1 : Input <math>\gamma_0, p_0, \sigma_{sd}^2, \mathcal{N}_0</math>. Calculate <math>P_0 = \frac{\gamma_0 \mathcal{N}_0}{\sigma_{sd}^2 \ln \frac{1}{1-p_0}}</math>.</p> <p>Step 2 : Set lower = 0 and upper = <math>P_0</math>.</p> <p>Step 3 : Let <math>P_1 = (\text{lower} + \text{upper})/2</math>, and calculate</p> $P_2 = \frac{\sigma_{sd}^2 P_1^2}{\gamma_0 \mathcal{N}_0},$ $P_k = \frac{\sigma_{sd}^2 (\sum_{i=1}^{k-1} P_i)^2}{\gamma_0 \mathcal{N}_0} \left[ 1 - e^{-\frac{P_{k-1} \gamma_0 \mathcal{N}_0}{\sigma_{sd}^2 (\sum_{i=1}^{k-1} P_i) (\sum_{i=1}^{k-2} P_i)}} \right],$ <p>for any <math>k = 3, 4, \dots, L</math>.</p> <p>Step 4 : Check if <math>\text{abs}(P_1 + P_2 + \dots + P_L - P_0) &lt; \epsilon (= 0.001)</math>, then stop and output power sequence <math>P_1, P_2, \dots, P_L</math>; otherwise,</p> <p>if <math>P_1 + P_2 + \dots + P_L - P_0 &lt; 0</math>, set lower = <math>P_1</math>;</p> <p>if <math>P_1 + P_2 + \dots + P_L - P_0 &gt; 0</math>, set upper = <math>P_1</math>;</p> <p>and go to Step 3.</p>
--

the resulting average total transmission power is  $\bar{P} = P_0$ , which is larger than the average total transmission power resulting from the power sequence associated with the Lagrangian solution. Therefore, the unique power sequence from the Lagrangian solution guarantees the global minima. We summarize the above discussion in the following theorem.

**Theorem 1** *In the H-ARQ transmission protocol, to minimize the average total transmission power, the optimal transmission power  $P_k$  at the  $k$ th,  $1 \leq k \leq L$ , transmission round must satisfy the following*

$$P_2 = \frac{\sigma_{sd}^2 P_1^2}{\gamma_0 \mathcal{N}_0}, \quad (78)$$

$$P_k = \frac{\sigma_{sd}^2 (\sum_{i=1}^{k-1} P_i)^2}{\gamma_0 \mathcal{N}_0} \left[ 1 - e^{-\frac{P_{k-1} \gamma_0 \mathcal{N}_0}{\sigma_{sd}^2 (\sum_{i=1}^{k-1} P_i) (\sum_{i=1}^{k-2} P_i)}} \right], \quad (79)$$

for  $k = 3, 4, \dots, L$ , and

$$P_1 + P_2 + \dots + P_L = P_0, \quad (80)$$

where  $P_0 \triangleq \frac{\gamma_0 \mathcal{N}_0}{\sigma_{sd}^2 \ln \frac{1}{1-p_0}}$ ,  $\gamma_0$  is the required SNR for correct decoding,  $\mathcal{N}_0$  is the additive white noise variance,  $\sigma_{sd}^2$  is the Rayleigh fading variance, and  $p_0$  is the targeted H-ARQ outage probability.  $\square$

From Theorem 1, we can see that the optimal transmission power sequence is uniquely determined by the set of equations (78)–(80). The optimal transmission power level for each (re)transmission round can be calculated recursively. According to (78) and (79), for any  $k = 2, 3, \dots, L$ , the optimal transmission power value  $P_k$  can be calculated based on  $P_1, P_2, \dots, P_{k-1}$ . So for any given power  $P_1$ , all other transmission power  $P_k, k = 2, 3, \dots, L$ , can be subsequently determined. The optimal initial power  $P_1$  can be numerically found based on (80) by the Newton method. A complete algorithm to recursively determine the optimal power assignment sequence  $P_k, k = 1, 2, \dots, L$ , is detailed in Table I.

When  $L = 2$ , we have a closed-form solution for the optimal power sequence. In this case,  $P_1 + P_2 = P_0$

and  $P_2 = \frac{\sigma_{sd}^2 P_1^2}{\gamma_0 \mathcal{N}_0}$ . By solving the two equations, the optimal transmission power  $P_1$  and  $P_2$  are given by

$$P_1 = \frac{2P_0}{1 + \sqrt{1 + \frac{4\sigma_{sd}^2 P_0}{\gamma_0 \mathcal{N}_0}}}, \quad (81)$$

$$P_2 = \frac{\gamma_0 \mathcal{N}_0}{4\sigma_{sd}^2} \left( \sqrt{1 + \frac{4\sigma_{sd}^2 P_0}{\gamma_0 \mathcal{N}_0}} - 1 \right)^2. \quad (82)$$

From (81) and (82), we can see that if  $\frac{\gamma_0 \mathcal{N}_0}{\sigma_{sd}^2} > \frac{P_0}{2}$ , then  $P_1 > \frac{P_0}{2}$ , which implies that  $P_1 > P_2$ , i.e. the power assigned in the first transmission round should be larger than that for the second retransmission round. The condition  $\frac{\gamma_0 \mathcal{N}_0}{\sigma_{sd}^2} > \frac{P_0}{2}$  means

$$\frac{\gamma_0 \mathcal{N}_0}{\sigma_{sd}^2} > \frac{1}{2} \frac{\gamma_0 \mathcal{N}_0}{\sigma_{sd}^2 \ln \frac{1}{1-p_0}},$$

which is true when  $p_0 > 1 - e^{-\frac{1}{2}} \approx 0.3935$ . On the other hand, if  $\frac{\gamma_0 \mathcal{N}_0}{\sigma_{sd}^2} < \frac{P_0}{2}$  (i.e.  $p_0 < 1 - e^{-\frac{1}{2}}$ ), then  $P_1 < \frac{P_0}{2}$ , which means  $P_1$  should be less than  $P_2$  (an opposite power assignment strategy compared to that of  $P_1 > P_2$ ). Especially, when the targeted outage probability is  $p_0 = 1 - e^{-\frac{1}{2}}$ , the optimal power assignment is  $P_1 = P_2$ , i.e. an equal power assignment, no matter what are the required SNR  $\gamma_0$ , the noise variance  $\mathcal{N}_0$  and the channel variance  $\sigma_{sd}^2$ . From the case of  $L = 2$ , we can see that the optimal power can be assigned either in an increasing, decreasing or equal way depending on the targeted outage probability performance of the H-ARQ protocol. This is different from the case in [35] where the optimal transmission power must be increasing in every retransmission.

For the general case of  $L > 2$ , numerical results (shown in Figs. 2-4 in Section 4) reveal that the optimal power assignment sequence can be neither increasing nor decreasing. Actually, from the theorem we can see that when  $P_1 < \frac{\gamma_0 \mathcal{N}_0}{\sigma_{sd}^2}$ , the optimal transmission power  $P_2$  is less than  $P_1$  according to (78). On the other hand, when  $P_1 > \frac{\gamma_0 \mathcal{N}_0}{\sigma_{sd}^2}$ , the optimal transmission power  $P_2$  is larger than  $P_1$ . This phenomenon is fundamentally different from the case in [35] where the optimal transmission power sequence is always increasing.

We note that if  $P_1 > \frac{\gamma_0 \mathcal{N}_0}{\sigma_{sd}^2}$ , then the optimal power assignment sequence in Theorem 1 is monotonically increasing, i.e.  $P_1 < P_2 < \dots < P_L$ . From (78), it is easy to see that  $P_2 > P_1$  in this case. For any  $k = 3, 4, \dots, L$ , since  $1 - e^{-x} > x - \frac{1}{2}x^2$  for any  $x > 0^2$ , so from (79) we have

$$\begin{aligned} P_k &> \frac{\sigma_{sd}^2 (\sum_{i=1}^{k-1} P_i)^2}{\gamma_0 \mathcal{N}_0} \left[ \frac{P_{k-1} \gamma_0 \mathcal{N}_0}{\sigma_{sd}^2 \left( \sum_{i=1}^{k-1} P_i \right) \left( \sum_{i=1}^{k-2} P_i \right)} - \frac{P_{k-1}^2 (\gamma_0 \mathcal{N}_0)^2}{2\sigma_{sd}^4 \left( \sum_{i=1}^{k-1} P_i \right)^2 \left( \sum_{i=1}^{k-2} P_i \right)^2} \right] \\ &= \left[ 1 + \frac{P_{k-1}}{\sum_{i=1}^{k-2} P_i} - \frac{P_{k-1} \gamma_0 \mathcal{N}_0}{2\sigma_{sd}^2 \left( \sum_{i=1}^{k-2} P_i \right)^2} \right] P_{k-1}. \end{aligned} \quad (83)$$

Since  $\frac{\gamma_0 \mathcal{N}_0}{\sigma_{sd}^2 (\sum_{i=1}^{k-2} P_i)} < \frac{\gamma_0 \mathcal{N}_0}{\sigma_{sd}^2 P_1} < 1$ , it is easy to see that

$$\frac{P_{k-1}}{\sum_{i=1}^{k-2} P_i} - \frac{P_{k-1} \gamma_0 \mathcal{N}_0}{2\sigma_{sd}^2 \left( \sum_{i=1}^{k-2} P_i \right)^2} = \frac{P_{k-1}}{\sum_{i=1}^{k-2} P_i} \left[ 1 - \frac{\gamma_0 \mathcal{N}_0}{2\sigma_{sd}^2 \left( \sum_{i=1}^{k-2} P_i \right)} \right] > 0. \quad (84)$$

<sup>2</sup>In this footnote, we would like to prove that  $G(x) \triangleq (1 - e^{-x}) - (x - \frac{1}{2}x^2) > 0$  for any  $x > 0$ . We can see that  $G'(x) = e^{-x} + x - 1$  and  $G''(x) = -e^{-x} + 1$ . Since  $G'(0) = 0$  and  $G''(x) > 0$  for any  $x > 0$ , so  $G'(x) > 0$  for any  $x > 0$ , i.e.  $G(x)$  is monotonically increasing for  $x > 0$ . With  $G(0) = 0$ , we conclude that  $G(x) > 0$  for any  $x > 0$ .

Combining (83) and (84), we conclude that  $P_k > P_{k-1}$  for any  $k = 3, 4, \dots, L$ . Thus, the optimal power assignment sequence in Theorem 1 is monotonically increasing in this case. Actually, in this case the optimal power assignment sequence increases as a function of  $P_1$  roughly in a polynomial way, which is shown in the next section.

### 3.2.3 Approximation of the Optimal Power Sequence

To reduce calculation complexity in the optimal power assignment, we present in this section a simple and tight approximation for the optimal transmission power sequence. The tight approximation allows us to get more insight understanding of the optimal power assignment strategy for the H-ARQ protocol.

Since  $1 - e^{-x} \approx x$  for small  $x$ , so for any  $k = 3, 4, \dots, L$ , the optimal transmission power  $P_k$  in (79) can be approximated as

$$P_k \approx \frac{\sigma_{sd}^2 (\sum_{i=1}^{k-1} P_i)^2}{\gamma_0 \mathcal{N}_0} \times \frac{P_{k-1} \gamma_0 \mathcal{N}_0}{\sigma_{sd}^2 (\sum_{i=1}^{k-1} P_i) (\sum_{i=1}^{k-2} P_i)} \quad (85)$$

$$= P_{k-1} + \frac{P_{k-1}^2}{\sum_{i=1}^{k-2} P_i}. \quad (86)$$

The approximation in (85) is tight when  $\frac{P_{k-1} \gamma_0 \mathcal{N}_0}{\sigma_{sd}^2 (\sum_{i=1}^{k-1} P_i) (\sum_{i=1}^{k-2} P_i)}$  is small and it is true in general. We can verify that when  $k = 3$ ,

$$\frac{P_{k-1} \gamma_0 \mathcal{N}_0}{\sigma_{sd}^2 (\sum_{i=1}^{k-1} P_i) (\sum_{i=1}^{k-2} P_i)} = \frac{1}{1 + \frac{\sigma_{sd}^2}{\gamma_0 \mathcal{N}_0} P_1}$$

which is strictly less than 1, and it becomes smaller when the power  $P_1$  is larger. When  $k > 3$ ,

$$\frac{P_{k-1} \gamma_0 \mathcal{N}_0}{\sigma_{sd}^2 (\sum_{i=1}^{k-1} P_i) (\sum_{i=1}^{k-2} P_i)} < \frac{\frac{\gamma_0 \mathcal{N}_0}{\sigma_{sd}^2}}{\sum_{i=1}^{k-2} P_i}$$

which is small when any of  $P_1, P_2, \dots, P_{k-2}$  is large.

When  $k = 3$ , substituting  $P_2 = \frac{\sigma_{sd}^2 P_1^2}{\gamma_0 \mathcal{N}_0}$  into (86), we have

$$P_3 \approx P_2 + \frac{P_2^2}{P_1} = \frac{\sigma_{sd}^2 P_1^2}{\gamma_0 \mathcal{N}_0} \left( 1 + \frac{\sigma_{sd}^2 P_1}{\gamma_0 \mathcal{N}_0} \right). \quad (87)$$

When  $k = 4$ , substituting  $P_2 = \frac{\sigma_{sd}^2 P_1^2}{\gamma_0 \mathcal{N}_0}$  and the above approximation of  $P_3$  into (86), we can approximate  $P_4$  as

$$P_4 \approx P_3 + \frac{P_3^2}{P_1 + P_2} = \frac{\sigma_{sd}^2 P_1^2}{\gamma_0 \mathcal{N}_0} \left( 1 + \frac{\sigma_{sd}^2 P_1}{\gamma_0 \mathcal{N}_0} \right)^2. \quad (88)$$

Assume that for any  $k \leq k_0 (> 2)$ , it is true that

$$P_k \approx \frac{\sigma_{sd}^2 P_1^2}{\gamma_0 \mathcal{N}_0} \left( 1 + \frac{\sigma_{sd}^2 P_1}{\gamma_0 \mathcal{N}_0} \right)^{k-2}, \quad k = 3, 4, \dots, k_0, \quad (89)$$

then for  $k = k_0 + 1$ , we have

$$P_{k_0+1} \approx P_{k_0} + \frac{P_{k_0}^2}{\sum_{i=1}^{k_0-1} P_i} \quad (90)$$

$$= \frac{\sigma_{sd}^2 P_1^2}{\gamma_0 \mathcal{N}_0} \left( 1 + \frac{\sigma_{sd}^2 P_1}{\gamma_0 \mathcal{N}_0} \right)^{k_0-2} + \frac{\left( \frac{\sigma_{sd}^2 P_1^2}{\gamma_0 \mathcal{N}_0} \right)^2 \left( 1 + \frac{\sigma_{sd}^2 P_1}{\gamma_0 \mathcal{N}_0} \right)^{2k_0-4}}{P_1 + \frac{\sigma_{sd}^2 P_1^2}{\gamma_0 \mathcal{N}_0} \sum_{i=2}^{k_0-1} \left( 1 + \frac{\sigma_{sd}^2 P_1}{\gamma_0 \mathcal{N}_0} \right)^{i-2}} \quad (91)$$

$$= \frac{\sigma_{sd}^2 P_1^2}{\gamma_0 \mathcal{N}_0} \left( 1 + \frac{\sigma_{sd}^2 P_1}{\gamma_0 \mathcal{N}_0} \right)^{(k_0+1)-2}, \quad (92)$$

Table 2: Algorithm to determine the approximation of the optimal power sequence  $P_k$  ( $1 \leq k \leq L$ )

<p>Step 1 : Input <math>\gamma_0, p_0, \sigma_{sd}^2, \mathcal{N}_0</math>. Calculate <math>P_0 = \frac{\gamma_0 \mathcal{N}_0}{\sigma_{sd}^2 \ln \frac{1}{1-p_0}}</math>.</p> <p>Step 2 : Set lower = 0 and upper = <math>P_0</math>.</p> <p>Step 3 : Let <math>P_1 = (\text{lower} + \text{upper})/2</math>, and calculate  <math display="block">\text{temp} = P_1 \left( 1 + \frac{\sigma_{sd}^2 P_1}{\gamma_0 \mathcal{N}_0} \right)^{L-1} - P_0.</math> Check if <math>\text{abs}(\text{Temp}) &lt; \epsilon</math> (<math>= 0.001</math>), then output the optimal power <math>P_1</math> and go to Step 4; otherwise  if <math>\text{temp} &lt; 0</math>, set lower = <math>P_1</math>;  if <math>\text{temp} &gt; 0</math>, set upper = <math>P_1</math>;  and repeat Step 3.</p> <p>Step 4 : Calculate the optimal transmission power <math>P_k</math> as follows :  <math display="block">P_k \approx \frac{\sigma_{sd}^2 P_1^2}{\gamma_0 \mathcal{N}_0} \left( 1 + \frac{\sigma_{sd}^2 P_1}{\gamma_0 \mathcal{N}_0} \right)^{k-2}, \quad k = 2, 3, \dots, L.</math></p>
---

i.e. the result in (89) is also true for  $k = k_0 + 1$ . Thus, by induction we can conclude that for any  $k = 2, 3, \dots, L$ , we have

$$P_k \approx \frac{\sigma_{sd}^2 P_1^2}{\gamma_0 \mathcal{N}_0} \left( 1 + \frac{\sigma_{sd}^2 P_1}{\gamma_0 \mathcal{N}_0} \right)^{k-2}. \quad (93)$$

Based on the approximation and the sum-power constraint in (80), we have a constraint on the optimal power  $P_1$  as follows

$$P_1 + \sum_{k=2}^L \frac{\sigma_{sd}^2 P_1^2}{\gamma_0 \mathcal{N}_0} \left( 1 + \frac{\sigma_{sd}^2 P_1}{\gamma_0 \mathcal{N}_0} \right)^{k-2} = P_0 \quad (94)$$

or equivalently

$$P_1 \left( 1 + \frac{\sigma_{sd}^2 P_1}{\gamma_0 \mathcal{N}_0} \right)^L = P_0. \quad (95)$$

The left-hand side of the equation (95) is an increasing function in terms of power  $P_1$ , so there is a unique solution for the equation. Thus, the optimal power  $P_1$  can be easily determined based on the equation in (95) by using the Newton method. We summarize the above discussion in the form of the following theorem.

**Theorem 2** *In the H-ARQ transmission protocol, the optimal transmission power at each round can be approximated as*

$$P_k \approx \frac{\sigma_{sd}^2 P_1^2}{\gamma_0 \mathcal{N}_0} \left( 1 + \frac{\sigma_{sd}^2 P_1}{\gamma_0 \mathcal{N}_0} \right)^{k-2} \quad (96)$$

for  $k = 2, 3, \dots, L$  where  $P_1$  is determined by the equation

$$P_1 \left( 1 + \frac{\sigma_{sd}^2 P_1}{\gamma_0 \mathcal{N}_0} \right)^{L-1} = P_0, \quad (97)$$

where  $P_0 = \frac{\gamma_0 \mathcal{N}_0}{\sigma_{sd}^2 \ln \frac{1}{1-p_0}}$ . □

From Theorem 2, we observe that for any  $k = 2, 3, \dots, L$ , the optimal transmission power  $P_k$  can be approximated as a function of  $P_1$ . The optimal transmission power  $P_1$  can be directly determined by the equation (97), then all other optimal transmission power values  $P_k, k = 2, 3, \dots, L$  can be obtained immediately based

on the closed-form expression in (96). The procedure is detailed in the algorithm in Table II. We can see that the calculation complexity of the algorithm in Table II is much less than that of the recursive algorithm in Table I. The approximation in Theorem 2 provides some insight understanding that the optimal transmission power in each retransmission round varies in term of  $P_1$  (the transmission power in the first round) in a polynomial way.

When  $L = 2$ , the constraint in (97) is reduced to  $P_1 \left(1 + \frac{\sigma_{sd}^2 P_1}{\gamma_0 \mathcal{N}_0}\right) = P_0$ . By solving the equation, we have the optimal power value for the first transmission round as  $P_1 = \frac{2P_0}{1 + \sqrt{1 + \frac{4\sigma_{sd}^2 P_0}{\gamma_0 \mathcal{N}_0}}}$ , which matches with the exact power value given in (81). When  $L > 2$ , based on the constraint in (97), the optimal transmission power  $P_1$  can be bounded as follows. Since the geometric mean is not greater than the arithmetic mean, we have

$$\frac{\sigma_{sd}^2}{\gamma_0 \mathcal{N}_0} P_0 = \frac{\sigma_{sd}^2 P_1}{\gamma_0 \mathcal{N}_0} \left(1 + \frac{\sigma_{sd}^2 P_1}{\gamma_0 \mathcal{N}_0}\right)^{L-1} < \left(\frac{(L-1) + L \frac{\sigma_{sd}^2 P_1}{\gamma_0 \mathcal{N}_0}}{L}\right)^L, \quad (98)$$

i.e.

$$P_1 > \frac{\gamma_0 \mathcal{N}_0}{\sigma_{sd}^2} \left[ \left(\frac{\sigma_{sd}^2 P_0}{\gamma_0 \mathcal{N}_0}\right)^{\frac{1}{L}} - \frac{L-1}{L} \right]. \quad (99)$$

On the other hand, since

$$P_0 = P_1 \left(1 + \frac{\sigma_{sd}^2 P_1}{\gamma_0 \mathcal{N}_0}\right)^{L-1} > \left(\frac{\sigma_{sd}^2}{\gamma_0 \mathcal{N}_0}\right)^{L-1} P_1^L, \quad (100)$$

so we have

$$P_1 < \frac{\gamma_0 \mathcal{N}_0}{\sigma_{sd}^2} \left(\frac{\sigma_{sd}^2 P_0}{\gamma_0 \mathcal{N}_0}\right)^{\frac{1}{L}}. \quad (101)$$

Therefore, the optimal transmission power  $P_1$  is bounded as follows

$$\frac{\gamma_0 \mathcal{N}_0}{\sigma_{sd}^2} \left[ \left(\frac{\sigma_{sd}^2 P_0}{\gamma_0 \mathcal{N}_0}\right)^{\frac{1}{L}} - \frac{L-1}{L} \right] < P_1 < \frac{\gamma_0 \mathcal{N}_0}{\sigma_{sd}^2} \left(\frac{\sigma_{sd}^2 P_0}{\gamma_0 \mathcal{N}_0}\right)^{\frac{1}{L}}, \quad (102)$$

in which the upper bound is tight when  $P_0$  is large. The difference between the lower bound and the upper bound is less than  $\frac{\gamma_0 \mathcal{N}_0}{\sigma_{sd}^2}$ .

In Figs. 10 and 11, we show comparisons of the approximation of the optimal transmission power sequence by Theorem 2 with the exact optimized power sequence by Theorem 1. In these two figures, we assumed that the targeted SNR is  $\gamma_0 = 10$  dB, the required outage performance is  $p_0 = 10^{-3}$ ,  $\sigma_{sd}^2 = 1$  and  $\mathcal{N}_0 = 1$ . The maximum number of transmission rounds is  $L = 3$  in Fig. 10, and  $L = 5$  in Fig. 11. We can see that the approximations of the optimal transmission power values (solid line with '\*' ) match very well with those based on exactly numerical calculation (solid line with 'o'). For comparison, we also include in the figures the transmission power level of the equal-power assignment strategy. We observe that in the first few (re)transmission rounds, the optimal power assignment strategy assigns significantly less transmission power compared to the equal-power assignment strategy.

The optimum transmission power sequence is increasing in both cases in Figs. 10 and 11. Actually, the optimum transmission power sequence can be neither increasing or decreasing, which is shown in Fig. 12. In this case, the maximum number of retransmission rounds is  $L = 10$ , the targeted SNR is  $\gamma_0 = 10$  dB and the required outage performance is  $p_0 = 10^{-1}$ . We can see that the optimal power assignment is decreasing in the first two rounds and increasing after that. Moreover, we observe that in this case there is a gap between the approximations of the optimal transmission power sequence and the exactly calculated sequence. Since when  $k = 3$ , the term  $\frac{P_{k-1} \gamma_0 \mathcal{N}_0}{\sigma_{sd}^2 (\sum_{i=1}^{k-1} P_i) (\sum_{i=1}^{k-2} P_i)} = \frac{1}{1 + \frac{\sigma_{sd}^2 P_1}{\gamma_0 \mathcal{N}_0}} \approx 0.63$  which is not small enough in this case, so the approximation of the exponential term in (85) is not tight. The difference between the approximated sequence and the exactly calculated power sequence can be more significant when the the maximum number

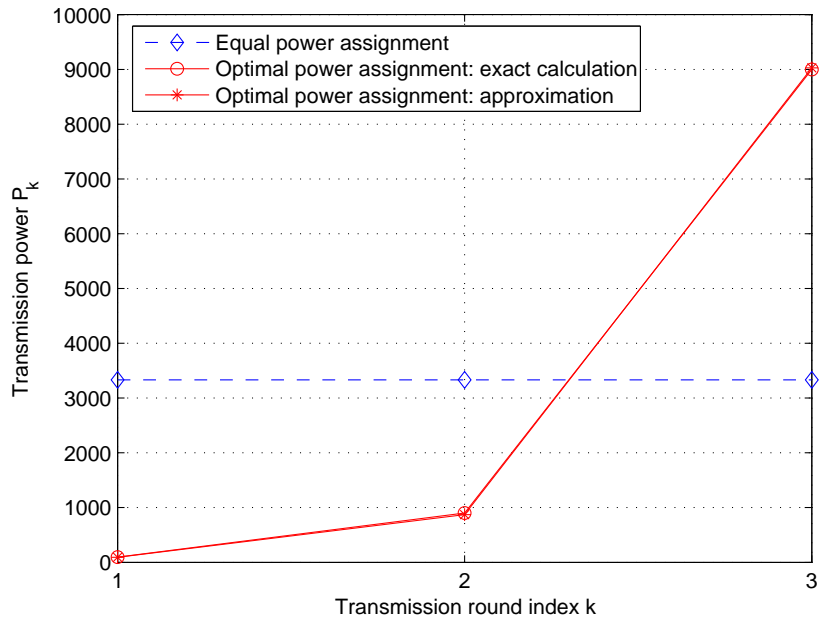


Figure 10: Transmission power sequence of the optimal power assignment strategy with  $L = 3$ ,  $\gamma_0 = 10$  dB,  $p_0 = 10^{-3}$ .

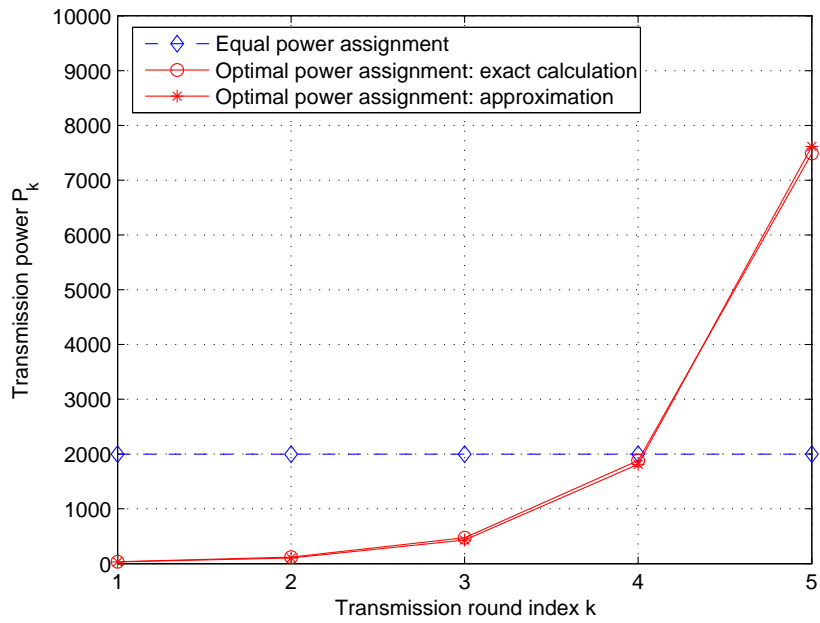


Figure 11: Transmission power sequence of the optimal power assignment strategy with  $L = 5$ ,  $\gamma_0 = 10$  dB,  $p_0 = 10^{-3}$ .

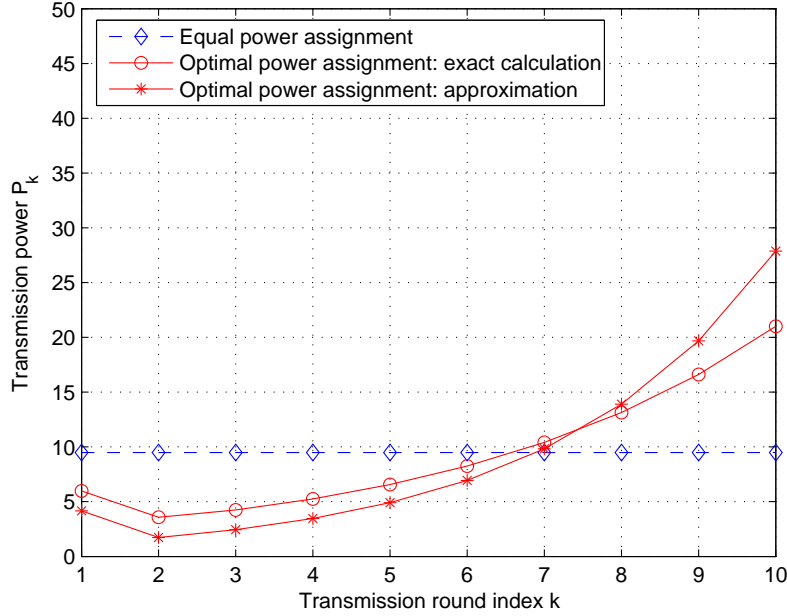


Figure 12: Transmission power sequence of the optimal assignment strategy with  $L = 10$ ,  $\gamma_0 = 10$  dB,  $p_0 = 10^{-1}$ .

of retransmission rounds  $L$  goes to infinity. Fortunately, this is not the case in practice where a reasonable  $L$  is normally less than 10 due to delay consideration.

Finally, based on the approximation of the optimal transmission power sequence, the average total transmission power of the H-ARQ protocol accounting for requested retransmissions can be approximated as follows

$$\begin{aligned}
\bar{P}_{opt} &\approx P_1 + \sum_{l=2}^L \frac{\sigma_{sd}^2 P_1^2}{\gamma_0 \mathcal{N}_0} \left(1 + \frac{\sigma_{sd}^2 P_1}{\gamma_0 \mathcal{N}_0}\right)^{l-2} \left[1 - e^{-\frac{\gamma_0 \mathcal{N}_0}{\sigma_{sd}^2 \sum_{i=1}^{l-1} \frac{\sigma_{sd}^2 P_1^2}{\gamma_0 \mathcal{N}_0} \left(1 + \frac{\sigma_{sd}^2 P_1}{\gamma_0 \mathcal{N}_0}\right)^{i-2}}}\right] \\
&= P_1 + \sum_{l=2}^L \frac{\sigma_{sd}^2 P_1^2}{\gamma_0 \mathcal{N}_0} \left(1 + \frac{\sigma_{sd}^2 P_1}{\gamma_0 \mathcal{N}_0}\right)^{l-2} \left[1 - e^{-\frac{\gamma_0 \mathcal{N}_0}{\sigma_{sd}^2 P_1} \left(1 + \frac{\sigma_{sd}^2 P_1}{\gamma_0 \mathcal{N}_0}\right)^{-l+2}}\right]. \tag{103}
\end{aligned}$$

The approximation of the average total transmission power is a function of  $P_1$ . Moreover, when  $P_1 > \frac{\gamma_0 \mathcal{N}_0}{\sigma_{sd}^2}$ , then using the approximation  $1 - e^{-x} \approx x$  for small  $x$ , the average total transmission power across requested retransmissions can be further approximated as

$$\bar{P}_{opt} \approx P_1 + \sum_{l=2}^L P_1 = LP_1. \tag{104}$$

This approximation is tight when  $L$  is small, since  $P_1$  is normally larger than  $\frac{\gamma_0 \mathcal{N}_0}{\sigma_{sd}^2}$  in this case. It shows that the average total transmission power is roughly the product of the transmission power in the first round and the number of retransmission rounds allowed in the H-ARQ protocol. If we approximate  $P_1$  as  $\frac{\gamma_0 \mathcal{N}_0}{\sigma_{sd}^2} \left(\frac{\sigma_{sd}^2 P_0}{\gamma_0 \mathcal{N}_0}\right)^{\frac{1}{L}}$  based on (101), then the average total transmission power with the optimal power assignment sequence can be approximated as

$$\bar{P}_{opt} \approx L \frac{\gamma_0 \mathcal{N}_0}{\sigma_{sd}^2} \left(\frac{\sigma_{sd}^2 P_0}{\gamma_0 \mathcal{N}_0}\right)^{\frac{1}{L}} = \frac{L}{\left(\ln \frac{1}{1-p_0}\right)^{\frac{1}{L}}} \frac{\gamma_0 \mathcal{N}_0}{\sigma_{sd}^2}. \tag{105}$$

### 3.2.4 Performance Comparisons between the Equal and Optimal Power Assignments

In this subsection, we compare the power efficiency of the H-ARQ protocols with the optimal power assignment strategy derived in this work and the conventional equal-power assignment approach. In numerical calculation, we assume that the variance of the channel  $h_{sd}$  is  $\sigma_{sd}^2 = 1$  and the noise variance is  $\mathcal{N}_0 = 1$ .

For a targeted outage probability  $p_0$ , according to (61), the equal-power assignment approach should also follow the power constraint

$$\sum_{l=1}^L P_l \geq P_0 = \frac{\gamma_0 \mathcal{N}_0}{\sigma_{sd}^2 \ln \frac{1}{1-p_0}}. \quad (106)$$

Thus, the equal-power assignment is  $P_l = P_0/L$  for each  $l = 1, 2, \dots, L$ . The corresponding average total transmission power is

$$\begin{aligned} \bar{P}_{equ} &= P_1 + \sum_{l=2}^L \frac{P_0}{L} \left[ 1 - e^{-\frac{\gamma_0 \mathcal{N}_0}{\sigma_{sd}^2 \sum_{i=1}^{l-1} \frac{P_0}{L}}} \right] \\ &= P_0 - \frac{P_0}{L} \sum_{l=2}^L e^{-\frac{L}{l-1} \frac{\gamma_0 \mathcal{N}_0}{\sigma_{sd}^2 P_0}}. \end{aligned} \quad (107)$$

When  $P_0$  is large, the average total transmission power of the equal-power assignment strategy can be approximated as

$$\bar{P}_{equ} \approx P_0 - \frac{P_0}{L} \sum_{l=2}^L \left( 1 - \frac{L}{l-1} \frac{\gamma_0 \mathcal{N}_0}{\sigma_{sd}^2 P_0} \right) = \frac{P_0}{L} + \frac{\gamma_0 \mathcal{N}_0}{\sigma_{sd}^2} \sum_{l=2}^L \frac{1}{l-1}. \quad (108)$$

Therefore, the power efficiency of the optimal power assignment strategy compared to the equal-power assignment approach can be quantified by the following ratio

$$\begin{aligned} \frac{\bar{P}_{equ}}{\bar{P}_{opt}} &= \frac{\frac{P_0}{L} + \frac{\gamma_0 \mathcal{N}_0}{\sigma_{sd}^2} \sum_{l=2}^L \frac{1}{l-1}}{L \frac{\gamma_0 \mathcal{N}_0}{\sigma_{sd}^2} \left( \frac{\sigma_{sd}^2 P_0}{\gamma_0 \mathcal{N}_0} \right)^{\frac{1}{L}}} \\ &= \frac{1}{L^2} \left( \ln \frac{1}{1-p_0} \right)^{\frac{1}{L}-1} + \frac{1}{L} \left( \ln \frac{1}{1-p_0} \right)^{\frac{1}{L}} \sum_{l=2}^L \frac{1}{l-1}. \end{aligned} \quad (109)$$

According to  $\ln \frac{1}{1-p_0} \approx p_0$ , the ratio can be approximated as

$$\frac{\bar{P}_{equ}}{\bar{P}_{opt}} \approx \frac{p_0^{\frac{1}{L}}}{L} \left( \frac{1}{L p_0} + \sum_{l=2}^L \frac{1}{l-1} \right). \quad (110)$$

For small targeted outage probability  $p_0$ , the ratio can be further approximated as  $\frac{\bar{P}_{equ}}{\bar{P}_{opt}} \approx \frac{p_0^{\frac{1}{L}-1}}{L^2}$ . We can see that the smaller the targeted outage probability  $p_0$ , the more power saving the optimal power assignment strategy compared to the equal-power assignment strategy.

For different targeted SNR  $\gamma_0$  (from 0 dB to 40 dB), we compare the average total transmission power of the optimal power assignment strategy and the equal-power assignment scheme in Figs. 13, 14, and 15 for the cases of  $L = 2$ ,  $L = 3$ , and  $L = 5$ , respectively. The required outage performance of the H-ARQ protocol is set at  $p_0 = 10^{-3}$ . When  $L = 2$ , from Fig. 13 we observe that the optimal power assignment saves about 9 dB in average total transmission power compared to the equal-power H-ARQ. When  $L = 3$ , we can see from Fig. 14 that the optimal power assignment shows about 10 dB gain compared to the equal-power assignment scheme. When  $L = 5$ , Fig. 15 shows that the optimal power assignment strategy significantly outperforms the equal-power assignment scheme with a performance improvement of about 11 dB. Moreover, it is interesting to observe that in each figure, the performance gain of the optimal power assignment strategy is almost constant

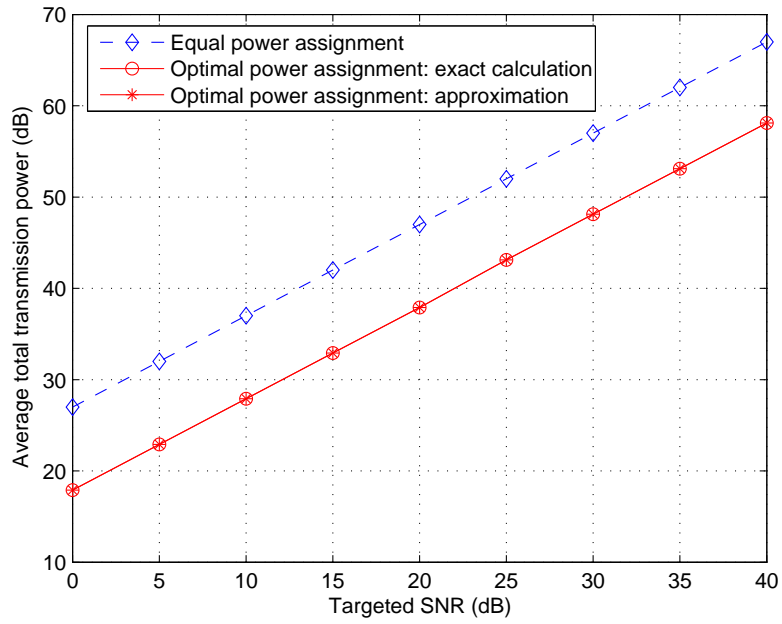


Figure 13: Comparisons of the average total transmission power between the equal and optimal power assignment strategies with different targeted SNRs.  $L = 2$ ,  $p_0 = 10^{-3}$ .

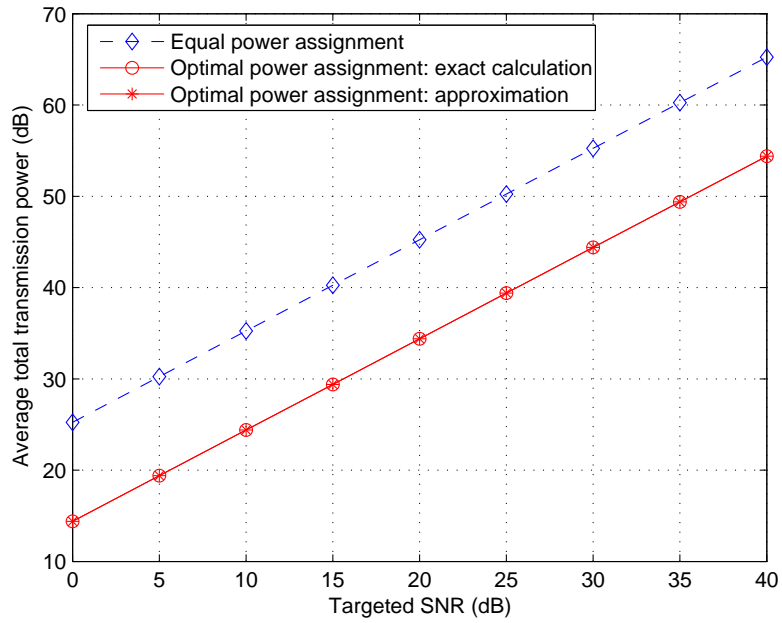


Figure 14: Comparisons of the average total transmission power of the equal and optimal power assignment strategies with different targeted SNRs.  $L = 3$ ,  $p_0 = 10^{-3}$ .

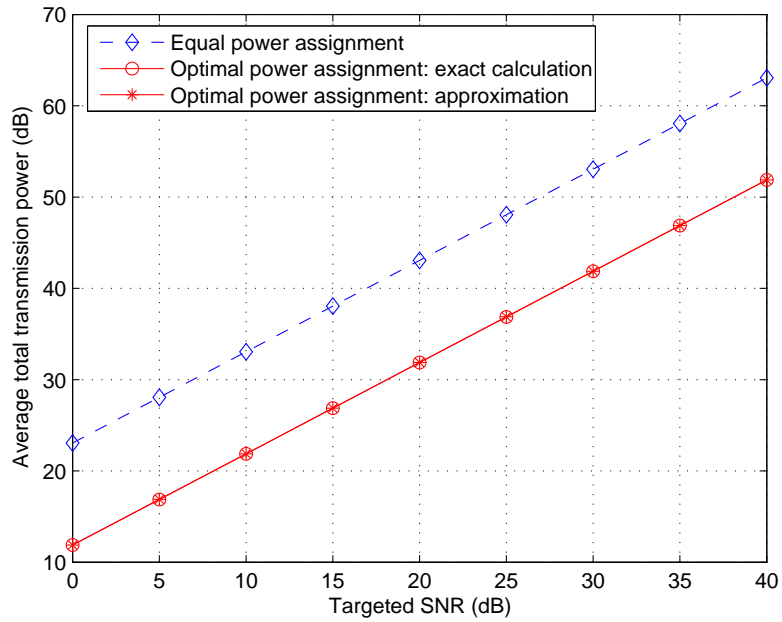


Figure 15: Comparisons of the average total transmission power of the equal and optimal power assignment strategies with different targeted SNRs.  $L = 5$ ,  $p_0 = 10^{-3}$ .

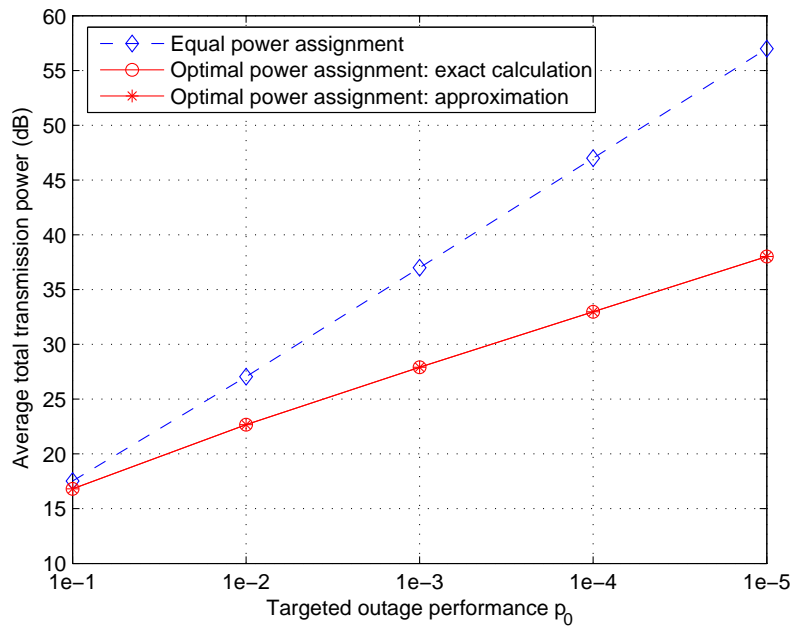


Figure 16: Comparisons of the average total transmission power of the equal and optimal power assignment strategies with different targeted outage probabilities.  $L = 2$ ,  $\gamma_0 = 10$  dB.

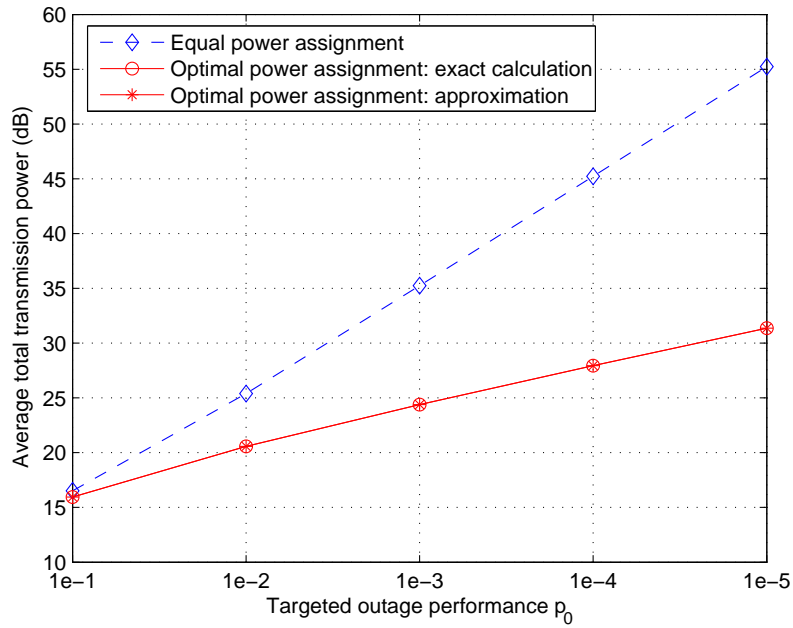


Figure 17: Comparisons of the average total transmission power of the equal and optimal power assignment strategies with different targeted outage probabilities.  $L = 3$ ,  $\gamma_0 = 10$  dB.

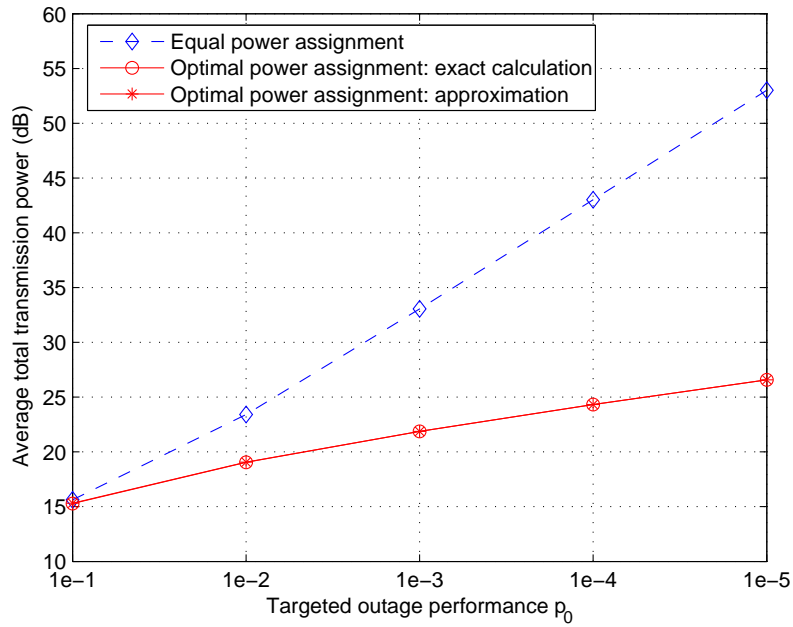


Figure 18: Comparisons of the average total transmission power of the equal and optimal power assignment strategies with different targeted outage probabilities.  $L = 5$ ,  $\gamma_0 = 10$  dB.

for different targeted SNR  $\gamma_0$  (from 0 dB to 40 dB). This is consistent with the theoretical approximation  $\frac{\bar{P}_{equ}}{P_{opt}}$  in (110) which does not rely on the targeted SNR  $\gamma_0$ . When  $L = 2$  and  $p_0 = 10^{-3}$ , the ratio in (110) is  $\frac{\bar{P}_{equ}}{P_{opt}} = 8.99$  dB (the observed power saving in Fig. 13 is 9 dB). When  $L = 3$  and  $p_0 = 10^{-3}$ , the ratio in (110) is  $\frac{\bar{P}_{equ}}{P_{opt}} = 10.48$  dB (the observed power saving in Fig. 14 is 10 dB).

We also compare the average total transmission power required in the two power assignment strategies with different targeted outage probability values. We assume the required SNR is  $\gamma_0 = 10$  dB. Figs. 16, 17 and 18 present comparison results for the cases of  $L = 2$ ,  $L = 3$ , and  $L = 5$ , respectively. From the three figures, we can see that for an outage performance of  $p_0 = 10^{-4}$ , the power savings of the optimal power assignment strategy compared to the equal-power assignment scheme are 15 dB when  $L = 2$ , 17 dB when  $L = 3$ , and 19 dB when  $L = 5$ . The lower the required outage probability, the more important optimization of the power sequence becomes. Moreover, we also observe that with the same targeted outage performance, the larger the number of retransmission rounds allowed in the H-ARQ protocol, the larger the performance gain between the optimal power assignment scheme and the equal-power assignment scheme.

We also show the average total transmission power based on the approximated optimal power sequence in the six figures. We can see that the average total transmission power based on the approximated power sequence matches tightly with that from the exact optimal power sequence in each case. Note that the exact calculation of the optimal transmission power sequence is based on Theorem 1 and the approximated power sequence comes from Theorem 2.

### 3.3 Differential Amplify-and-Forward Relaying: Performance Analysis and Power Optimization

In this subsection, first we briefly review the DAF relaying scheme. Second, we present our exact outage probability result and the asymptotically tight approximation. Third, the asymptotically optimum power allocation scheme is presented. At the end of this subsection, numerical and simulation results are given and a few conclusions are made.

#### 3.3.1 System Model

We consider a system model which consists of one source, one relay, and one destination using a DAF relaying protocol, as shown in Figure 1. In DAF transmissions, each information symbol  $v_m$  is first differentially encoded at the source as

$$x^\tau = v_m x^{\tau-1} \quad (111)$$

where  $x^\tau$  denoted the signal to be transmitted from the source at time  $\tau$ ,  $v_m = e^{j\phi_m}$ , and  $\{\phi_m\}_0^{M-1}$  is a set of  $M$  information phases [44, 45]. We consider a cooperative strategy with two phases, in which users transmit their information through orthogonal channels by frequency division or time division multiplexing.

In phase 1, the source broadcasts the signal  $x^\tau$  to the destination and the relay. Then the received signals at the destination and at the relay can be modeled, respectively, as

$$y_{s,d}^\tau = \sqrt{P_1} h_{s,d} x^\tau + \eta_{s,d}^\tau \quad (112)$$

$$y_{s,r}^\tau = \sqrt{P_1} h_{s,r} x^\tau + \eta_{s,r}^\tau \quad (113)$$

where  $P_1$  is the transmitted power at the source,  $h_{s,d}$  and  $h_{s,r}$  are the channel coefficients from the source to the destination and to the relay respectively,  $\eta_{s,d}^\tau$  and  $\eta_{s,r}^\tau$  are additive noise, respectively.

In Phase 2, the relay amplifies the received signal and forwards it to the destination with an amplification factor  $\alpha$ . The received signal at the destination can be written as

$$y_{r,d}^\tau = \sqrt{P_2} h_{r,d} \alpha y_{s,r}^\tau + \eta_{r,d}^\tau \quad (114)$$

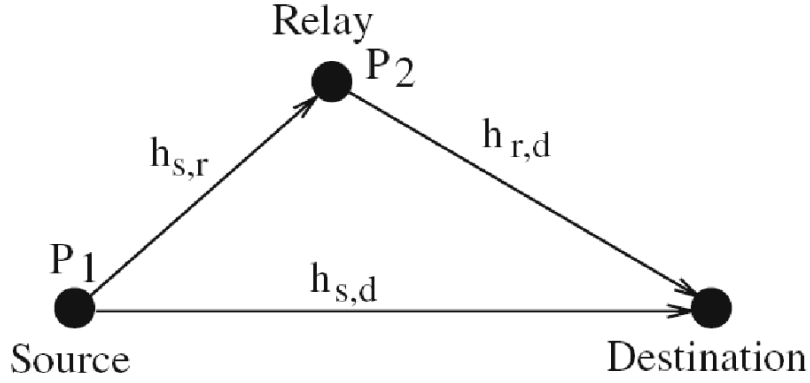


Figure 19: An illustrative cooperative system model.

where  $P_2$  is the transmitted power at the relay,  $h_{r,d}$  is the channel coefficient from the relay to the destination, and  $\eta_{r,d}^\tau$  is additive noise.

The channel coefficients  $h_{s,d}$ ,  $h_{s,r}$  and  $h_{r,d}$  are modeled as independent zero-mean complex Gaussian random variables with variances  $\delta_{s,d}^2$ ,  $\delta_{s,r}^2$  and  $\delta_{r,d}^2$ , respectively. The noise  $\eta_{s,d}^\tau$ ,  $\eta_{s,r}^\tau$  and  $\eta_{r,d}^\tau$  are modeled as independent complex Gaussian random variables with zero mean and variance  $N_0$ . Note that  $|h_{i,j}|^2$ ,  $(i,j) \in \{(s,d), (s,r), (r,d)\}$  are exponential random variables with PDF  $p_{|h_{i,j}|^2}(t) = \frac{1}{\delta_{i,j}^2} \exp(-\frac{t}{\delta_{i,j}^2})$ . To normalize the transmitted power at the relay, we consider

$$\alpha^2 = \frac{1}{P_1 \delta_{s,r}^2 + N_0}. \quad (115)$$

From (113)-(115), the received signal at the destination in Phase 2 can be rewritten as

$$y_{r,d}^\tau = \tilde{h}_{r,d} x^\tau + \tilde{\eta}_{r,d}^\tau \quad (116)$$

where

$$\tilde{h}_{r,d} = \sqrt{\frac{P_1 P_2}{P_1 \delta_{s,r}^2 + N_0}} h_{r,d} h_{s,r} \quad (117)$$

$$\tilde{\eta}_{r,d}^\tau = \sqrt{\frac{P_2}{P_1 \delta_{s,r}^2 + N_0}} h_{r,d} \eta_{s,r}^\tau + \eta_{r,d}^\tau \quad (118)$$

and  $\tilde{\eta}_{r,d}^\tau$  is a zero-mean complex Gaussian random variable with variance  $(\frac{P_2 |h_{r,d}|^2}{P_1 \delta_{s,r}^2 + N_0} + 1) N_0$ .

For differential demodulation at the receiver side, the fading coefficients are assumed to be approximately the same over two consecutive symbol periods. Then, according to (111) and (112), we may rewrite the received signal at the destination in Phase 1 as

$$y_{s,d}^\tau = y_{s,d}^{\tau-1} v_m + n_{s,d}^\tau \quad (119)$$

where  $n_{s,d}^\tau = \eta_{s,d}^\tau - v_m \eta_{s,d}^{\tau-1}$ . Similarly, with (111) and (116), we have

$$y_{r,d}^\tau = y_{r,d}^{\tau-1} v_m + n_{r,d}^\tau \quad (120)$$

where  $n_{r,d}^\tau = \tilde{\eta}_{r,d}^\tau - v_m \tilde{\eta}_{r,d}^{\tau-1}$ . Finally, at the destination, we combine the received signal from the source in Phase 1 and that from the relay in Phase 2 to jointly detect the transmitted information. Based on the maximum ratio combining (MRC) detection [46], the combined output at the destination is

$$y^\tau = a_1 (y_{s,d}^{\tau-1})^* y_{s,d}^\tau + a_2 (y_{r,d}^{\tau-1})^* y_{r,d}^\tau \quad (121)$$

where the coefficients  $a_1$  and  $a_2$  are given by [42, 37]

$$\begin{aligned} a_1 &= \frac{1}{N_0} \\ a_2 &= \frac{P_1 \delta_{s,r}^2 + N_0}{N_0(P_1 \delta_{s,r}^2 + P_2 |h_{r,d}|^2 + N_0)} \end{aligned} \quad (122)$$

which maximize the SNR of the combined output. The transmitted information symbol is detected as follows

$$\hat{v}_m = \arg \max_{m=0,1,\dots,M-1} \text{Re}\{v_m^* y^T\} \quad (123)$$

Note that the optimum combining coefficient in (122) needs the instantaneous amplitude square of the channel  $h_{r,d}$ . In practice, this may be replaced by the statistics of the channel such as the variance of the channel, which results in the following combining coefficients [42]

$$\begin{aligned} \hat{a}_1 &= \frac{1}{N_0} \\ \hat{a}_2 &= \frac{P_1 \delta_{s,r}^2 + N_0}{N_0(P_1 \delta_{s,r}^2 + P_2 \delta_{r,d}^2 + N_0)} \end{aligned} \quad (124)$$

It was observed in [42] that the performances of the two combining coefficients (122) and (124) are close. Since the analysis of the outage probability based on the combining coefficient (124) is intractable which may not provide any insight understanding, we consider in the following the analysis based on the combining coefficient (122). The analysis will provide a benchmark for the performance of the DAF relaying scheme and reveal some insight understanding of the DAF relaying.

### 3.3.2 Outage Analysis for The DAF Relaying

In the DAF relaying scheme, the instantaneous SNR  $\gamma$  of the combining output at the destination based on the MRC combining coefficients (122) can be represented as [42, 37]

$$\gamma = \gamma_1 + \gamma_2, \quad (125)$$

where

$$\gamma_1 = \frac{P_1 |h_{s,d}|^2}{N_0}, \quad (126)$$

$$\gamma_2 = \frac{P_1 P_2 |h_{s,r}|^2 |h_{r,d}|^2}{N_0(P_1 \delta_{s,r}^2 + P_2 |h_{r,d}|^2 + N_0)}. \quad (127)$$

An outage is declared if the instantaneous SNR  $\gamma$  falls below a certain specified threshold  $\gamma_{th}$ , so the outage probability is  $P_{out} = Pr\{0 \leq \gamma \leq \gamma_{th}\}$  [47]. If we denote the CDF of the SNR  $\gamma$  as  $F_\gamma(x)$ , then the outage probability of the DAF relaying is  $P_{out} = F_\gamma(\gamma_{th})$ .

We develop the CDF of the SNR  $\gamma$  as follows. Note that  $\gamma_1$  and  $\gamma_2$  are two independent random variables. Hence the CDF of  $\gamma$  is

$$\begin{aligned} F_\gamma(x) &= Pr\{0 \leq \gamma_1 + \gamma_2 \leq x\} \\ &= \int_0^x Pr\{0 \leq \gamma_2 \leq x - \gamma_1\} p_{\gamma_1}(\gamma_1) d\gamma_1. \end{aligned} \quad (128)$$

Let  $\beta_{s,d} = \frac{N_0}{P_1 \delta_{s,d}^2}$ ,  $\beta_{s,r} = \frac{N_0}{P_1 \delta_{s,r}^2}$  and  $\beta_{r,d} = \frac{N_0}{P_2 \delta_{r,d}^2}$ , then  $p_{\gamma_1}(\gamma_1)$ , the PDF of  $\gamma_1$ , in (128) is given by  $p_{\gamma_1}(\gamma_1) = \beta_{s,d} e^{-\beta_{s,d} \gamma_1}$ . Furthermore, if we denote  $\gamma_{s,r} = P_1 |h_{s,r}|^2 / N_0$  and  $\gamma_{r,d} = P_2 |h_{r,d}|^2 / N_0$ , then the CDF of  $\gamma_2$  can

be determined as

$$\begin{aligned}
F_{\gamma_2}(x) &= Pr\left\{0 \leq \frac{\gamma_{s,r}\gamma_{r,d}}{1 + 1/\beta_{s,r} + \gamma_{r,d}} \leq x\right\} \\
&= \int_0^\infty Pr\left\{0 \leq \gamma_{s,r} \leq \frac{(1 + 1/\beta_{s,r})x}{\gamma_{r,d}} + x\right\} p_{\gamma_{r,d}}(\gamma_{r,d}) d\gamma_{r,d} \\
&= \int_0^\infty \left(1 - e^{-\beta_{s,r}\left(\frac{(1+1/\beta_{s,r})x}{\gamma_{r,d}} + x\right)}\right) \beta_{r,d} e^{-\beta_{r,d}\gamma_{r,d}} d\gamma_{r,d} \\
&= 1 - \beta_{r,d} e^{-\beta_{s,r}x} \int_0^\infty e^{-\beta_{r,d}\gamma_{r,d} - \frac{(1+\beta_{s,r})x}{\gamma_{r,d}}} d\gamma_{r,d}. \tag{129}
\end{aligned}$$

Substitute (129) with argument  $x - \gamma_1$  into (128), we have

$$\begin{aligned}
F_\gamma(x) &= \int_0^x \beta_{s,d} e^{-\beta_{s,d}\gamma_1} d\gamma_1 \\
&\quad - \int_0^x \beta_{r,d} e^{-\beta_{s,r}(x-\gamma_1)} \left(\int_0^\infty e^{-\beta_{r,d}t - \frac{(1+\beta_{s,r})(x-\gamma_1)}{t}} dt\right) \beta_{s,d} e^{-\beta_{s,d}\gamma_1} d\gamma_1. \tag{130}
\end{aligned}$$

In (130), the first part is  $\int_0^x \beta_{s,d} e^{-\beta_{s,d}\gamma_1} d\gamma_1 = 1 - e^{-\beta_{s,d}x}$ . The second part can be further calculated by switching the integration order, i.e. integrating in terms of the variable  $\gamma_1$  first and then for the variable  $t$ , as follows:

$$\begin{aligned}
&\int_0^\infty \int_0^x \beta_{r,d} \beta_{s,d} e^{-\beta_{s,r}(x-\gamma_1) - \beta_{r,d}t - \frac{(1+\beta_{s,r})(x-\gamma_1)}{t} - \beta_{s,d}\gamma_1} d\gamma_1 dt \\
&= \int_0^\infty \frac{\beta_{r,d} \beta_{s,d} e^{-\beta_{r,d}t}}{\beta_{s,d} - \beta_{s,r} - (1 + \beta_{s,r})/t} \left(e^{-\left(\frac{1+\beta_{s,r}}{t} + \beta_{s,r}\right)x} - e^{-\beta_{s,d}x}\right) dt.
\end{aligned}$$

By combining the above two parts, we obtain the CDF of the SNR  $\gamma$ . Therefore, the outage probability of the DAF relaying can be specifically given by

$$\begin{aligned}
P_{out}(\gamma_{th}) &= 1 - e^{-\beta_{s,d}\gamma_{th}} - \int_0^\infty \frac{\beta_{r,d} \beta_{s,d} e^{-\beta_{r,d}t}}{\beta_{s,d} - \beta_{s,r} - \frac{1+\beta_{s,r}}{t}} \\
&\quad \times \left(e^{-\left(\frac{1+\beta_{s,r}}{t} + \beta_{s,r}\right)\gamma_{th}} - e^{-\beta_{s,d}\gamma_{th}}\right) dt. \tag{131}
\end{aligned}$$

Comparing to the result in [43], in which the outage probability was presented by a triple integral, our result involves only a single integral, which can be easier to calculate numerically.

For a special case of  $\beta_{s,d} = \beta_{s,r}$ , i.e. the source-destination and source-relay links have the same channel variance, the outage probability in (131) can be simplified as

$$\begin{aligned}
P_{out}(\gamma_{th}) &= 1 - e^{-\beta_{s,r}\gamma_{th}} \\
&\quad - \frac{\beta_{s,r}\beta_{r,d}}{1 + \beta_{s,r}} e^{-\beta_{s,r}\gamma_{th}} \int_0^\infty t e^{-\beta_{r,d}t} \left(1 - e^{-\frac{(1+\beta_{s,r})\gamma_{th}}{t}}\right) dt, \tag{132}
\end{aligned}$$

which can be further represented as

$$\begin{aligned}
P_{out}(\gamma_{th}) &= 1 - e^{-\beta_{s,r}\gamma_{th}} - e^{-\beta_{s,r}\gamma_{th}} \frac{\beta_{s,r}}{(1 + \beta_{s,r})\beta_{r,d}} \\
&\quad + e^{-\beta_{s,r}\gamma_{th}} 2\beta_{s,r}\gamma_{th} K_2(2\sqrt{(1 + \beta_{s,r})\beta_{r,d}\gamma_{th}}), \tag{133}
\end{aligned}$$

where  $K_2(\cdot)$  is the 2<sup>nd</sup> order modified Bessel function of the second kind [48, (3.478.4)].

Although the exact expression in (131) is much simpler than the result in [43], it still involves an integral. To get further insight understanding of the DAF relaying scheme, we try to approximate the outage probability in the following. With the aid of an approximation of the modified Bessel function, we can obtain an asymptotically tight approximation for the outage probability at high SNR. We have the following result.

**Theorem 3** If all channel links  $h_{s,d}$ ,  $h_{s,r}$  and  $h_{r,d}$  are available, i.e.  $\delta_{s,d} \neq 0$ ,  $\delta_{s,r} \neq 0$ , and  $\delta_{r,d} \neq 0$ , then for sufficiently high SNR, the outage probability  $P_{out}$  of the DAF relaying can be approximated as

$$P_{out} \approx \frac{\gamma_{th}^2 N_0^2}{2P_1 \delta_{s,d}^2} \left[ \frac{1}{P_1 \delta_{s,r}^2} + \frac{\frac{1}{2} - \ln\left(\frac{\gamma_{th} N_0}{P_2 \delta_{r,d}^2}\right)}{P_2 \delta_{r,d}^2} \right]. \quad (134)$$

**Proof:** First, we try to approximate the CDF of  $\gamma_2$  in (129) as follows. Denote  $t = \beta_{r,d} \gamma_{r,d}$  and  $y = (1 + \beta_{s,r}) \beta_{r,d} x$ , then the CDF of  $\gamma_2$  (129) can be rewritten as

$$1 - e^{-\frac{\beta_{s,r} y}{(1 + \beta_{s,r}) \beta_{r,d}}} \int_0^\infty e^{-t - \frac{y}{t}} dt.$$

For simplicity, denote  $g(y) = \int_0^\infty e^{-t - \frac{y}{t}} dt$ , then

$$g'(y) = - \int_0^\infty \frac{e^{-t - \frac{y}{t}}}{t} dt = -2K_0(2\sqrt{y}),$$

where  $K_0(\cdot)$  is the zero-order modified Bessel function of the second kind. Note that for sufficiently high SNR,  $y = (1 + \beta_{s,r}) \beta_{r,d} x$  is small, which may go to zero. For small  $y$ , there exists a positive value  $y_0$  ( $0 < y_0 < y$ ) such that

$$g(y) \approx g(y_0) + g'(y_0)y,$$

where for small  $y_0$ ,  $g(y_0)$  and  $g'(y_0)$  can be approximated as [49]

$$g(y_0) \approx 1, \\ g'(y_0) = -2K_0(2\sqrt{y_0}) \approx \ln(y_0).$$

Thus, for sufficiently small variable  $y$ , we have

$$g(y) \approx 1 + \ln(y_0)y \approx 1 + \ln(y)y. \quad (135)$$

With the approximation in (135) and  $e^{-\beta_{s,r}x} \approx 1 - \beta_{s,r}x$ , we have an approximation for the CDF of  $\gamma_2$  in (129) as follows:

$$F_{\gamma_2}(x) \approx \beta_{s,r}x - \beta_{r,d}x \ln(\beta_{r,d}x). \quad (136)$$

Substituting the approximation (136) into (128), and with  $e^{-\beta_{s,d}\gamma_1} \approx 1 - \beta_{s,d}\gamma_1$  for sufficiently small argument  $\beta_{s,d}\gamma_1$ , the CDF of  $\gamma$ ,  $F_\gamma(x)$ , can be approximated as

$$F_\gamma(x) \approx \int_0^x [\beta_{s,r}(x - \gamma_1) - \beta_{r,d}(x - \gamma_1) \ln(\beta_{r,d}(x - \gamma_1))] \\ \times [\beta_{s,d}(1 - \beta_{s,d}\gamma_1)] d\gamma_1 \\ \triangleq I_1 + I_2 + I_3 + I_4, \quad (137)$$

where

$$I_1 = \beta_{s,d} \beta_{s,r} \int_0^x (x - \gamma_1) d\gamma_1 = \frac{1}{2} \beta_{s,d} \beta_{s,r} x^2, \\ I_2 = -\beta_{s,d}^2 \beta_{s,r} \int_0^x (x - \gamma_1) \gamma_1 d\gamma_1 = -\frac{1}{6} \beta_{s,d}^2 \beta_{s,r} x^3, \\ I_3 = -\beta_{s,d} \beta_{r,d} \int_0^x (x - \gamma_1) \ln(\beta_{r,d}(x - \gamma_1)) d\gamma_1 \\ = \frac{1}{4} \beta_{s,d} \beta_{r,d} x^2 - \frac{1}{2} \beta_{s,d} \beta_{r,d} x^2 \ln(\beta_{r,d} x), \\ I_4 = \beta_{s,d}^2 \beta_{r,d} \int_0^x (x - \gamma_1) \gamma_1 \ln(\beta_{r,d}(x - \gamma_1)) d\gamma_1 \\ = -\frac{5}{36} \beta_{s,d}^2 \beta_{r,d} x^3 + \frac{1}{6} \beta_{s,d}^2 \beta_{r,d} x^3 \ln(\beta_{r,d} x). \quad (138)$$

Substituting  $I_1, I_2, I_3$  and  $I_4$  into (137), we have

$$F_\gamma(x) = \frac{1}{2}\beta_{s,d}\beta_{s,r}x^2 + \frac{1}{4}\beta_{s,d}\beta_{r,d}x^2 - \frac{1}{2}\beta_{s,d}\beta_{r,d}x^2 \ln(\beta_{r,d}x) - \frac{1}{6}\beta_{s,d}^2\beta_{s,r}x^3 - \frac{5}{36}\beta_{s,d}^2\beta_{r,d}x^3 + \frac{1}{6}\beta_{s,d}^2\beta_{r,d}x^3 \ln(\beta_{r,d}x). \quad (139)$$

We observe that when  $\beta_{s,d}, \beta_{s,r}$  and  $\beta_{r,d}$  go to zero, the terms involving  $\beta_{s,d}^2\beta_{s,r}$  and  $\beta_{s,d}^2\beta_{r,d}$  go to zero faster than the terms with  $\beta_{s,d}\beta_{s,r}$  and  $\beta_{s,d}\beta_{r,d}$ . As a result, for high SNR, the CDF of  $\gamma$  can be approximated as

$$F_\gamma(x) \approx \frac{1}{2}\beta_{s,d}\beta_{s,r}x^2 + \frac{1}{4}\beta_{s,d}\beta_{r,d}x^2 - \frac{1}{2}\beta_{s,d}\beta_{r,d}x^2 \ln(\beta_{r,d}x), \quad (140)$$

which implies the approximation of the outage probability in the theorem.

### 3.3.3 Optimum Power Assignment

Based on the closed-form tight approximation of the outage probability in (134), we can determine an asymptotically optimum power allocation scheme for the DAF cooperation scheme. For a given total transmitted power budget of  $P_1 + P_2 = P$ , we try to minimize the outage approximation to find an optimum power allocation ratio.

Let  $P_1 = rP$ ,  $P_2 = (1-r)P$ , and denote  $B = \frac{1}{2} - \ln\left(\frac{\gamma_{th}N_0}{P\delta_{r,d}^2}\right)$ , then the outage approximation (134) can be rewritten as

$$P_{out} = \frac{\gamma_{th}^2 N_0^2}{2P^2 \delta_{s,d}^2} \left( \frac{1}{r^2 \delta_{s,r}^2} + \frac{B + \ln(1-r)}{r(1-r)\delta_{r,d}^2} \right). \quad (141)$$

To find an optimum power ratio  $r$ , it is equivalent to minimize

$$f(r) \triangleq \frac{1}{r^2 \delta_{s,r}^2} + \frac{B + \ln(1-r)}{r(1-r)\delta_{r,d}^2} \quad (142)$$

By taking derivative of (142) with respect to  $r$ , we have

$$\begin{aligned} \frac{\partial f(r)}{\partial r} &= -\frac{2}{r^3 \delta_{s,r}^2} - \frac{B(1-2r)}{\delta_{r,d}^2 r^2 (1-r)^2} \\ &\quad - \frac{1}{\delta_{r,d}^2 r (1-r)^2} - \frac{\ln(1-r)(1-2r)}{\delta_{r,d}^2 r^2 (1-r)^2}. \end{aligned} \quad (143)$$

Set the derivative (143) equal to 0, we have

$$\begin{aligned} 2(1-r)^2 + \frac{\delta_{s,r}^2 B}{\delta_{r,d}^2} (1-2r)r \\ + \frac{\delta_{s,r}^2}{\delta_{r,d}^2} r^2 + \frac{\delta_{s,r}^2}{\delta_{r,d}^2} \ln(1-r)(1-2r)r = 0. \end{aligned} \quad (144)$$

For simplicity, denote  $u(r) = \ln(1-r)(1-2r)r$ , then  $u(\frac{1}{2}) = 0$ ,  $u'(\frac{1}{2}) = \ln(2)$  and  $u''(\frac{1}{2}) = 4\ln(2) + 4$ . Therefore, the first three terms of the Taylor expansion to approximate  $u(r)$  are

$$\begin{aligned} \ln(1-r)(1-2r)r &\approx u\left(\frac{1}{2}\right) + u'\left(\frac{1}{2}\right)\left(r - \frac{1}{2}\right) + \frac{1}{2}u''\left(\frac{1}{2}\right)\left(r - \frac{1}{2}\right)^2 \\ &= (2\ln(2) + 2)r^2 - (\ln(2) + 2)r + \frac{1}{2}. \end{aligned} \quad (145)$$

By plugging (145) into (144), we obtain the following equation

$$C_2 r^2 + C_1 r + C_0 = 0, \quad (146)$$

in which  $C_0 = \frac{\delta_{s,r}^2}{2\delta_{r,d}^2} + 2$ ,  $C_1 = \frac{\delta_{s,r}^2}{\delta_{r,d}^2}(-\ln(2) - 2 + B) - 4$ , and  $C_2 = \frac{\delta_{s,r}^2}{\delta_{r,d}^2}(2\ln(2) + 3 - 2B) + 2$ . Solving the equation, we obtain the following power allocation result.

Table 3: Comparing the optimum power ratio by exhaustive search and approximation, assuming  $\{\delta_{s,d}^2, \delta_{s,r}^2, \delta_{r,d}^2\} = \{1, 1, 1\}$

P in dB	$\{\delta_{s,d}^2, \delta_{s,r}^2, \delta_{r,d}^2\} = \{1, 1, 1\}$	
	Exhaustive search $r$	Approximated $r$
25	0.6746	0.6662
30	0.6296	0.6272
35	0.6052	0.6041
40	0.5891	0.5886

Table 4: Comparing the optimum power ratio by exhaustive search and approximation, assuming  $\{\delta_{s,d}^2, \delta_{s,r}^2, \delta_{r,d}^2\} = \{1, 1, 100\}$

P in dB	$\{\delta_{s,d}^2, \delta_{s,r}^2, \delta_{r,d}^2\} = \{1, 1, 100\}$	
	Exhaustive search $r$	Approximated $r$
25	0.8690	0.8607
30	0.8580	0.8513
35	0.8485	0.8429
40	0.8401	0.8354

**Theorem 4** *If all channel links  $h_{s,d}$ ,  $h_{s,r}$  and  $h_{r,d}$  are available, i.e.  $\delta_{s,d} \neq 0$ ,  $\delta_{s,r} \neq 0$ , and  $\delta_{r,d} \neq 0$ , then for sufficiently high SNR, the optimum power allocation ratio  $r = P_1/P$  for the DAF relaying is*

$$r \approx \frac{(C_{r,d}-2)\delta_{s,r}^2 - 4\delta_{r,d}^2 + \sqrt{(C_{r,d}^2-2)\delta_{s,r}^4 + (8C_{r,d}-12)\delta_{s,r}^2\delta_{r,d}^2}}{(4C_{r,d}-6)\delta_{s,r}^2 - 4\delta_{r,d}^2} \quad (147)$$

where  $C_{r,d} = -\ln\left(\frac{2N_0\gamma_{th}}{P\delta_{r,d}^2}\right) + \frac{1}{2}$ . Furthermore, when SNR goes to infinity,  $C_{r,d}$  is sufficiently large and then the ratio (147) can be further approximated as:

$$r \approx \frac{1 + \sqrt{1 + \frac{8\delta_{r,d}^2}{\delta_{s,r}^2 C_{r,d}}}}{4} \rightarrow \frac{1}{2}. \quad (148)$$

We list in Tables 3 and 4 the comparisons of the optimum power ratio  $r$  based on the closed-form approximation presented in Theorem 4 and the ratio obtained by exhaustive search based on the exact expression in (142). The comparison results are shown for various total transmitted power budget  $P$ , and for variances  $\{\delta_{s,d}^2, \delta_{s,r}^2, \delta_{r,d}^2\} = \{1, 1, 1\}$  and  $\{1, 1, 100\}$ , respectively. From the tables, we can see that the power ratios calculated based on Theorem 4 are very close to those by exhaustive search.

From Theorem 4, we observe that for high SNR, the asymptotically optimum power ratio does not depend on the source-destination link, and it depends only on the variances of the source-relay and relay-destination links. Moreover, as the total transmitted power  $P$  goes to infinity, the optimum ratio  $r$  goes to 0.5, which implies that an equal power allocation scheme ( $P_1 = P_2 = P/2$ ) is optimum in this case.

### 3.3.4 Simulation Results and Discussions

To verify our analytical results, we carried out some computer simulations. In our simulations, we assume that the variance of the noise is 1 (i.e.  $N_0 = 1$ ), and the outage SNR threshold is  $\gamma_{th} = 10$  dB.

Figures 20-22 depict the simulated outage probability performance curves, the outage probability approximation based on Theorem 1, and numerical calculation based on the close-form expression in (131) for three

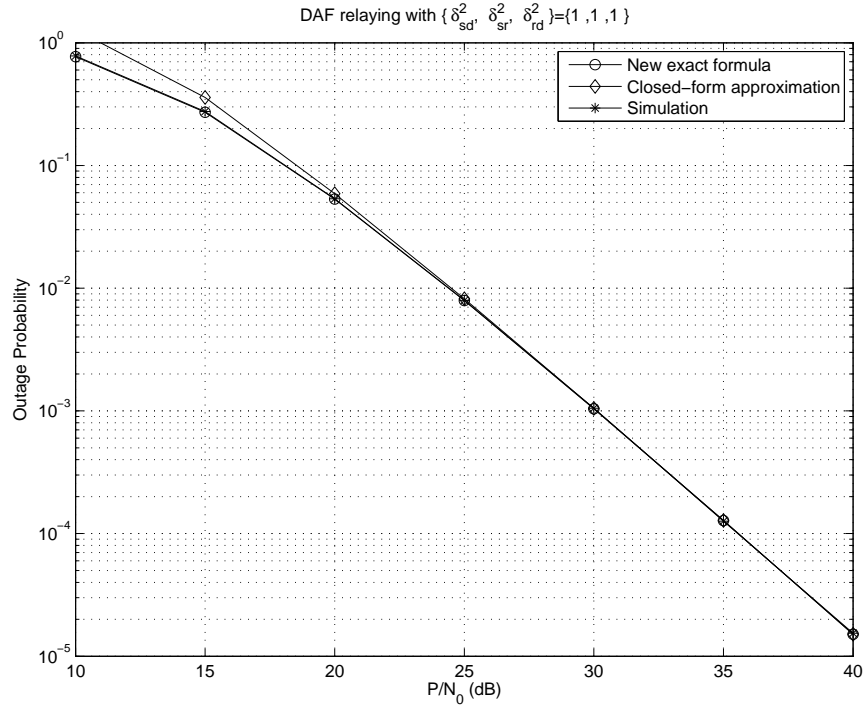


Figure 20: Outage probability of the DAF relaying with variances  $\{\delta_{s,d}^2, \delta_{s,r}^2, \delta_{r,d}^2\} = \{1, 1, 1\}$ .

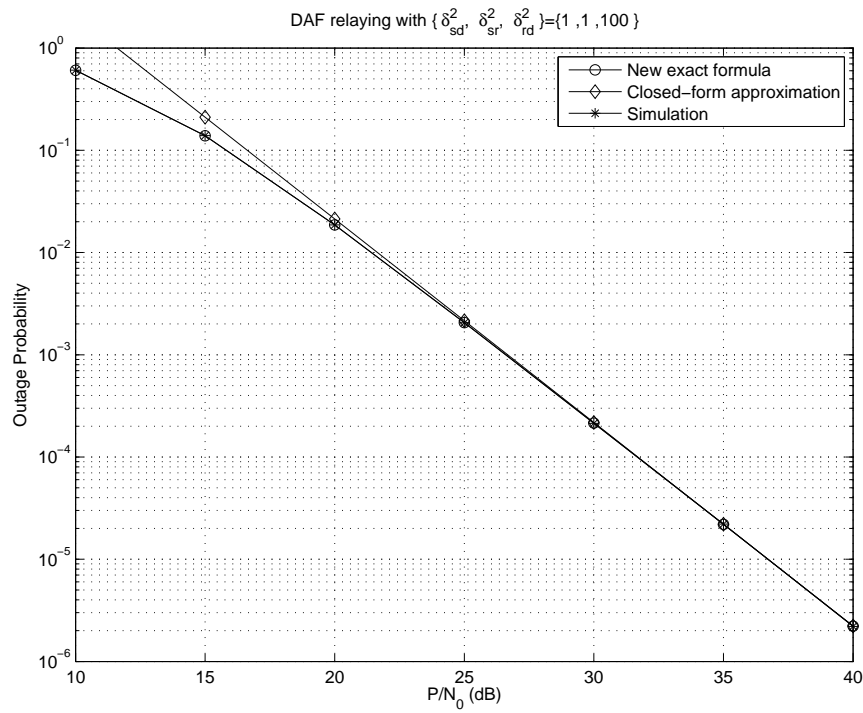


Figure 21: Outage probability of the DAF relaying with variances  $\{\delta_{s,d}^2, \delta_{s,r}^2, \delta_{r,d}^2\} = \{1, 1, 100\}$ .

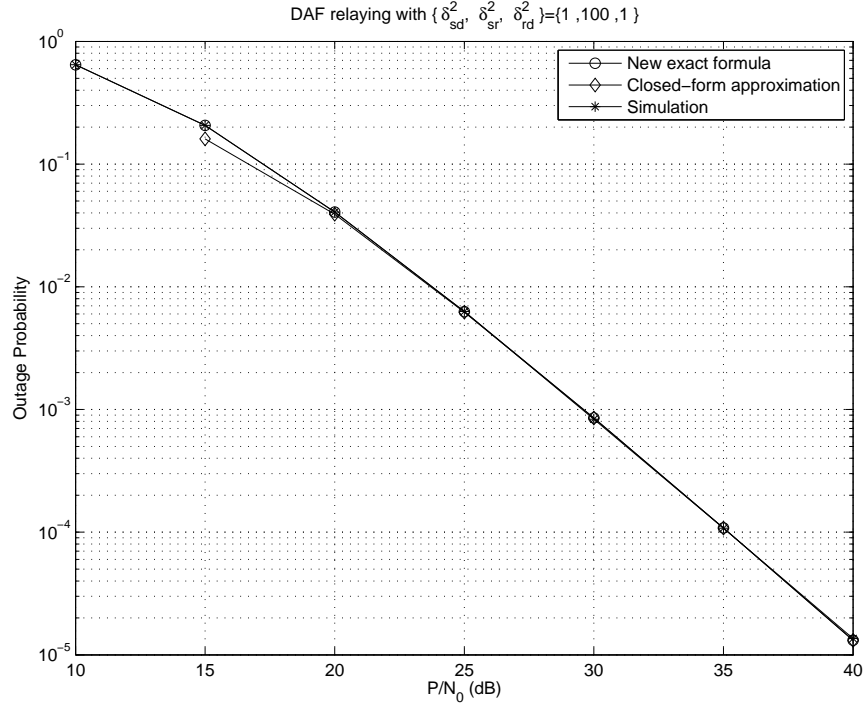


Figure 22: Outage probability of the DAF relaying with variances  $\{\delta_{s,d}^2, \delta_{s,r}^2, \delta_{r,d}^2\} = \{1, 100, 1\}$ .

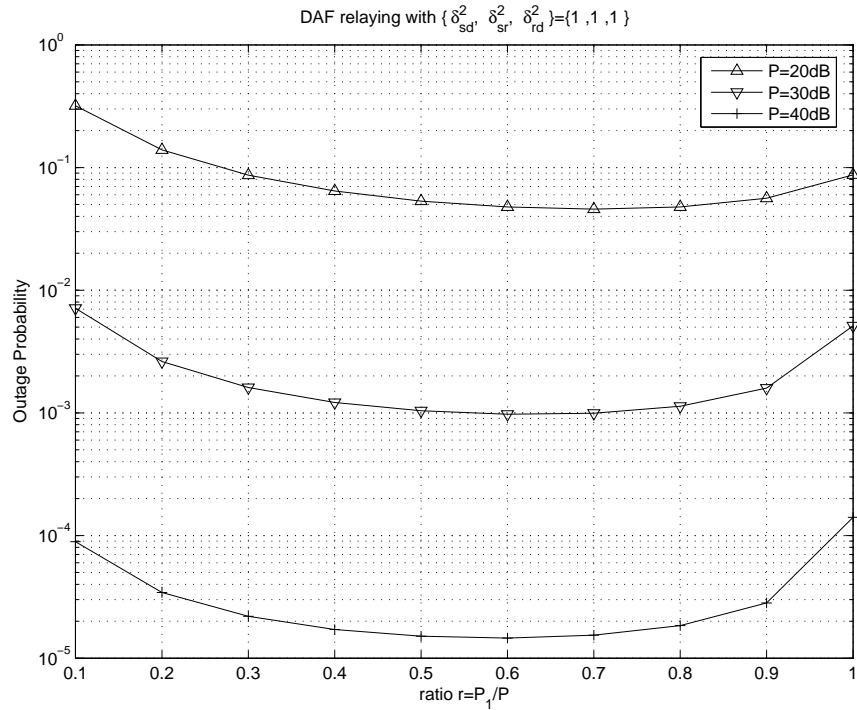


Figure 23: Numerical search of the optimum power ratio  $r$  for the DAF relaying with variances  $\{\delta_{s,d}^2, \delta_{s,r}^2, \delta_{r,d}^2\} = \{1, 1, 1\}$ , and different transmit power  $P=20\text{dB}$ ,  $30\text{dB}$  and  $40\text{dB}$ .

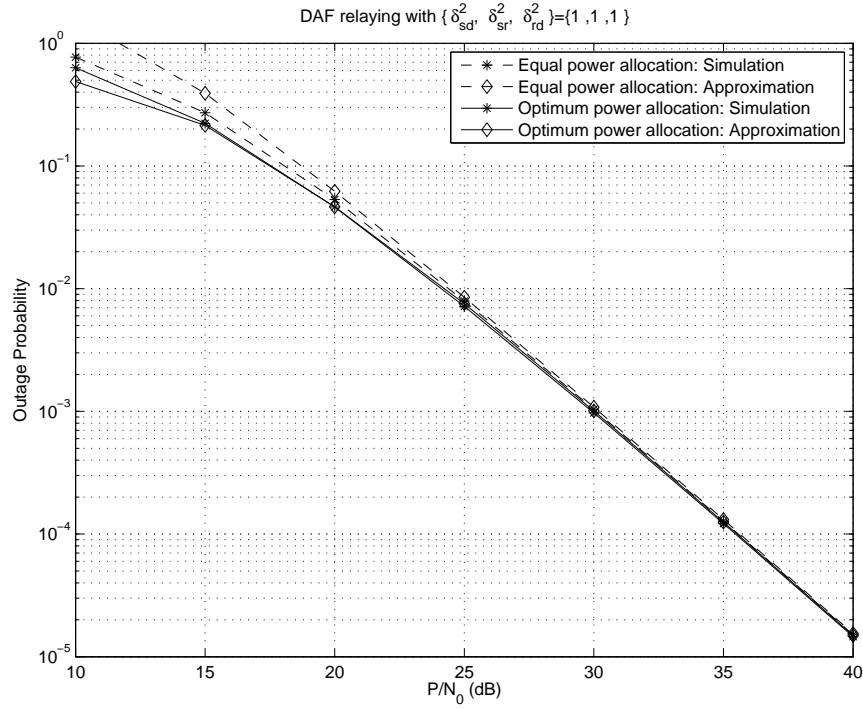


Figure 24: Performance comparison of the DAF relaying with the equal and the optimum power allocation, with variances  $\{\delta_{s,d}^2, \delta_{s,r}^2, \delta_{r,d}^2\} = \{1, 1, 1\}$ .

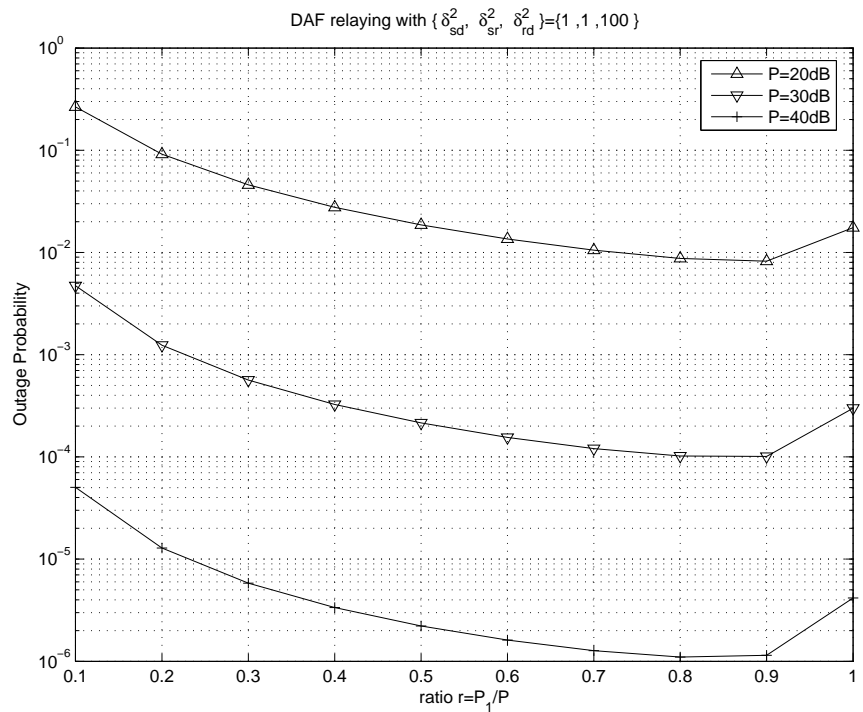


Figure 25: Numerical search of the optimum power ratio  $r$  for the DAF relaying with variances  $\{\delta_{s,d}^2, \delta_{s,r}^2, \delta_{r,d}^2\} = \{1, 1, 100\}$ , and different transmit power  $P=20\text{dB}$ ,  $30\text{dB}$  and  $40\text{dB}$ .

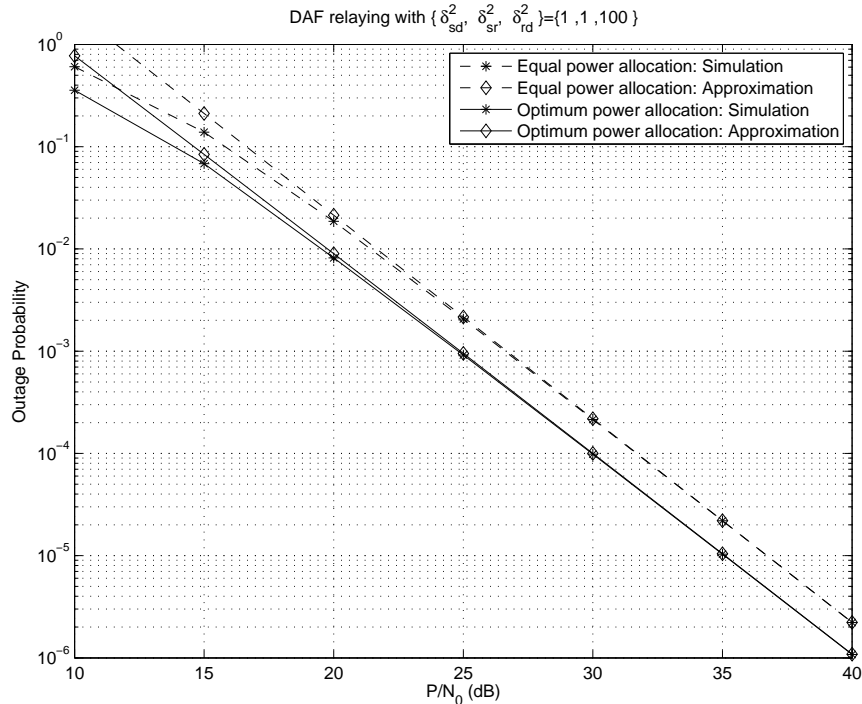


Figure 26: Performance comparison of the DAF relaying with the equal and the optimum power allocation, with variances  $\{\delta_{s,d}^2, \delta_{s,r}^2, \delta_{r,d}^2\} = \{1, 1, 100\}$ .

scenarios:  $\{\delta_{s,d}^2, \delta_{s,r}^2, \delta_{r,d}^2\} = \{1, 1, 1\}$ ,  $\{\delta_{s,d}^2, \delta_{s,r}^2, \delta_{r,d}^2\} = \{1, 1, 100\}$ , and  $\{\delta_{s,d}^2, \delta_{s,r}^2, \delta_{r,d}^2\} = \{1, 100, 1\}$ , respectively. We equally allocated power for the source and the relay in the three scenarios. We can see that the numerical results based on the exact expression in (131) matches with the simulation results. The outage probability approximation is loose at low SNR and it merges with the simulation curve around  $10^{-2}$  which is tight in all the three scenarios.

Figure 23 shows the outage probability performance versus power ratio  $r = P_1/P$  for different total transmitted power budgets, in which the channel variances are  $\{\delta_{s,d}^2, \delta_{s,r}^2, \delta_{r,d}^2\} = \{1, 1, 1\}$ . In this case, the optimum power ratio is close to  $1/2$ . The performance of the optimum power allocation scheme is close to that of the equal power allocation scheme in this case, which is shown in Figure 24.

Figure 25 shows the outage probability performance versus power ratio  $r = P_1/P$  for the case of  $\{\delta_{s,d}^2, \delta_{s,r}^2, \delta_{r,d}^2\} = \{1, 1, 100\}$ . In this case, the optimum power ratio is around 0.85. Simulation results in Figure 26 show that the performance of the optimum power allocation scheme is about 2 dB better than that of the equal power allocation scheme in this case.

### 3.4 Joint Power Optimization for Multi-Source and Multi-Destination Relay Network

In this subsection, first we introduce briefly the system model of a multi-source multi-destination relay network where transmissions occur over non-orthogonal, in general, channels. Second, we determine the maximum ratio combining of the received signals at each intended destination and exploit the resulting SINR. Third, we determine the optimum power assignment for the sources and the relay that minimizes the total power consumption under the condition that the SINR requirement of each source-destination pair is satisfied. Fourth, we determine the optimum power assignment that maximizes the minimum SINR among all source-destination pairs subject to any given total power budget. Finally, numerical studies are provided and some discussion are made at the end.

The following notation is used throughout this subsection. Bold letters in uppercase and lowercase denote matrices and vectors, respectively.  $(\cdot)^*$ ,  $(\cdot)^T$  and  $(\cdot)^H$  represent the conjugate, the transpose and the Hermitian transpose operation, respectively.  $|\cdot|$  and  $\|\cdot\|$  represent Euclidean norm of a complex number and a vector,

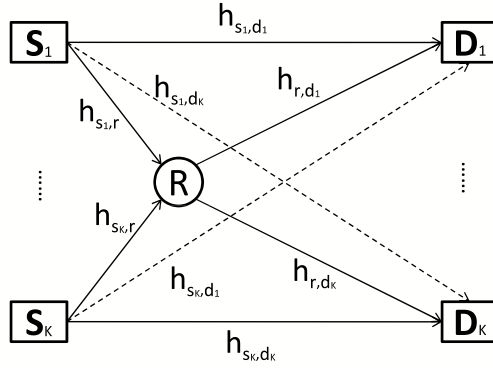


Figure 27: Multi-source multi-destination relay network.

respectively.  $\mathbf{I}_L$  is an  $L \times L$  identity matrix.  $\text{diag}(h_1, h_2, \dots, h_L)$  is an  $L \times L$  diagonal matrix with diagonal elements  $h_1, h_2, \dots, h_L$ .  $\mathbf{A}_{\bar{k}}$  denotes a sub-matrix of  $\mathbf{A}$  obtained by deleting the  $k^{\text{th}}$  column and  $k^{\text{th}}$  row of  $\mathbf{A}$ . If  $\mathbf{a}_k$  represents the  $k^{\text{th}}$  column of the matrix  $\mathbf{A}$ , then  $\mathbf{a}_{\bar{k}}$  denotes the vector obtained after removing the  $k^{\text{th}}$  entry from  $\mathbf{a}_k$ .

### 3.4.1 System Model

For illustration purposes and simplicity in presentation, we consider a single relay code division multiplexing system with  $K$  sources and  $K$  destinations as shown in Fig. 27, where transmissions occur over non-orthogonal, in general, channels. Our developments can be generalized to multiple-relay systems and other multiplexing schemes in frequency and/or time. Let  $S_k$  denote the  $k^{\text{th}}$  source and  $D_k$  the corresponding destination,  $k = 1, 2, \dots, K$ , and let  $R$  denote the relay. The relay forwards simultaneously the signals received from all sources. Let  $b_k$  denote the transmitted information symbol of the source  $S_k$  with unity energy, i.e.  $E\{|b_k|^2\} = 1, \forall k$ . The signal sent by the source  $S_k$  can be expressed as

$$\mathbf{s}_k = \mathbf{c}_k b_k,$$

where  $\mathbf{c}_k = (c_k^{(1)}, c_k^{(2)}, \dots, c_k^{(L)})^T$  is the code/signature of the source  $S_k$ , which is a unit-energy column vector with length  $L$ . The codes/channels of different sources are, in general, correlated. Let  $\rho_{kj} \triangleq \mathbf{c}_k^T \mathbf{c}_j$  denote the cross-correlation between codes/channels  $k$  and  $j$ , where  $\rho_{kj} \in [0, 1)$  for  $k \neq j$ , and  $\rho_{kk} = 1$ . Let  $\mathbf{R} \triangleq (\rho_{kj})$  denote the  $K \times K$  cross-correlation matrix, i.e.

$$\mathbf{R} = (\mathbf{c}_1, \mathbf{c}_2, \dots, \mathbf{c}_K)^T (\mathbf{c}_1, \mathbf{c}_2, \dots, \mathbf{c}_K). \quad (149)$$

We consider the following two-phase amplify-and-forward relay strategy with  $L$  time slots in each phase. In Phase 1, each source  $S_k$  transmits the signal  $\mathbf{s}_k$  with transmitted power  $P_k$ . Then, the received signals at the destination  $D_k$  and at the relay  $R$  during the  $i$ -th ( $1 \leq i \leq L$ ) time slot can be modeled, respectively, as

$$y_{s,d_k}^{(i)} = \sum_{l=1}^K \sqrt{P_l} h_{s_l,d_k}^{(i)} c_l^{(i)} b_l + n_{s,d_k}^{(i)}, \quad 1 \leq i \leq L, \quad (150)$$

$$y_{s,r}^{(i)} = \sum_{l=1}^K \sqrt{P_l} h_{s_l,r}^{(i)} c_l^{(i)} b_l + n_{s,r}^{(i)}, \quad 1 \leq i \leq L. \quad (151)$$

In Phase 2, the relay amplifies the received signals and forwards them to the destination with an amplification factor  $\alpha$  and transmission power  $P_r$ . The received signal at the destination  $D_k$  during the  $i$ -th ( $1 \leq i \leq L$ ) time slot can be written as

$$y_{r,d_k}^{(i)} = \sqrt{P_r} h_{r,d_k}^{(i)} \alpha y_{s,r}^{(i)} + n_{r,d_k}^{(i)}, \quad i = 1, 2, \dots, L. \quad (152)$$

In (150)-(152),  $h_{s_l, d_k}^{(i)}$ ,  $h_{s_l, r}^{(i)}$ , and  $h_{r, d_k}^{(i)}$ , ( $l, k = 1, \dots, K$ ) are the coefficients of the channels between the source  $S_l$  and the destination  $D_k$ , between the source  $S_l$  and the relay  $R$ , and between the relay  $R$  and the destination  $D_k$ , respectively, during the  $i$ -th ( $1 \leq i \leq L$ ) time slot.  $n_{s, d_k}^{(i)}$  and  $n_{r, d_k}^{(i)}$  represent noise at the destination  $D_k$  during the  $i$ -th time slot of Phase 1 and Phase 2, correspondingly, while  $n_{s, r}^{(i)}$  represents noise at the relay  $R$  during the  $i$ -th time slot. The channels  $h_{s_l, d_k}^{(i)}$ ,  $h_{s_l, r}^{(i)}$ , and  $h_{r, d_k}^{(i)}$  are assumed to be independent Gaussian random variables with zero-mean and variances  $\sigma_{s_l, d_k}^2$ ,  $\sigma_{s_l, r}^2$ , and  $\sigma_{r, d_k}^2$ , respectively. All noise terms are assumed to be independent Gaussian random variables with zero-mean and variances  $\sigma^2$ . Without loss of generality, we assume  $\sigma^2 = 1$ .

The channel coefficients in matrix format can be given as  $\mathbf{H}_{s_l, d_k} = \text{diag}(h_{s_l, d_k}^{(1)}, \dots, h_{s_l, d_k}^{(L)})$ ,  $\mathbf{H}_{s_l, r} = \text{diag}(h_{s_l, r}^{(1)}, \dots, h_{s_l, r}^{(L)})$  and  $\mathbf{H}_{r, d_k} = \text{diag}(h_{r, d_k}^{(1)}, \dots, h_{r, d_k}^{(L)})$ . Then, the received signals can be expressed as follows:

$$\mathbf{y}_{s, d_k} = \sum_{l=1}^K \sqrt{P_l} \mathbf{H}_{s_l, d_k} \mathbf{c}_l b_l + \mathbf{n}_{s, d_k}, \quad (153)$$

$$\mathbf{y}_{s, r} = \sum_{l=1}^K \sqrt{P_l} \mathbf{H}_{s_l, r} \mathbf{c}_l b_l + \mathbf{n}_{s, r}, \quad (154)$$

$$\mathbf{y}_{r, d_k} = \sqrt{P_r} \alpha \mathbf{H}_{r, d_k} \mathbf{y}_{s, r} + \mathbf{n}_{r, d_k}, \quad (155)$$

where  $\mathbf{y}_{s, d_k} = (y_{s, d_k}^{(1)}, y_{s, d_k}^{(2)}, \dots, y_{s, d_k}^{(L)})^T$ ,  $\mathbf{y}_{s, r} = (y_{s, r}^{(1)}, y_{s, r}^{(2)}, \dots, y_{s, r}^{(L)})^T$  and  $\mathbf{y}_{r, d_k} = (y_{r, d_k}^{(1)}, y_{r, d_k}^{(2)}, \dots, y_{r, d_k}^{(L)})^T$ . In (153)–(155), the noise vectors  $\mathbf{n}_{s, d_k}$ ,  $\mathbf{n}_{s, r}$  and  $\mathbf{n}_{r, d_k}$  have elements that are independent Gaussian random variables with zero mean and unit variance. The amplification factor in (155) is specified as

$$\alpha^2 = \frac{1}{E\{\|\mathbf{y}_{s, r}\|^2\}} = \frac{1}{\sum_{l=1}^K P_l \beta_{s_l, r} + L}, \quad (156)$$

where  $\beta_{s_l, r} = \mathbf{c}_l^H E\{\mathbf{H}_{s_l, r}^H \mathbf{H}_{s_l, r}\} \mathbf{c}_l$ . By substituting (154) and (156) into (155), we obtain

$$\mathbf{y}_{r, d_k} = \sqrt{P_r} \alpha \mathbf{H}_{r, d_k} \sum_{l=1}^K \sqrt{P_l} \mathbf{H}_{s_l, r} \mathbf{c}_l b_l + \sqrt{P_r} \alpha \mathbf{H}_{r, d_k} \mathbf{n}_{s, r} + \mathbf{n}_{r, d_k}. \quad (157)$$

The destination  $D_k$  combines the signals received from the sources in Phase 1 and the signals received from the relay in Phase 2 to jointly detect the information symbol transmitted by the source  $S_k$ . The combined received signal from Phase 1 and Phase 2 at destination  $D_k$  can be expressed in vector form as follows:

$$\mathbf{y}_k \triangleq \begin{pmatrix} \mathbf{y}_{s, d_k} \\ \mathbf{y}_{r, d_k} \end{pmatrix} = \mathbf{H}_{k, k} \mathbf{c}_k b_k + \sum_{l=1, l \neq k}^K \mathbf{H}_{l, k} \mathbf{c}_l b_l + \mathbf{n}_k,$$

where

$$\mathbf{H}_{l, k} = \begin{pmatrix} \sqrt{P_l} \mathbf{H}_{s_l, d_k} \\ \sqrt{P_l} \alpha \mathbf{H}_{s_l, r} \mathbf{H}_{r, d_k} \end{pmatrix}$$

is a  $2L \times L$  virtual channel matrix from the source  $S_l$  to the destination  $D_k$ , and

$$\mathbf{n}_k = \begin{pmatrix} \mathbf{n}_{s, d_k} \\ \sqrt{P_r} \alpha \mathbf{H}_{r, d_k} \mathbf{n}_{s, r} + \mathbf{n}_{r, d_k} \end{pmatrix}$$

is an equivalent noise vector of length  $2L$ . We note that  $\mathbf{H}_{k, k}$  is the channel matrix associated with the desired source  $S_k$ , while  $\mathbf{H}_{l, k}$ , ( $l \neq k$ ) are the channel matrices of the interfering sources. Based on maximum ratio combining (MRC) detection [?], the transmitted signal from the source  $S_k$  is generally detected as,

$$\hat{b}_k = \arg \min_{b_k \in \mathbb{A}} \|\mathbf{w}_{k, o}^H \mathbf{y}_k - b_k\|^2,$$

where  $\mathbb{A}$  is the transmitted signal set. For example,

$$\hat{b}_k = \text{sign}(\text{Re}\{\mathbf{w}_{k,o}^H \mathbf{y}_k\}),$$

for BPSK and

$$\hat{b}_k = \text{sign}(\text{Re}\{\mathbf{w}_{k,o}^H \mathbf{y}_k\}) + \text{sign}(\text{Im}\{\mathbf{w}_{k,o}^H \mathbf{y}_k\})j,$$

for QPSK in which  $j = \sqrt{-1}$ . The combining weight vector  $\mathbf{w}_{k,o}$  of size  $2L$  is chosen to maximize the SINR at the destination  $D_k$ , which is given by

$$\text{SINR}(\mathbf{w}_k) = \frac{E\{|\mathbf{w}_k^H \mathbf{H}_{k,k} \mathbf{c}_k b_k|^2\}}{E\{|\mathbf{w}_k^H (\sum_{l=1, l \neq k}^K \mathbf{H}_{l,k} \mathbf{c}_l b_l + \mathbf{n}_k)|^2\}}, \quad (158)$$

i.e.

$$\mathbf{w}_{k,o} = \arg \max_{\mathbf{w}_k} \text{SINR}(\mathbf{w}_k).$$

Note that in (158), the expected value in numerator is taken over the random variable  $b_k$ , while the expected value in denominator is taken over the random variables  $b_l, l \neq k$  and all independent noise terms in  $\mathbf{n}_k$ .

### 3.4.2 System Performance Analysis

To determine the maximum SINR weight vector  $\mathbf{w}_{k,o}$  and the corresponding SINR at the destination  $D_k$ , we first define

$$\begin{aligned} \mathbf{U}_k &\triangleq \sum_{l=1, l \neq k}^K \mathbf{H}_{l,k} \mathbf{c}_l \mathbf{c}_l^H \mathbf{H}_{l,k}^H + \mathbf{\Gamma}_k, \\ \mathbf{\Gamma}_k &\triangleq E\{\mathbf{n}_k \mathbf{n}_k^H\} = \begin{pmatrix} \mathbf{I}_L & 0 \\ 0 & P_r \alpha^2 \mathbf{H}_{r,d_k} \mathbf{H}_{r,d_k}^H + \mathbf{I}_L \end{pmatrix}. \end{aligned}$$

Then by taking the expectation over the signals  $b_k$  in numerator,  $b_l, l \neq k$  and noises in denominator, the SINR in (158) with any given combining weight vector  $\mathbf{w}_k$  can be written as

$$\text{SINR}(\mathbf{w}_k) = \frac{|\mathbf{w}_k^H \mathbf{H}_{k,k} \mathbf{c}_k|^2}{\mathbf{w}_k^H \mathbf{U}_k \mathbf{w}_k}. \quad (159)$$

It is easy to check that  $\mathbf{U}_k$  is Hermitian and it can be represented in terms of its eigenvalues  $\lambda_1, \lambda_2, \dots, \lambda_K$  and their associated eigenvectors  $\mathbf{q}_1, \mathbf{q}_2, \dots, \mathbf{q}_K$  as follows:

$$\mathbf{U}_k = \sum_{k=1}^K \lambda_k \mathbf{q}_k \mathbf{q}_k^H,$$

where  $\lambda_k \geq 0, \forall k$  and  $\mathbf{q}_k^H \mathbf{q}_l = 0, \forall k, l, k \neq l$ . Let

$$\mathbf{U}_k^{\frac{1}{2}} \triangleq \sum_{k=1}^K \lambda_k^{\frac{1}{2}} \mathbf{q}_k \mathbf{q}_k^H,$$

then  $\mathbf{U}_k^{\frac{1}{2}}$  is Hermitian and  $\mathbf{U}_k = \mathbf{U}_k^{\frac{1}{2}} \mathbf{U}_k^{\frac{1}{2}}$ . Moreover,

$$\mathbf{U}_k^{-\frac{1}{2}} = \sum_{k=1}^K \lambda_k^{-\frac{1}{2}} \mathbf{q}_k \mathbf{q}_k^H,$$

which is also Hermitian. According to Schwartz inequality, we have

$$\begin{aligned}
\frac{|\mathbf{w}_k^H \mathbf{H}_{k,k} \mathbf{c}_k|^2}{\mathbf{w}_k^H \mathbf{U}_k \mathbf{w}_k} &= \frac{|\mathbf{w}_k^H \mathbf{U}_k^{-\frac{1}{2}} \mathbf{U}_k^{\frac{1}{2}} \mathbf{H}_{k,k} \mathbf{c}_k|^2}{\mathbf{w}_k^H \mathbf{U}_k^{\frac{1}{2}} \mathbf{U}_k^{\frac{1}{2}} \mathbf{w}_k} \\
&\leq \frac{\|\mathbf{w}_k^H \mathbf{U}_k^{\frac{1}{2}}\|^2 \|\mathbf{U}_k^{-\frac{1}{2}} \mathbf{H}_{k,k} \mathbf{c}_k\|^2}{\|\mathbf{w}_k^H \mathbf{U}_k^{\frac{1}{2}}\|^2} \\
&= \|\mathbf{U}_k^{-\frac{1}{2}} \mathbf{H}_{k,k} \mathbf{c}_k\|^2,
\end{aligned}$$

where the equality holds when  $\mathbf{w}_k^H \mathbf{U}_k^{\frac{1}{2}} = (\mathbf{U}_k^{-\frac{1}{2}} \mathbf{H}_{k,k} \mathbf{c}_k)^H$ . Thus, the maximum SINR weight vector  $\mathbf{w}_{k,o}$  is given by

$$\mathbf{w}_{k,o} = \mathbf{U}_k^{-1} \mathbf{H}_{k,k} \mathbf{c}_k.$$

The corresponding maximum SINR at the destination  $D_k$  with the optimum weight vector  $\mathbf{w}_{k,o}$  is equal to

$$\text{SINR}_k = \mathbf{c}_k^H \mathbf{H}_{k,k}^H \mathbf{U}_k^{-1} \mathbf{H}_{k,k} \mathbf{c}_k. \quad (160)$$

In order to optimally allocate power to all sources, we further exploit  $\text{SINR}_k$  in (160) as follows. We define  $\hat{\mathbf{C}}_k \triangleq \text{diag}(\mathbf{c}_1, \dots, \mathbf{c}_{k-1}, \mathbf{c}_{k+1}, \dots, \mathbf{c}_K)$ , which is a  $L(K-1) \times (K-1)$  block diagonal matrix formed by placing all code vectors except  $\mathbf{c}_k$  in the diagonal positions, and  $\hat{\mathbf{H}}_k \triangleq [\mathbf{H}_{1,k}, \dots, \mathbf{H}_{k-1,k}, \mathbf{H}_{k+1,k}, \dots, \mathbf{H}_{K,k}]$  which is a  $2L \times L(K-1)$  interference channel matrix. Using the above notation,  $\text{SINR}_k$  can be expressed as

$$\text{SINR}_k = \mathbf{c}_k^H \mathbf{H}_{k,k}^H (\hat{\mathbf{H}}_k \hat{\mathbf{C}}_k \hat{\mathbf{C}}_k^H \hat{\mathbf{H}}_k^H + \mathbf{\Gamma}_k)^{-1} \mathbf{H}_{k,k} \mathbf{c}_k. \quad (161)$$

According to the Woodbury matrix inversion lemma [75], we have

$$(\hat{\mathbf{H}}_k \hat{\mathbf{C}}_k \hat{\mathbf{C}}_k^H \hat{\mathbf{H}}_k^H + \mathbf{\Gamma}_k)^{-1} = \mathbf{\Gamma}_k^{-1} - \mathbf{\Gamma}_k^{-1} \hat{\mathbf{H}}_k \hat{\mathbf{C}}_k (\mathbf{I}_{K-1} + \hat{\mathbf{C}}_k^H \hat{\mathbf{H}}_k^H \mathbf{\Gamma}_k^{-1} \hat{\mathbf{H}}_k \hat{\mathbf{C}}_k)^{-1} \hat{\mathbf{C}}_k^H \hat{\mathbf{H}}_k^H \mathbf{\Gamma}_k^{-1}.$$

Let us now define the following matrix  $\mathbf{F}^{(k)} \triangleq (f_{mn}^{(k)})$ , where

$$f_{mn}^{(k)} = \rho_{mn} \sqrt{P_m P_n} \left( h_{s_m, d_k}^* h_{s_n, d_k} + \frac{\alpha^2 P_r |h_{r, d_k}|^2 h_{s_m, r}^* h_{s_n, r}}{\alpha^2 P_r |h_{r, d_k}|^2 + 1} \right), \quad (162)$$

and denote by  $\mathbf{f}_k^{(k)}$  the  $k^{\text{th}}$  column vector of the matrix  $\mathbf{F}^{(k)}$ . Then, after some algebraic calculations, we can see that

$$\begin{cases}
f_{kk}^{(k)} &= \mathbf{c}_k^H \mathbf{H}_{k,k}^H \mathbf{\Gamma}_k^{-1} \mathbf{H}_{k,k} \mathbf{c}_k \\
\mathbf{f}_k^{(k)} &= \hat{\mathbf{C}}_k^H \hat{\mathbf{H}}_k^H \mathbf{\Gamma}_k^{-1} \mathbf{H}_{k,k} \mathbf{c}_k \\
\mathbf{F}_k^{(k)} &= \hat{\mathbf{C}}_k^H \hat{\mathbf{H}}_k^H \mathbf{\Gamma}_k^{-1} \hat{\mathbf{H}}_k \hat{\mathbf{C}}_k,
\end{cases} \quad (163)$$

where  $\mathbf{f}_k^{(k)}$  contains the channels and the cross-correlation between the intended source  $S_k$  and the interfering sources, while  $\mathbf{F}_k^{(k)}$  contains the channels and the cross-correlation among interfering sources. Based on (161)-(163), we can represent  $\text{SINR}_k$  as

$$\text{SINR}_k = f_{kk}^{(k)} - \mathbf{f}_k^{(k)H} (\mathbf{I}_{K-1} + \mathbf{F}_k^{(k)})^{-1} \mathbf{f}_k^{(k)}, \quad (164)$$

where the superscript  $(\cdot)^{(k)}$  indicates the corresponding destination  $D_k$ .

Note that when all the channels are quasi-static over an information symbol period  $L$ , i.e. when  $h_{s_n, d_k}^{(i)} = h_{s_n, d_k}$ ,  $h_{s_n, r}^{(i)} = h_{s_n, r}$  and  $h_{r, d_k}^{(i)} = h_{r, d_k} \forall i = 1, 2, \dots, L$  and  $\forall n, k = 1, 2, \dots, K$ , then  $f_{mn}^{(k)}$  in (162) can be reduced to

$$f_{mn}^{(k)} = \rho_{mn} \sqrt{P_m P_n} \left( h_{s_m, d_k}^* h_{s_n, d_k} + \frac{\alpha^2 P_r |h_{r, d_k}|^2 h_{s_m, r}^* h_{s_n, r}}{\alpha^2 P_r |h_{r, d_k}|^2 + 1} \right). \quad (165)$$

When there are only two source-destination pairs with one relay, i.e.  $K = 2$ , the SINR $_k$  in (164) with quasi-static channels is specified as

$$\begin{aligned} \text{SINR}_k &= f_{kk}^{(k)} - |f_{kj}^{(k)}|^2 (1 + f_{jj}^{(k)})^{-1} \\ &= P_k \left( |h_{s_k, d_k}|^2 + \frac{\alpha^2 P_r |h_{r, d_k}|^2 |h_{s_k, r}|^2}{\alpha^2 P_r |h_{r, d_k}|^2 + 1} \right) - \\ &\quad \rho^2 P_k P_j \left| h_{s_k, d_k}^* h_{s_j, d_k} + \frac{\alpha^2 P_r |h_{r, d_k}|^2 h_{s_k, r}^* h_{s_j, r}}{\alpha^2 P_r |h_{r, d_k}|^2 + 1} \right|^2 \left( 1 + P_j |h_{s_j, d_k}|^2 + \frac{\alpha^2 P_r |h_{r, d_k}|^2 P_j |h_{s_j, r}|^2}{\alpha^2 P_r |h_{r, d_k}|^2 + 1} \right)^{-1}, \end{aligned}$$

where  $\rho = \rho_{12} = \rho_{21}$  and the subscript  $j = 2$  if  $k = 1$  while  $j = 1$  if  $k = 2$ . Furthermore, when the code/channel vectors  $\mathbf{c}_k$  are orthogonal to each other, i.e.  $\rho_{kj} = \mathbf{c}_k^T \mathbf{c}_j = 0$ , for  $j \neq k$ , then  $\mathbf{f}_k^{(k)} = \mathbf{0}$  for quasi-static channels. Hence the SINR at destination  $D_k$  is given by

$$\text{SINR}_k = f_{kk}^{(k)} = P_k |h_{s_k, d_k}|^2 + \frac{\alpha^2 P_r |h_{r, d_k}|^2 P_k |h_{s_k, r}|^2}{\alpha^2 P_r |h_{r, d_k}|^2 + 1}, \quad (166)$$

which is the sum of the SINRs of the direct link and the relay link.

### 3.4.3 Optimum Power Assignment Under SINR Constraints for All Source-Destination Pairs

In this subsection, we determine the optimum power assignment for the sources and the relay that minimizes the total power consumption under the condition that the SINR requirement of each source-destination pair is satisfied. First, we consider the power optimization for the relay network in a general setting where codes/channels of different sources may have arbitrary correlation. Then, we discuss a simplified power optimization scheme for a special case where codes/channels of different sources are orthogonal, and provide an intuitive interpretation for the proposed scheme.

Let us assume that the SINR requirement for the source-destination pair  $(S_k, D_k)$  is  $\gamma_k$ ,  $k = 1, 2, \dots, K$ . Then, the problem of optimizing power to minimize the total power consumption and satisfy all source-destination SINR requirements can be formulated as:

$$\begin{cases} \min_{P_1, \dots, P_K; P_r} & \sum_{k=1}^K P_k + P_r, \\ \text{s. t.} & \text{SINR}_k \geq \gamma_k, \quad 1 \leq k \leq K, \end{cases} \quad (167)$$

where the transmission power terms  $P_1, P_2, \dots, P_k$  and  $P_r$  are all non-negative.

Let us define a normalized power factor at the relay as follows

$$x \triangleq \alpha^2 P_r, \quad (168)$$

where  $\alpha$  is the amplification factor specified in (156). The parameter  $x$  will play a key role in the optimization procedure. Let us also denote by  $\mathbf{G}^{(k)} = (g_{mn}^{(k)})$  a matrix with elements

$$g_{mn}^{(k)} \triangleq \rho_{mn} \left( h_{s_m, d_k}^* h_{s_n, d_k} + \frac{x |h_{r, d_k}|^2 h_{s_m, r}^* h_{s_n, r}}{x |h_{r, d_k}|^2 + 1} \right), \quad (m, n = 1, 2, \dots, K). \quad (169)$$

for any  $m, n = 1, 2, \dots, K$ . Then, from (162), we can represent each entry in  $\mathbf{F}^{(k)}$  by

$$f_{mn}^{(k)} = \sqrt{P_m P_n} g_{mn}^{(k)}.$$

It is straightforward to verify that

$$\det(\mathbf{F}^{(k)}) = \left( \prod_{l=1}^K P_l \right) \det(\mathbf{G}^{(k)}), \quad (170)$$

$$\det(\mathbf{F}_{\bar{k}}^{(k)}) = \left( \prod_{l=1, l \neq k}^K P_l \right) \det(\mathbf{G}_{\bar{k}}^{(k)}). \quad (171)$$

From (164), we know that  $\mathbf{I}_{K-1} + \mathbf{F}_{\bar{k}}^{(k)}$  is invertible. So, based on the Schur complement formula<sup>3</sup>, we have

$$\begin{aligned} & \det(\mathbf{I}_K + \mathbf{F}^{(k)}) \\ &= \det \begin{pmatrix} 1 + f_{kk}^{(k)} & \mathbf{f}_{\bar{k}}^{(k)H} \\ \mathbf{f}_{\bar{k}}^{(k)} & \mathbf{I}_{K-1} + \mathbf{F}_{\bar{k}}^{(k)} \end{pmatrix} \\ &= \det(\mathbf{I}_{K-1} + \mathbf{F}_{\bar{k}}^{(k)}) \cdot \left[ 1 + f_{kk}^{(k)} - \mathbf{f}_{\bar{k}}^{(k)H} (\mathbf{I}_{K-1} + \mathbf{F}_{\bar{k}}^{(k)})^{-1} \mathbf{f}_{\bar{k}}^{(k)} \right] \\ &= \det(\mathbf{I}_{K-1} + \mathbf{F}_{\bar{k}}^{(k)}) \cdot (1 + \text{SINR}_k), \end{aligned} \quad (172)$$

where the last equality follows from the expression of  $\text{SINR}_k$  in (164). Thus, we have

$$1 + \text{SINR}_k = \frac{\det(\mathbf{I}_K + \mathbf{F}^{(k)})}{\det(\mathbf{I}_{K-1} + \mathbf{F}_{\bar{k}}^{(k)})}. \quad (173)$$

We note that for moderate or high SINR, we can approximate  $1 + \text{SINR}_k \approx \text{SINR}_k$  and  $1 + f_{ll}^{(k)} \approx f_{ll}^{(k)}$ ,  $\forall k, l = 1, \dots, K$  [55][74]. So, based on (173), we can approximate  $\text{SINR}_k$  as follows:

$$\text{SINR}_k \approx \frac{\det(\mathbf{F}^{(k)})}{\det(\mathbf{F}_{\bar{k}}^{(k)})} = \frac{P_k \det(\mathbf{G}^{(k)})}{\det(\mathbf{G}_{\bar{k}}^{(k)})}. \quad (174)$$

Therefore, the optimization problem in (167) can be written as

$$\begin{cases} \min_{P_1, \dots, P_K; P_r} \sum_{k=1}^K P_k + P_r, \\ \text{s. t. } \frac{P_k \det(\mathbf{G}^{(k)})}{\det(\mathbf{G}_{\bar{k}}^{(k)})} \geq \gamma_k, \quad 1 \leq k \leq K. \end{cases} \quad (175)$$

Let  $V$  denote the feasible set of the optimization problem in (175), i.e.

$$V = \{P_1, \dots, P_K, P_r \mid \text{SINR}_k \geq \gamma_k, \forall 1 \leq k \leq K\}.$$

We may partition  $V$  into disjoint subsets such as

$$V = \bigcup_{x \geq 0} V_x,$$

---

<sup>3</sup>If matrix  $\mathbf{D}$  is invertible, then [75]

$$\det \begin{pmatrix} \mathbf{A} & \mathbf{B} \\ \mathbf{C} & \mathbf{D} \end{pmatrix} = \det(\mathbf{D}) \cdot \det(\mathbf{A} - \mathbf{B}\mathbf{D}^{-1}\mathbf{C}).$$

where

$$V_x = \{P_1, \dots, P_K, P_r \mid \text{SINR}_k \geq \gamma_k, \forall 1 \leq k \leq K, \alpha^2 P_r = x\}$$

for any  $x \geq 0$ .

We note that for any given value of the parameter  $x$  in (168), the transmission power at the relay,  $P_r$ , can be determined from (156) as

$$P_r = \frac{x}{\alpha^2} = x \sum_{k=1}^K P_k \beta_{s_k, r} + xL. \quad (176)$$

Thus, for any given  $x \geq 0$ , the optimization problem in (175) over the feasible set  $V_x$  becomes

$$\begin{cases} \min_{P_1, \dots, P_K} \sum_{k=1}^K (x\beta_{s_k, r} + 1)P_k + xL, \\ \text{s. t. } P_k \geq \frac{\gamma_k \det(\mathbf{G}_k^{(k)})}{\det(\mathbf{G}^{(k)})}, 1 \leq k \leq K. \end{cases} \quad (177)$$

We observe that in (177), for any given  $x \geq 0$ ,  $\frac{\gamma_k \det(\mathbf{G}_k^{(k)})}{\det(\mathbf{G}^{(k)})}$  is a constant which is independent of  $P_k$  ( $k = 1, 2, \dots, K$ ). Hence the minimal value in (177) is obtained when all constraints hold with equality, i.e.

$$P_k = \frac{\gamma_k \det(\mathbf{G}_k^{(k)})}{\det(\mathbf{G}^{(k)})}, \quad k = 1, 2, \dots, K. \quad (178)$$

Then, the corresponding minimal total power of (177) is

$$v(x) \triangleq \sum_{k=1}^K \gamma_k (x\beta_{s_k, r} + 1) \frac{\det(\mathbf{G}_k^{(k)})}{\det(\mathbf{G}^{(k)})} + xL, \quad (179)$$

which is a function of  $x \geq 0$ . Let us denote  $v^*$  as the minimal value of the objective function over (175) in the feasible set  $V$ . Then, we can see that

$$v^* = \min_{x \geq 0} v(x). \quad (180)$$

The above discussion shows that we are able to convert the optimization problem in (167) over a multi-dimension space to the minimization problem in (180), which depends only on one variable  $x \geq 0$ , i.e. over a one-dimension space. The minimization of  $v(x)$  in (179) can be easily solved by a numerical search for the optimal value of the parameter  $x \geq 0$ . With the optimal value  $x^*$  that minimizes the function  $v(x)$  in (179), we can obtain the corresponding optimal power  $P_k^*$  and  $P_r^*$  based on (178) and (176), respectively.

In the previous section, we solved the optimization problem for a general multi-source multi-destination relay network with arbitrary correlation among user codes. In this subsection, we are able to further simplify the optimization when the signatures of different sources are orthogonal and the fading channels are quasi-static during the transmission period of a signature code.

In particular, for multi-source multi-destination relay networks with orthogonal transmissions, the cross-correlation matrix  $\mathbf{R}$  in (149) is an identity matrix, so both  $\mathbf{G}_k^{(k)}$  and  $\mathbf{G}^{(k)}$  in (174) are diagonal matrices, and

$$\frac{\det(\mathbf{G}_k^{(k)})}{\det(\mathbf{G}^{(k)})} = \frac{\prod_{l=1, l \neq k}^K g_{ll}^{(k)}}{\prod_{l=1}^K g_{ll}^{(k)}} = \frac{1}{g_{kk}^{(k)}}, \quad (181)$$

where  $g_{kk}^{(k)}$  is specified in (169). Under the assumption of quasi-static channels, we can write  $h_{s_k, r}^{(i)} = h_{s_k, r}$ ,  $h_{s_k, d_k}^{(i)} = h_{s_k, d_k}$ , and  $h_{r, d_k}^{(i)} = h_{r, d_k}$ ,  $\forall i = 1, 2, \dots, L$ , and  $\forall k = 1, 2, \dots, K$ . We note that  $\beta_{s_k, r} = \sigma_{s_k, r}^2$  where

$\sigma_{s_k,r}^2$  is the variance of the source-relay channel  $h_{s_k,r}$ , i.e.  $\sigma_{s_k,r}^2 = E\{|h_{s_k,r}|^2\}$ . Thus, by substituting (181) into (179), we have

$$\begin{aligned} v(x) &= \sum_{k=1}^K \frac{\gamma_k(x\sigma_{s_k,r}^2 + 1)}{|h_{s_k,d_k}|^2 + \frac{x|h_{r,d_k}|^2|h_{s_k,r}|^2}{x|h_{r,d_k}|^2+1}} + xL \\ &= \sum_{k=1}^K \gamma_k(c_k + b_kx + \frac{a_k}{x + d_k}), \end{aligned} \quad (182)$$

where

$$\begin{aligned} a_k &= \frac{|h_{s_k,r}|^2}{A^2|h_{r,d_k}|^2} \left(1 - \frac{|h_{s_k,d_k}|^2\sigma_{s_k,r}^2}{A|h_{r,d_k}|^2}\right), \\ b_k &= \frac{L}{K\gamma_k} + \frac{\sigma_{s_k,r}^2}{A}, \\ c_k &= \frac{1}{A} + \frac{|h_{s_k,r}|^2\sigma_{s_k,r}^2}{A^2|h_{r,d_k}|^2}, \\ d_k &= \frac{|h_{s_k,d_k}|^2}{A|h_{r,d_k}|^2}, \end{aligned} \quad (183)$$

and  $A = |h_{s_k,d_k}|^2 + |h_{s_k,r}|^2$ .

We note that for any  $k = 1, 2, \dots, K$ , if  $a_k > 0$ , each term  $c_k + b_kx + \frac{a_k}{x+d_k}$  in (182) is convex with respect to  $x \geq 0$ , and it can be minimized by

$$x = \max(0, -d_k + \sqrt{\frac{a_k}{b_k}}).$$

If  $a_k \leq 0$ ,  $c_k + b_kx + \frac{a_k}{x+d_k}$  is increasing in  $[0, +\infty)$ , it implies that the minimum point occurs at  $x = 0$ . Let us denote

$$x_{min} \triangleq \min(x_1, x_2, \dots, x_K), \quad (184)$$

$$x_{max} \triangleq \max(x_1, x_2, \dots, x_K), \quad (185)$$

where for any  $k = 1, 2, \dots, K$

$$x_k = \begin{cases} \max(0, -d_k + \sqrt{\frac{a_k}{b_k}}) & \text{if } a_k > 0, \\ 0 & \text{if } a_k \leq 0. \end{cases} \quad (186)$$

Then, each term  $c_k + b_kx + \frac{a_k}{x+d_k}$  in (182) is decreasing in the range  $[0, x_{min}]$  and increasing in the range  $[x_{max}, +\infty)$ , which implies that the optimal solution  $x^*$  that minimizes the function  $v(x)$  in (182) is bounded as

$$x_{min} \leq x^* \leq x_{max}. \quad (187)$$

Thus, to find the optimal solution  $x^*$ , we only need to search within the range  $[x_{min}, x_{max}]$ . We note that  $x_{min} = 0$  if there exists  $k \in \{1, 2, \dots, K\}$  such that  $a_k \leq 0$ .

From (186), we can see that the necessary condition for  $x_k > 0$  is

$$a_k > b_k d_k^2,$$

which implies that

$$\frac{|h_{s_k,r}|^2|h_{r,d_k}|^2}{\sigma_{s_k,r}^2} > |h_{s_k,d_k}|^2. \quad (188)$$

In a non-fading or *slow-fading* scenario, where the coherence time of the channel is much longer than the delay requirement of the channel. In this situation, the channel gain remains roughly constant over all the time [76], then we can safely assume that  $|h_{i,j}|^2 \approx \sigma_{i,j}^2$ , where  $\sigma_{i,j}^2$  is the variance of the channel  $h_{i,j}$ . Then (188) is equivalent to

$$\sigma_{r,d_k}^2 > \sigma_{s_k,d_k}^2. \quad (189)$$

If none of the inequalities in (189) is true, i.e.  $\sigma_{r,d_k}^2 \leq \sigma_{s_k,d_k}^2$  for all  $k = 1, 2, \dots, K$ , then  $x_{max} = 0$ , which implies that the optimal solution  $x^* = 0$ . So, the corresponding optimum power at the relay  $P_r^* = 0$ , which means that the relay is not needed. In other words, if each relay-destination channel link is weaker than the intended source-destination channel link, then we should not use relay.

In addition, if  $a_k \leq 0, \forall k = 1, 2, \dots, K$ , then each term  $c_k + b_k x + \frac{a_k}{x+d_k}$  in (182) is an increasing function of  $x \in [0, +\infty)$ , therefore the optimal solution is  $x^* = 0$ . Given that  $a_k \leq 0$  is equivalent to

$$|h_{s_k,d_k}|^2 \sigma_{s_k,r}^2 \geq (|h_{s_k,d_k}|^2 + |h_{s_k,r}|^2) |h_{r,d_k}|^2, \quad (190)$$

it implies that if all channels  $|h_{s_k,d_k}|^2, (k = 1, 2, \dots, K)$  that correspond to direct links are strong enough or all channels of the relay links  $|h_{r,d_k}|^2, (k = 1, 2, \dots, K)$  are weak, then avoiding use of the relay can lead to power savings. In other words, if there is at least one relay-destination link that is better than the corresponding source-destination link, the relay should forward its received signal to the destinations in order to help reduce the overall power consumption while maintaining at the same time the target performance level.

Finally, for a symmetric system where  $\sigma_{s_1,d_1}^2 = \sigma_{s_2,d_2}^2 = \dots = \sigma_{s_K,d_K}^2, \sigma_{s_1,r}^2 = \sigma_{s_2,r}^2 = \dots = \sigma_{s_K,r}^2$  and  $\sigma_{r,d_1}^2 = \sigma_{r,d_2}^2 = \dots = \sigma_{r,d_K}^2$ , we are able to obtain an analytical solution for the minimization of  $v(x)$ . In this case, all  $d_k$  are equal, say  $d = d_k, \forall k$ . Then

$$v(x) = c + bx + \frac{a}{x+d}, \quad (191)$$

where  $c = \sum_{k=1}^K \gamma_k c_k, b = \sum_{k=1}^K \gamma_k b_k, a = \sum_{k=1}^K \gamma_k a_k$ . Consequently, the value  $x^*$  that minimizes  $v(x)$  in (191) is

$$x^* = \begin{cases} -d + \sqrt{\frac{a}{b}} & \text{if } a > 0, \\ 0 & \text{if } a \leq 0. \end{cases} \quad (192)$$

Substituting (192) into (178) and (176), we obtain the optimal power  $P_k^*$  and  $P_r^*$ , respectively.

We note that for a symmetric system, all  $a_k$  are equal. When the SINR requirement is high enough at each destination,  $L/(K\gamma_k)$  is relatively small compared to  $\frac{\sigma_{s_k,r}^2}{A}$ , so all  $b_k$ 's are approximately the same ( $k = 1, 2, \dots, K$ ). As a consequence, the ratio  $a/b$  in (192) is independent of  $\gamma_k$ . Hence, the optimal value  $x^*$  in (192) is independent of the SINR thresholds  $\gamma_k$  in this case.

In the following, for comparison purposes, we discuss the equal power allocation scheme where all the sources and the relay are allocated the same power  $P$ . In this case, the corresponding parameter  $x$  in (168) is

$$x = \frac{1}{\sum_{k=1}^K \sigma_{s_k,r}^2 + \frac{L}{P}}. \quad (193)$$

To find the optimal power  $P$  that minimizes the total power of the system under the constraints that the SINR requirements of all source-destination pairs are satisfied, we can follow the procedure described in the previous section, i.e.

$$\begin{cases} \min_P & P \sum_{k=1}^K (x \sigma_{s_k,r}^2 + 1) + xL, \\ \text{s.t.} & P \geq \frac{\gamma_k \det(\mathbf{G}_k^{(k)})}{\det(\mathbf{G}^{(k)})}, \quad k = 1, 2, \dots, K. \end{cases} \quad (194)$$

We note that the objective function in (194) is increasing in terms of increasing  $P > 0$ . Thus, the optimal solution  $P^*$  of (194) is given as

$$P^* = \max_{k=1, \dots, K} \left\{ \frac{\gamma_k \det(\mathbf{G}_k^{(k)})}{\det(\mathbf{G}^{(k)})} \right\}. \quad (195)$$

Since the channel quality is not the same, in general, for all links, it is implied that the terms  $\frac{\gamma_k \det(\mathbf{G}_k^{(k)})}{\det(\mathbf{G}^{(k)})}$ ,  $k = 1, 2, \dots, K$  in (194) are not equal in general, which means that the equality in (194) might not hold for all  $k$ . As a result, the equal power allocation strategy generally spends more power than what is needed.

#### 3.4.4 Optimum Power Assignment Under a Total Power Budget Constraint

In this subsection, we will apply the methodology that we developed in Section 4 to solve a related max-min SINR based power optimization problem for multi-source multi-destination relay networks. Specifically, we will design a power assignment scheme that maximizes the minimum SINR among all source-destination pairs subject to any given total power budget. We may say that such a scheme introduces a type of fairness among different source-destination pairs. The optimization problem can be formulated as follows:

$$\begin{cases} \max_{P_1, \dots, P_K; P_r} \min_{k=1, \dots, K} \{ \text{SINR}_k \}, \\ \text{s.t.} \quad \sum_{k=1}^K P_k + P_r \leq P_{total} \end{cases} \quad (196)$$

where  $P_{total}$  is the given power budget of the system.

Let us denote

$$z \triangleq \min_{k=1, \dots, K} \{ \text{SINR}_k \}, \quad (197)$$

then (196) is equivalent to

$$\begin{cases} \max_{P_1, \dots, P_K; P_r} z, \\ \text{s.t.} \quad \sum_{k=1}^K P_k + P_r \leq P_{total}, \\ \text{SINR}_k \geq z, k = 1, \dots, K. \end{cases} \quad (198)$$

According to (174), we may approximate  $\text{SINR}_k$  as

$$\text{SINR}_k \approx \frac{P_k \det(\mathbf{G}^{(k)})}{\det(\mathbf{G}_k^{(k)})}, \quad (199)$$

where the matrices  $\mathbf{G}^{(k)}$  and  $\mathbf{G}_k^{(k)}$  are specified in (169). If we define  $x \triangleq \alpha^2 P_r$ , then for any given  $x \geq 0$ , the transmission power at the relay  $P_r$  is determined as

$$P_r = \frac{x}{\alpha^2} = x \sum_{k=1}^K P_k \beta_{s_k, r} + xL. \quad (200)$$

As a consequence, we can reformulate the problem in (198) as

$$\begin{cases} \max_{P_1, \dots, P_K; z} z, \\ \text{s.t.} \quad \sum_{k=1}^K (x \beta_{s_k, r} + 1) P_k + xL \leq P_{total}, \\ P_k \geq z \cdot \frac{\det(\mathbf{G}_k^{(k)})}{\det(\mathbf{G}^{(k)})}, 1 \leq k \leq K. \end{cases} \quad (201)$$

For any  $x \geq 0$ , we denote the maximal value of the objective function in (201) as  $z(x)$ . Then,  $z(x)$  must satisfy

$$P_k \geq z(x) \cdot \frac{\det(\mathbf{G}_k^{(k)})}{\det(\mathbf{G}^{(k)})}, \quad \forall k = 1, 2, \dots, K. \quad (202)$$

Substituting the above constraints into the total power constraint in (201), we have

$$\sum_{k=1}^K (x\beta_{s_k,r} + 1)z(x) \cdot \frac{\det(\mathbf{G}_k^{(k)})}{\det(\mathbf{G}^{(k)})} + xL \leq P_{total}. \quad (203)$$

Thus, for any fixed  $x \geq 0$ , the maximal value of the objective function in (201) is

$$z(x) = \frac{P_{total} - xL}{\sum_{k=1}^K (x\beta_{s_k,r} + 1) \cdot \frac{\det(\mathbf{G}_k^{(k)})}{\det(\mathbf{G}^{(k)})}}. \quad (204)$$

We can see that maximizing  $z(x)$  can be implemented by a numerical search of single (one-dimension) parameter ( $x \geq 0$ ). If we denote the optimal parameter of (204) as  $x^*$ , then the optimum power assignment to the sources is

$$P_k^* = z(x^*) \cdot \frac{\det(\mathbf{G}_k^{(k)})}{\det(\mathbf{G}^{(k)})}, \quad k = 1, 2, \dots, K, \quad (205)$$

and the corresponding power assigned to the relay is

$$P_r^* = x^* \left( \sum_{k=1}^K P_k^* \beta_{s_k,r} + L \right). \quad (206)$$

We note that  $z(x)$  in (204) should be non-negative for any given  $x$ , which implies that  $P_{total} - xL \geq 0$ , i.e.  $x \leq \frac{P_{total}}{L}$ . Thus, we only need to search the single variable  $x$  over the interval  $[0, \frac{P_{total}}{L}]$  to obtain the optimal solution  $x^*$  that maximizes the function  $z(x)$ .

From (199) and (205), we can see that for any  $k = 1, 2, \dots, K$ ,  $\text{SINR}_k = z(x^*)$ , which implies that the optimum power assignment achieved through the max-min SINR based optimization in (196) leads to the same SINR values for all source-destination pairs. We recall that for the total power minimization problem in (167), the optimal power assignment ensures that the resulting SINR for each source-destination pair is equal to the SINR requirement of the corresponding source-destination pair, i.e.  $\text{SINR}_k = \gamma_k$ ,  $k = 1, \dots, K$ . It is natural to expect that when all source-destination SINR requirements  $\gamma_k$  in (167) are the same, the power assignment strategy for the max-min SINR based optimization and that for the total power minimization based optimization would be the same. This intuitive interpretation can be seen from the derivations in (179) and (204). We note that for reasonably high power budget  $P_{total}$ , the term  $xL$  in (204) can be ignored, and maximization of  $z(x)$  in (204) is equivalent to minimization of the denominator which is related to the objective function in (179). If all the source-destination pairs' SINR requirements in (179) are the same, i.e.  $\gamma_k$ ,  $k = 1, \dots, K$ , then the optimal solutions  $x^*$  of  $z(x)$  in (204) is also optimal in minimizing  $v(x)$  in (179).

For comparison purposes, in the following we illustrate the max-min SINR problem under equal power allocation. The optimization problem in (196) with an equal power assignment can be expressed as

$$\begin{cases} \max_P \min_{k=1, \dots, K} \{ \text{SINR}_k \}, \\ \text{s. t. } (K+1)P \leq P_{total}, \end{cases} \quad (207)$$

where all the sources and the relay are assigned the same transmission power  $P$ . With the SINR approximation in (199) and  $z = \min_{1 \leq k \leq K} \{ \text{SINR}_k \}$ , we have

$$\begin{cases} \max_P z, \\ \text{s. t. } P \leq \frac{P_{total}}{K+1}, \\ P \geq z \cdot \frac{\det(\mathbf{G}_k^{(k)})}{\det(\mathbf{G}^{(k)})}, \quad k = 1, \dots, K. \end{cases} \quad (208)$$

Table 5: Optimum power assignment that minimizes the total power under given SINR constraints using the proposed method and the exhaustive search method for an *asymmetric* setting ( $K = 2$ )

	$(\gamma_1, \gamma_2)$ (dB)	$P_1$ (dB)	$P_2$ (dB)	$P_r$ (dB)
Proposed method	(10,10)	13.14	19.89	20.54
Exhaustive search	(10,10)	13.22	19.91	20.41
Proposed method	(10,20)	11.59	27.34	29.74
Exhaustive search	(10,20)	11.76	27.28	29.70

Table 6: Optimum power assignment that minimizes the total power under given SINR constraints using the proposed method and the exhaustive search method for a *symmetric* setting ( $K = 2$ )

	$(\gamma_1, \gamma_2)$ (dB)	$P_1$ (dB)	$P_2$ (dB)	$P_r$ (dB)
Proposed method	(10,10)	14.56	14.56	15.86
Exhaustive search	(10,10)	14.91	14.91	15.31
Proposed method	(10,20)	13.25	23.25	22.44
Exhaustive search	(10,20)	13.32	23.32	22.34

Thus, the optimal solution is  $P = \frac{P_{total}}{K+1}$  and the maximal value of the worst-case SINR is given by

$$z = \frac{P_{total}}{K+1} \cdot \max_{1 \leq k \leq K} \left\{ \frac{\det(\mathbf{G}^{(k)})}{\det(\mathbf{G}_k^{(k)})} \right\}. \quad (209)$$

We can see that in the equal power assignment scheme, the minimum SINR value among all source-destination pairs is directly determined by the given total power budget value.

### 3.4.5 Numerical Results and Discussions

In this subsection, we perform numerical studies to illustrate the proposed optimum power assignment algorithms. In our studies, we consider a *slow fading* scenario and then approximate  $|h_{i,j}|^2$  by  $\sigma_{i,j}^2$ . The channel gain for each channel link is assumed to follow a path loss model, where the variance of channel coefficient is given by  $\sigma_{i,j}^2 = \delta_{i,j}^{-\lambda}$  ( $i, j \in \{s_k, d_k, r\}$ ) with  $\delta_{i,j}$  as the distance of the channel link and  $\lambda$  as the path-loss exponent ( $\lambda = 3$  in our numerical studies).

In the first set of numerical studies, we illustrate the optimum power assignment that minimizes the total power consumption under the condition that the SINR requirement of each source-destination pair is satisfied. First, we consider a system with two source-destination pairs and one relay, i.e.  $K = 2$ , and the cross-correlation of the two source codes is  $\rho = 0.25$ . We study two sets of SINR requirements for the two source-destination pairs: (i)  $[\gamma_1, \gamma_2] = [10, 10]$ dB, and (ii)  $[\gamma_1, \gamma_2] = [10, 20]$ dB.

Fig. 28 plots the total power consumption with varying parameter  $x \geq 0$  for an *asymmetric* system, where the values of the distance between nodes are set as follows:  $\delta_{s_1, d_1} = 2, \delta_{s_1, d_2} = 3, \delta_{s_1, r} = \delta_{s_2, r} = \delta_{s_2, d_1} = \delta_{r, d_1} = 1, \delta_{s_2, d_2} = 3$  and  $\delta_{r, d_2} = 2$ . The optimal values of the parameter that minimize the total power consumption are  $x^* = 0.63$  and  $x^* = 1.52$  for  $[\gamma_1, \gamma_2] = [10, 10]$ dB and  $[10, 20]$ dB, respectively. Based on the optimal value  $x^*$ , we obtain the corresponding optimal power assignment  $P_1, P_2$  and  $P_r$  according to (178) and (176), as listed in Table 5. In this table, we also compare the optimal power values obtained by our proposed approximation method and those obtained by exhaustive search based on the optimization in (167). We observe that the optimal power values obtained by the two methods are almost indistinguishable. In Fig. 29, we plot

the total power consumption with varying parameter  $x \geq 0$  for a *symmetric* system, where the values of the distance between nodes are set as:  $\delta_{s_1,d_1} = \delta_{s_2,d_2} = \delta_{s_1,d_2} = \delta_{s_2,d_1} = 2$  and  $\delta_{s_1,r} = \delta_{s_2,r} = \delta_{r,d_1} = \delta_{r,d_2} = 1$ . The optimal values of the parameter are  $x^* = 0.32$  and  $x^* = 0.59$  for  $[\gamma_1, \gamma_2] = [10, 10]$ dB and  $[10, 20]$ dB, respectively. Based on the optimal value  $x^*$ , we obtain the corresponding optimal power allocation  $P_1, P_2$  and  $P_r$  again according to (178) and (176), as listed in Table 6. We observe that when the SINR requirements of the two source-destination pairs are equal, the power assignments to the two sources are the same. However, when the SINR requirements are different ( $[\gamma_1, \gamma_2] = [10, 20]$ dB), the equal power assignment is not optimum anymore. We can see in Table 6 that the optimal power values obtained by our proposed approximation method are indistinguishable from those obtained by the exhaustive search based on the optimization in (167).

We now repeat our studies for a system with three source-destination pairs and one relay, i.e.  $K = 3$ , where the signatures of the three sources are orthogonal to each other. We examine both an asymmetric case (Fig. 30) and a symmetric case (Fig. 31). In both figures, we consider three sets of SINR requirements for the three source-destination pairs, namely: (i)  $[\gamma_1, \gamma_2, \gamma_3] = [20, 20, 20]$ dB, (ii)  $[\gamma_1, \gamma_2, \gamma_3] = [10, 20, 20]$ dB, and (iii)  $[\gamma_1, \gamma_2, \gamma_3] = [10, 10, 20]$ dB. In Fig. 30, we consider an asymmetric system where the distance values are set as  $\delta_{s_k,r} = 1, (k = 1, 2, 3), \delta_{r,d_1} = 1, \delta_{r,d_2} = 2, \delta_{r,d_3} = 3$  and  $\delta_{s_1,d_1} = 2, \delta_{s_2,d_2} = 3$  and  $\delta_{s_3,d_3} = 4$ . In this case, the optimal values of the parameter that minimize the total power consumption are  $x^* = 2.34, x^* = 2.77$  and  $x^* = 3.17$  for the three sets of SINR requirements, respectively. Based on the optimal values, the optimum power assignments  $P_1, P_2, P_3$  and  $P_r$  can be obtained accordingly based on (178) and (176). In Fig. 31, we consider a symmetric system with  $\delta_{s_k,r} = \delta_{r,d_k} = 1, (k = 1, 2, 3)$  and  $\delta_{s_k,d_k} = 2, (k = 1, 2, 3)$ . The optimal values of the parameter are  $x^* = 0.77, x^* = 0.76$  and  $x^* = 0.75$  for the three sets of SINR requirements, respectively. We can see that the optimal values  $x^*$  in the symmetric system are almost the same for the three sets of SINR requirements. This result is consistent with the theoretical discussion that the optimal value  $x^*$  is independent of the SINR requirement  $\gamma_k$  but it depends on the channel condition.

In Table 7, we show the power efficiency of the proposed optimum power assignment scheme by listing the resulting total power consumption, compared to the total power consumption that results from the equal power assignment scheme. We consider both an asymmetric case (the system setup is the same as that in Fig. 30) and a symmetric case (the system setup is the same as that in Fig. 31). We can see that in the asymmetric system, the power savings of the optimum power assignment scheme is 4–6dB for the three sets of SINR requirements. The more unbalanced the SINR requirements of the three source-destination pairs are, the more power savings of the optimum power assignment scheme compared to the equal power assignment scheme can be achieved. In the symmetric system, the power savings of the optimum power assignment scheme is 0.5–4.5dB for the three sets of SINR requirements. Comparing the results between the asymmetric system and the symmetric system, we observe that the optimum power assignment scheme gains more power savings in the asymmetric system than in the symmetric system. Also, we observe that the total power consumption of the equal power assignment scheme is the same in each of the asymmetric and symmetric systems, which is consistent with our previous discussion that the equal power assignment depends only on the most challenging/weakest source-destination pair.

In the second set of numerical studies, we illustrate the optimum power assignment algorithm that maximizes the minimum SINR among all source-destination pairs under a given total power budget. We consider a system with two source-destination pairs and one relay, i.e.  $K = 2$ , with a total power budget  $P_{total} = 30$ dB. We assume that the cross-correlation of the two source codes is  $\rho = 0.25$ . We consider both an asymmetric case (the system setup is the same as that in Fig. 28) and a symmetric case (the system setup is the same as that in Fig. 29).

Fig. 32 shows the maximization of the minimum SINR with varying parameter  $x \geq 0$  for both the asymmetric and symmetric systems, respectively. The optimal values of the parameter that maximize the minimum SINR of all source-destination pairs are  $x^* = 1.16$  for the asymmetric system and  $x^* = 0.69$  for the symmetric system. For both the asymmetric and symmetric cases, the optimum power assignments  $P_1, P_2$  and  $P_r$  are determined based on (205) and (206) with the corresponding optimal value  $x^*$ , listed in Table 8. In Table 8, we also compare the optimal power values obtained by the proposed approximation method and those obtained by exhaustive search based on the optimization in (198). We observe that the optimal power values of the power assignment obtained by the two methods are indistinguishable. We note that for the symmetric case, the sources

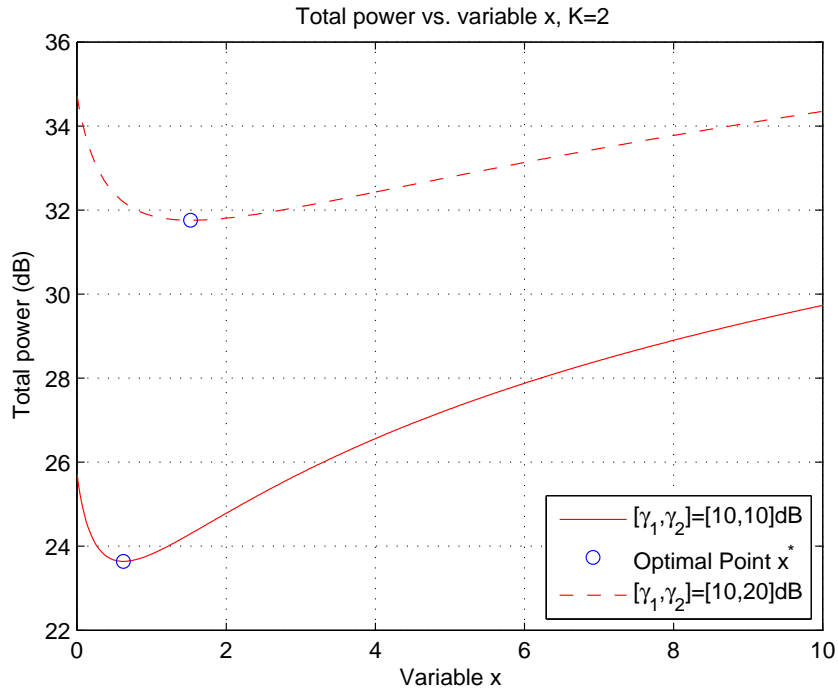


Figure 28: Minimization of the total power consumption under varying parameter  $x$  for an *asymmetric* multi-source multi-destination relay network with given SINR constraints ( $K = 2$ ).

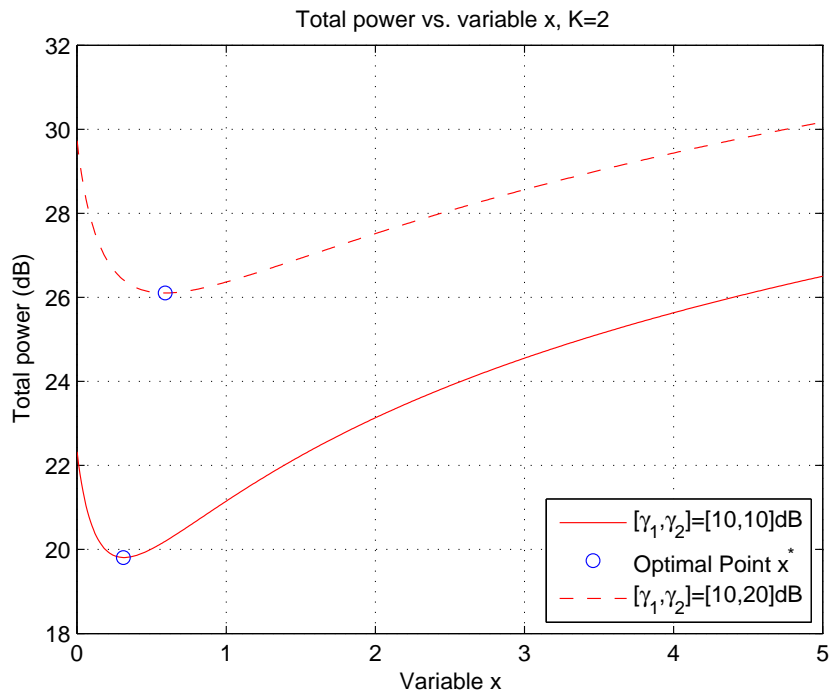


Figure 29: Minimization of the total power consumption with varying parameter  $x$  for a *symmetric* multi-source multi-destination relay network under given SINR constraints ( $K = 2$ ).

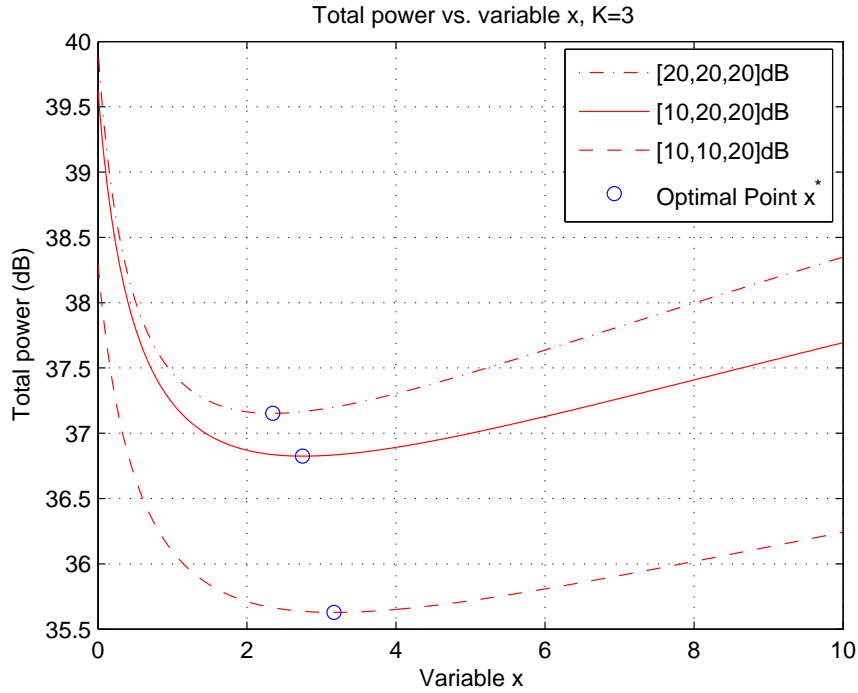


Figure 30: Minimization of the total power consumption with varying parameter  $x$  for an *asymmetric* multi-source multi-destination relay network under given SINR constraints ( $K = 3$ ).

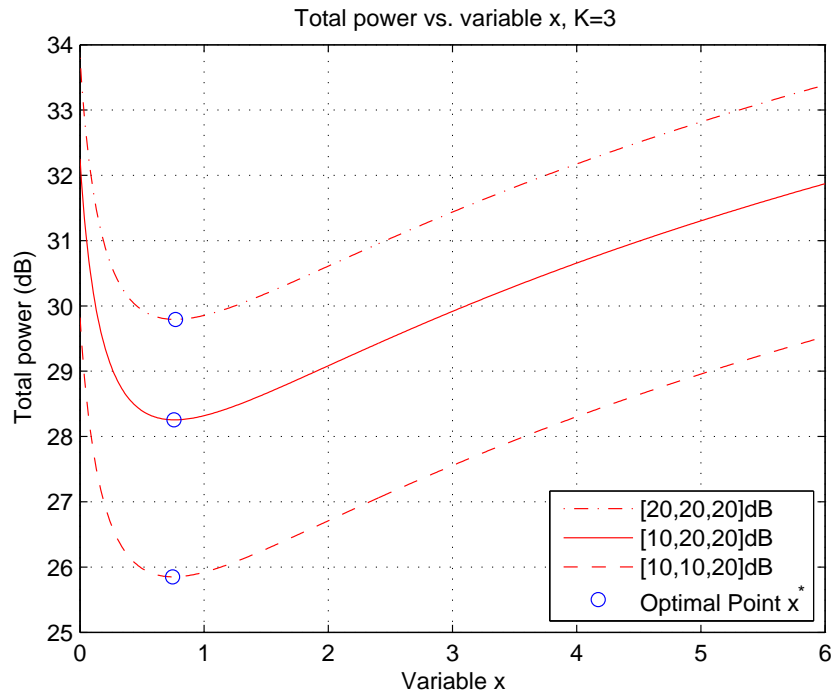


Figure 31: Minimization of the total power consumption with varying parameter  $x$  for a *symmetric* multi-source multi-destination relay network under given SINR constraints ( $K = 3$ ).

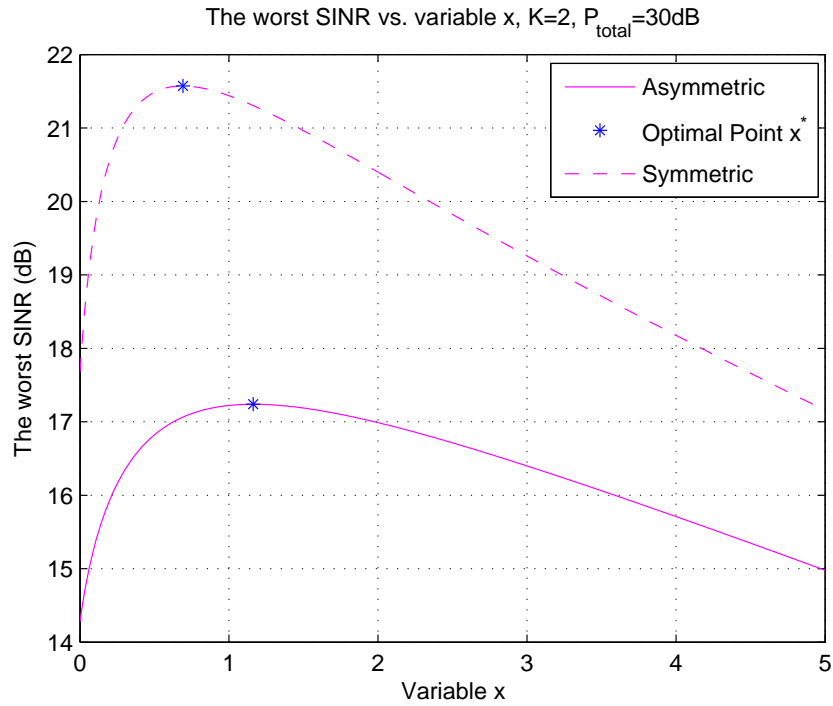


Figure 32: Maximization of the minimum SINR among all source-destination pairs under given total power budget  $P_{total} = 30\text{dB}$  ( $K = 2$ ).

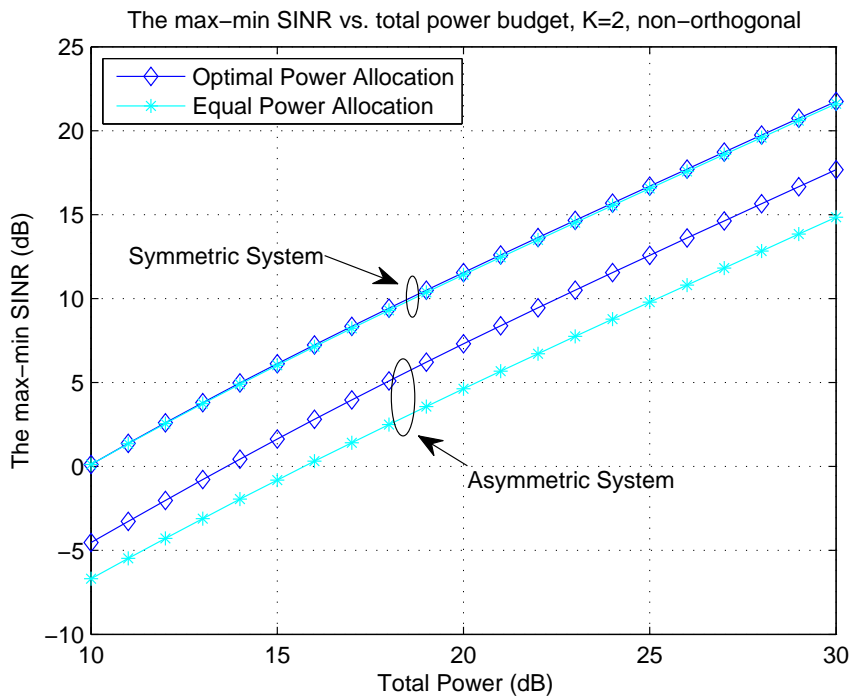


Figure 33: Comparison of the minimum SINR resulting from the proposed optimum power assignment scheme and the equal power assignment scheme with any given total power budget ( $K = 2$ ).

Table 7: Comparison of the total power consumption resulting from the optimum power assignment scheme and the equal power assignment scheme ( $K = 3$ )

	$\gamma_1, \gamma_2, \gamma_3$ (dB)	Total Power Consumption (dB)	
		Optimum	Equal
<i>Asymmetric System</i>	[20,20,20]	37.15	41.58
	[10,20,20]	36.82	41.58
	[10,10,20]	35.63	41.58
<i>Symmetric System</i>	[20,20,20]	29.79	30.30
	[10,20,20]	28.25	30.30
	[10,10,20]	25.85	30.30

Table 8: Optimum power assignment that maximizes the minimum SINR among two source-destination pairs under given total power budget  $P_{total} = 30$ dB, by using the proposed method and the exhaustive search method ( $K = 2$ )

		$P_1$ (dB)	$P_2$ (dB)	$P_r$ (dB)
<i>Asymmetric System</i>	Proposed method	19.22	25.34	27.59
	Exhaustive search	19.37	25.45	27.66
<i>Symmetric System</i>	Proposed method	24.49	24.49	26.41
	Exhaustive search	24.64	24.64	26.50

are allocated equal power under the max-min SINR optimization scheme, while the relay utilizes transmission power which is some what different from that allocated to the sources.

Finally, in Fig. 33, we compare the minimum SINR resulting from the proposed optimum power assignment scheme and the minimum SINR resulting from the equal power assignment scheme. We consider both an asymmetric case and a symmetric case, and the system setup is the same as that in Fig. 32. We can see that in the asymmetric case, the minimum SINR of the two source-destination pairs is improved significantly (by at least 2dB) when we use the proposed optimum power assignment scheme instead of the equal power assignment scheme. In the symmetric case, we can see that the performance of the equal power assignment scheme is very close to that of the optimum power assignment scheme (actually, in this case all the source-destination pairs have the same performance).

### 3.5 Cognitive Code-Division Channelization

In this subsection, first we briefly describe the CR CDMA system model and our formulation of the optimization problem. Then, we present in detail our proposed power and code-channel allocation solution. The performance of the proposed scheme is evaluated through simulations and a few concluding remarks are drawn at the end.

#### 3.5.1 System Model and Problem Formulation

We consider a primary CDMA system with processing gain (code sequence length)  $L$ ,  $K$  primary transmitters  $PT_i, i = 1, 2, \dots, K$ , and a primary receiver  $PR$  (for example,  $K$  uplink transmissions by users  $PT_i, i = 1, 2, \dots, K$ , to base station  $PR$ ). We also consider a potential concurrent secondary code-division link in the spectrum band of the primary system between a secondary transmitter  $ST$  and receiver  $SR$  (Fig. 34). All signals, primary and secondary, are supposed to propagate over flat-fading channels and experience additive white Gaussian noise. We denote by  $h_i, q_i, i = 1, 2, \dots, K$ , the path coefficients from  $PT_i$  to  $PR$  and  $SR$ ,

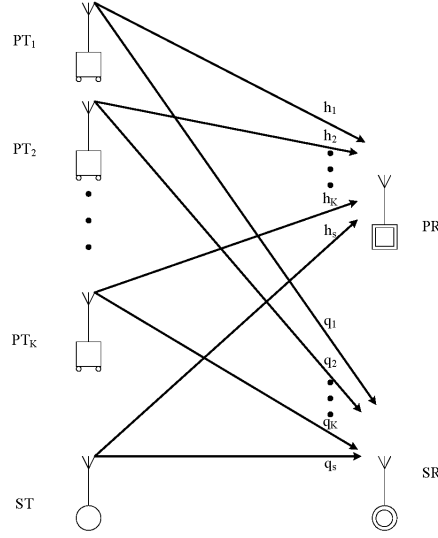


Figure 34: Primary/secondary CDMA system model of  $K$  primary transmitters  $PT_i, i = 1, 2, \dots, K$ , a primary receiver  $PR$ , and a secondary transmitter-receiver pair  $ST, SR$ . All paths  $h_1, \dots, h_K, q_1, \dots, q_K, h_s, q_s$  exhibit independent (quasi-static) Rayleigh fading.

respectively. The path coefficients from  $ST$  to  $PR, SR$  are denoted by  $h_s$  and  $q_s$ , respectively. All path coefficients are modeled as Rayleigh distributed random variables that are independent across user signals and remain constant during several symbol intervals (quasi-static fading).

After carrier demodulation, chip-matched filtering and sampling at the chip rate over the duration of a symbol (bit) period of  $L$  chips, the received signal at the primary receiver  $PR$  can be represented as

$$\mathbf{r} = \sum_{i=1}^K \sqrt{E_i} h_i \mathbf{s}_i b_i + \sqrt{E_s} h_s \mathbf{s}_s b_s + \mathbf{n}_p, \quad (210)$$

while the secondary signal received by  $SR$  is

$$\mathbf{y} = \sum_{i=1}^K \sqrt{E_i} q_i \mathbf{s}_i b_i + \sqrt{E_s} q_s \mathbf{s}_s b_s + \mathbf{n}_s \quad (211)$$

where  $E_i > 0$ ,  $b_i \in \{\pm 1\}$ , and  $\mathbf{s}_i \in \mathbb{R}^L$ ,  $\|\mathbf{s}_i\| = 1$ , denote bit energy, information bit, and normalized signature vector of primary user  $i$ ,  $i = 1, 2, \dots, K$ , respectively;  $E_s > 0$ ,  $b_s \in \{\pm 1\}$ , and  $\mathbf{s}_s \in \mathbb{R}^L$ ,  $\|\mathbf{s}_s\| = 1$ , denote the bit energy, information bit, and normalized signature vector, respectively, of the secondary transmitter  $ST$ ;  $\mathbf{n}_p$  and  $\mathbf{n}_s$  represent additive white Gaussian noise (AWGN) at  $PR$  and  $SR$ , correspondingly, independent from each other with  $\mathbf{0}$  mean and autocovariance matrix  $\sigma^2 \mathbf{I}$ .

The linear filters at the primary and secondary receivers that exhibit maximum output SINR [91] can be found to be

$$\begin{aligned} \mathbf{w}_{maxSINR,i} &= c_1 \mathbf{R}_p^{-1} \mathbf{s}_i, \quad i = 1, 2, \dots, K, \\ \mathbf{w}_{maxSINR,s} &= c_2 \mathbf{R}_s^{-1} \mathbf{s}_s, \end{aligned}$$

where  $\mathbf{R}_p = E\{\mathbf{r}\mathbf{r}^T\}$ ,  $\mathbf{R}_s = E\{\mathbf{y}\mathbf{y}^T\}$ ,  $c_1, c_2 > 0$  ( $E\{\cdot\}$  denotes statistical expectation and  $T$  is the transpose operator). The output SINR at  $PR$  with respect to the signal transmitted by  $PT_i$ ,  $SINR_i$ , is given below followed by the output SINR at  $SR$ ,  $SINR_s$ ,

$$SINR_i = \frac{E\{|\mathbf{w}_{maxSINR,i}^T (\sqrt{E_i} h_i b_i \mathbf{s}_i)|^2\}}{E\{|\mathbf{w}_{maxSINR,i}^T (\sum_{k=1, k \neq i}^K \sqrt{E_k} h_k \mathbf{s}_k b_k + \sqrt{E_s} h_s \mathbf{s}_s b_s + \mathbf{n}_p)|^2\}} = E_i h_i^2 \mathbf{s}_i^T \mathbf{R}_p^{-1} \mathbf{s}_i, \quad (212)$$

$$SINR_s = \frac{E\{|\mathbf{w}_{maxSINR,s}^T(\sqrt{E_s}q_s b_s \mathbf{s}_s)|^2\}}{E\{|\mathbf{w}_{maxSINR,s}^T(\sum_{k=1}^K \sqrt{E_k}q_k \mathbf{s}_k b_k + \mathbf{n}_s)|^2\}} = E_s q_s^2 \mathbf{s}_s^T \mathbf{R}_{s/s}^{-1} \mathbf{s}_s \quad (213)$$

where  $\mathbf{R}_{p/i}$  and  $\mathbf{R}_{s/s}$  are the ‘‘exclude  $i$ ’’ and ‘‘exclude  $s$ ’’ input data autocorrelation matrices at  $PR$  and  $SR$ , respectively, defined by

$$\begin{aligned} \mathbf{R}_{p/i} &\triangleq \sum_{k=1, k \neq i}^K E_k h_k^2 \mathbf{s}_k \mathbf{s}_k^T + E_s h_s^2 \mathbf{s}_s \mathbf{s}_s^T + \sigma^2 \mathbf{I}, \\ \mathbf{R}_{s/s} &\triangleq \sum_{k=1}^K E_k q_k^2 \mathbf{s}_k \mathbf{s}_k^T + \sigma^2 \mathbf{I}. \end{aligned}$$

In our cognitive radio setup, the secondary transmitter has to guarantee the SINR QoS of all primary users. In this spirit, our objective is to find the transmission bit energy  $E_s$  and the real-valued normalized signature vector  $\mathbf{s}_s$  that maximize  $SINR_s$  under the constraints that  $SINR_i$ ,  $i = 1, 2, \dots, K$ , are all above a certain threshold  $\alpha > 0$ , i.e. we would like to identify the optimal pair

$$\begin{aligned} (E_s, \mathbf{s}_s)^{opt} &= \arg \max_{E_s > 0, \mathbf{s}_s \in \mathbb{R}^L} E_s \mathbf{s}_s^T \mathbf{R}_{s/s}^{-1} \mathbf{s}_s \\ &\text{subject to } E_i h_i^2 \mathbf{s}_i^T \mathbf{R}_{p/i}^{-1} \mathbf{s}_i \geq \alpha, \quad i = 1, 2, \dots, K, \\ &\mathbf{s}_s^T \mathbf{s}_s = 1, E_s \leq E_{max} \end{aligned} \quad (214)$$

where  $E_{max}$  denotes the maximum available/allowable bit energy for the secondary user.

The optimization task of maximizing a quadratic objective function ( $\mathbf{R}_{s/s}^{-1}$  is positive definite) subject to the constraints in (214) is, unfortunately, a non-convex NP-hard (in  $L$ ) optimization problem [92]. In the following section, we delve into the details of the problem and derive a novel realizable suboptimum solution.

### 3.5.2 Proposed Cognitive Secondary Channel Design

Using the matrix inversion lemma [93] on  $\mathbf{R}_{p/i}^{-1}$ , we can express the key quadratic constraint expression  $\mathbf{s}_i^T \mathbf{R}_{p/i}^{-1} \mathbf{s}_i$  in (214) as

$$\mathbf{s}_i^T \mathbf{R}_{p/i}^{-1} \mathbf{s}_i = \frac{\mathbf{s}_i^T \mathbf{R}_p^{-1} \mathbf{s}_i}{1 - E_i h_i^2 \mathbf{s}_i^T \mathbf{R}_p^{-1} \mathbf{s}_i}, \quad i = 1, 2, \dots, k, \quad (215)$$

where we recall that  $\mathbf{R}_p = E\{\mathbf{r}\mathbf{r}^T\}$  is the autocorrelation matrix of the whole input to the primary receiver  $PR$ . Then, the  $PR$  SINR constraints in (214) become

$$\mathbf{s}_i^T \mathbf{R}_p^{-1} \mathbf{s}_i \geq \frac{\alpha}{E_i h_i^2 + \alpha E_i h_i^2} \triangleq \gamma_i, \quad i = 1, 2, \dots, K, \quad (216)$$

and the optimization problem can be rewritten as

$$\begin{aligned} (E_s, \mathbf{s}_s)^{opt} &= \arg \max_{E_s > 0, \mathbf{s}_s \in \mathbb{R}^L} E_s \mathbf{s}_s^T \mathbf{R}_{s/s}^{-1} \mathbf{s}_s \\ &\text{subject to } \mathbf{s}_i^T \mathbf{R}_p^{-1} \mathbf{s}_i \geq \gamma_i, \quad i = 1, 2, \dots, K, \\ &\mathbf{s}_s^T \mathbf{s}_s = 1, E_s \leq E_{max}. \end{aligned} \quad (217)$$

Using the matrix inversion lemma on  $\mathbf{R}_p^{-1}$  this time, we see that

$$\mathbf{R}_p^{-1} = \mathbf{R}_{p/s}^{-1} - \frac{E_s h_s^2 \mathbf{R}_{p/s}^{-1} \mathbf{s}_s \mathbf{s}_s^T \mathbf{R}_{p/s}^{-1}}{1 + E_s h_s^2 \mathbf{s}_s^T \mathbf{R}_{p/s}^{-1} \mathbf{s}_s} \quad (218)$$

where  $\mathbf{R}_{p/s}$  is the autocorrelation matrix of the input to the primary receiver  $PR$  excluding the secondary transmission,

$$\begin{aligned}\mathbf{R}_{p/s} &\triangleq E\left\{\left(\sum_{i=1}^K \sqrt{E_i} h_i \mathbf{s}_i b_i + \mathbf{n}_p\right)\left(\sum_{i=1}^K \sqrt{E_i} h_i \mathbf{s}_i b_i + \mathbf{n}_p\right)^T\right\} \\ &= \sum_{i=1}^K E_i h_i^2 \mathbf{s}_i \mathbf{s}_i^T + \sigma^2 \mathbf{I}.\end{aligned}$$

Then, inserting (218) in (217) we can express the optimization constraints as explicit functions of the code sequence of the secondary user  $\mathbf{s}_s$ , i.e.

$$\mathbf{s}_i^T \mathbf{R}_{p/s}^{-1} \mathbf{s}_i \geq \frac{E_s h_s^2 \mathbf{s}_i \mathbf{R}_{p/s}^{-1} \mathbf{s}_s \mathbf{s}_s^T \mathbf{R}_{p/s}^{-1} \mathbf{s}_i}{1 + E_s h_s^2 \mathbf{s}_s^T \mathbf{R}_{p/s}^{-1} \mathbf{s}_s} + \gamma_i, \quad i = 1, 2, \dots, K. \quad (219)$$

For notational simplicity, define the  $L \times L$  matrix

$$\mathbf{B}_i \triangleq h_s^2 \mathbf{R}_{p/s}^{-1} \mathbf{s}_i \mathbf{s}_i^T \mathbf{R}_{p/s}^{-1} - \beta_i h_s^2 \mathbf{R}_{p/s}^{-1} \quad (220)$$

where

$$\beta_i \triangleq \mathbf{s}_i^T \mathbf{R}_{p/s}^{-1} \mathbf{s}_i - \gamma_i, \quad i = 1, 2, \dots, K. \quad (221)$$

Then, the optimization problem in (217) can be rewritten -for one more time- as

$$\begin{aligned}\mathbf{x}^{opt} &= \arg \max_{\mathbf{x} \in \mathbb{R}^L} \mathbf{x}^T \mathbf{R}_{s/s}^{-1} \mathbf{x} \\ \text{subject to} & \quad \mathbf{x}^T \mathbf{B}_i \mathbf{x} - \beta_i \leq 0, \quad i = 1, 2, \dots, K, \\ & \quad \mathbf{x}^T \mathbf{x} \leq E_{max}\end{aligned} \quad (222)$$

where  $\mathbf{x}$  is the amplitude-including transmitted signature vector of the secondary user,  $\mathbf{x} \triangleq \sqrt{E_s} \mathbf{s}_s$ . We notice that for (222) to be solved at the secondary transmitter  $ST$ , the primary receiver  $PR$  must communicate the matrix parameters  $\mathbf{B}_i$  and scalars  $\beta_i$ ,  $i = 1, 2, \dots, K$ . Therefore, no explicit communication of the primary channel codes and gains is required that may directly compromise the privacy/security of the primary system. In terms of the computational effort, however, (i)  $\mathbf{B}_i$ ,  $i = 1, 2, \dots, K$ , are not necessarily positive semidefinite, hence the problem in (222) is in general a non-convex quadratically constrained quadratic program (non-convex QCQP), and (ii) the complexity of a solver of (222) is exponential in the dimension  $L$  (NP-hard problem).

To circumvent these two difficulties, we first observe that if we use the trace property of matrices  $\mathbf{U}, \mathbf{V}$ ,  $Tr\{\mathbf{UV}\} = Tr\{\mathbf{VU}\}$ , we are able to represent the objective function in (222) as

$$\mathbf{x}^T \mathbf{R}_{s/s}^{-1} \mathbf{x} = Tr\{\mathbf{R}_{s/s}^{-1} \mathbf{X}\} \quad (223)$$

where  $\mathbf{X} = \mathbf{x} \mathbf{x}^T$ . Thus, the optimization problem in (222) takes the new equivalent matrix form

$$\begin{aligned}\mathbf{X}^{opt} &= \arg \max_{\mathbf{X} \in \mathbb{R}^{L \times L}} Tr\{\mathbf{R}_{s/s}^{-1} \mathbf{X}\} \\ \text{subject to} & \quad Tr\{\mathbf{B}_i \mathbf{X}\} \leq \beta_i, \quad i = 1, 2, \dots, K, \\ & \quad Tr\{\mathbf{X}\} \leq E_{max}, \quad \mathbf{X} \succeq \mathbf{0}, \quad rank(\mathbf{X}) = 1\end{aligned} \quad (224)$$

where  $\mathbf{X} \succeq \mathbf{0}$  denotes that the matrix  $\mathbf{X}$  is positive semidefinite.

So far, we have shown that the original secondary cognitive link design problem in (214) is equivalent to the one in (217), (222), and finally (224), and is non-convex NP-hard. To effectively attack the problem anyway, we now propose to *relax the rank constraint* in (224) and proceed by solving the following problem *instead*,

$$\begin{aligned}\mathbf{X}' &= \arg \max_{\mathbf{X} \in \mathbb{R}^{L \times L}} Tr\{\mathbf{R}_{s/s}^{-1} \mathbf{X}\} \\ \text{subject to} & \quad Tr\{\mathbf{B}_i \mathbf{X}\} \leq \beta_i, \quad i = 1, 2, \dots, K, \\ & \quad Tr\{\mathbf{X}\} \leq E_{max}, \quad \mathbf{X} \succeq \mathbf{0}.\end{aligned} \quad (225)$$

Then, (225) is a convex polynomial-complexity problem that can be solved using semidefinite programming. Strictly speaking, we can solve (225) in polynomial time within an error  $\epsilon > 0$  from its value at the optimum point  $\mathbf{X}'$ . More specifically, let  $f_o \triangleq Tr\{\mathbf{R}_{s/s}^{-1}\mathbf{X}\}|_{\mathbf{x}=\mathbf{X}'}$ , i.e.  $f_o$  is the optimum value of the constrained (affine) objective function in (225). Then, for any given  $\epsilon > 0$ , semidefinite programming guarantees that we can converge in polynomial time (polynomial in the input size  $L$  and in the error requirement function  $\log 1/\epsilon$ ) to a solution that lies in  $(f_o - \epsilon, f_o)$  [94]. In this paper, for the semidefinite programming problem in (225), we propose to use a primal-dual interior-point method [95]. In particular, we consider the problem in (225) as the primal optimization problem, we create a differently parameterized equivalent dual problem, and then solve both problems iteratively in a coupled fashion. Then, each iteration can be implemented in  $O(L^3)$  and the algorithm converges after  $O(L \log 1/\epsilon)$  iterations to the matrix  $\mathbf{X}''$  that makes the objective function  $Tr\{\mathbf{R}_{s/s}^{-1}\mathbf{X}\}$  attain a value within  $(f_o - \epsilon, f_o)$ . The proposed method is outlined in Fig. 35. We note that relaxing the rank constraint of the non-convex NP-hard problem in (224) we created the convex optimization problem in (225) that can be solved in  $O(L^4 \log 1/\epsilon)$  time (by semidefinite programming methods as described in Fig. 35). Of course, because of the constraint relaxation itself the objective function evaluated at the optimum point  $\mathbf{X}'$  in (225) is just an upper bound on the value of the objective function evaluated at the optimum point of interest  $\mathbf{X}^{opt}$  of (224),  $Tr\{\mathbf{R}_{s/s}^{-1}\mathbf{X}^{opt}\} \leq Tr\{\mathbf{R}_{s/s}^{-1}\mathbf{X}'\}$ . Moreover,  $\mathbf{X}'$  is not available exactly either and instead we have  $\mathbf{X}''$  with  $Tr\{\mathbf{R}_{s/s}^{-1}\mathbf{X}''\} \in (Tr\{\mathbf{R}_{s/s}^{-1}\mathbf{X}'\} - \epsilon, Tr\{\mathbf{R}_{s/s}^{-1}\mathbf{X}'\})$ .

To summarize our developments so far for the cognitive design of a code-division secondary link, first, for the given primary SINR-QoS threshold  $\alpha > 0$ , we test whether  $\beta_i$ ,  $i = 1, 2, \dots, K$ , in (221) are all greater than zero. If this is not true, then the SINR-QoS constraints for the primary users cannot be met and outright no secondary transmission is allowed (see flow-chart in Fig. 36). Otherwise, we run the procedure of Fig. 35 which returns matrix  $\mathbf{X}''$ . If the rank of  $\mathbf{X}''$  is 1 with eigenvalue, eigenvector pair  $\lambda_1, \mathbf{a}_1$ , then we already have our secondary link design with signature  $\mathbf{s}_s = \mathbf{a}_1$  and transmission amplitude  $E_s = \lambda_1$ . If the rank of  $\mathbf{X}''$  is not 1, further work is needed as described below.

When  $\mathbf{X}'$  of (225) (or in practice  $\mathbf{X}''$  returned by Fig. 35) happens to be of rank 1 with eigenvalue, eigenvector pair  $\lambda_1, \mathbf{a}_1$ , then  $\mathbf{X}' \equiv \mathbf{X}^{opt}$  in (224) and  $\mathbf{x}^{opt} = \sqrt{\lambda_1}\mathbf{a}_1$  in (222). Otherwise, there is no direct path from  $\mathbf{X}'$  of (225) to  $\mathbf{x}^{opt}$  in (222). In this case, we may simply consider changing the search for an optimal vector in (222) to a search for an optimal probability density function (pdf) of vectors that maximizes the average objective function subject to average constraints, i.e.

$$\begin{aligned} f^{opt}(\mathbf{x}) &= \arg \max_{f(\mathbf{x})} E\{\mathbf{x}^T \mathbf{R}_{s/s}^{-1} \mathbf{x}\} \\ \text{subject to } & E\{\mathbf{x}^T \mathbf{B}_i \mathbf{x}\} \leq \beta_i, \quad i = 1, 2, \dots, K, \\ & E\{\mathbf{x}^T \mathbf{x}\} \leq E_{max} \end{aligned} \quad (226)$$

where  $f(\mathbf{x})$  denotes the probability density function of  $\mathbf{x}$ . This switch to a statistical optimization problem has been known as the ‘‘randomized method’’ in semidefinite programming literature [94]. Using the commutative property between trace and expectation operators, the pdf optimization problem in (226) takes the equivalent form

$$\begin{aligned} f^{opt}(\mathbf{x}) &= \arg \max_{f(\mathbf{x})} Tr\{\mathbf{R}_{s/s}^{-1} E\{\mathbf{x}\mathbf{x}^T\}\} \\ \text{subject to } & Tr\{\mathbf{B}_i E\{\mathbf{x}\mathbf{x}^T\}\} \leq \beta_i, \quad i = 1, 2, \dots, K, \\ & Tr\{E\{\mathbf{x}\mathbf{x}^T\}\} \leq E_{max}. \end{aligned} \quad (227)$$

We can show that  $f^{opt}(\mathbf{x})$  is in fact Gaussian with  $\mathbf{0}$  mean and covariance matrix  $\mathbf{X}'$ ,  $f^{opt}(\mathbf{x}) = \mathcal{N}(\mathbf{0}, \mathbf{X}')$ . With  $\mathbf{X}''$  from Fig. 35 as a close approximation of  $\mathbf{X}'$ , we can draw now a sequence of samples  $\mathbf{x}_1, \mathbf{x}_2, \dots, \mathbf{x}_P$  from  $\mathcal{N}(\mathbf{0}, \mathbf{X}'')$ . We test all of them for ‘‘feasibility’’ on the constraints of (222) whether  $\mathbf{x}_p^T \mathbf{B}_i \mathbf{x}_p \leq \beta_i$ ,  $\forall i = 1, 2, \dots, K$ , and  $\mathbf{x}_p^T \mathbf{x}_p \leq E_{max}$ ,  $p = 1, 2, \dots, P$ , and among the feasible vectors (if any) we choose the one, say  $\mathbf{x}^{(0)}$ , with maximum  $\mathbf{x}^T \mathbf{R}_{s/s}^{-1} \mathbf{x}$  objective function value (see flow-chart in Fig. 36). We could have suggested at this time a cognitive secondary link design with  $\sqrt{E_s} \mathbf{s}_s = \mathbf{x}^{(0)}$ . Instead, we will use  $\mathbf{x}^{(0)}$  as an

Formulate the pair of primal and dual semidefinite programming problems:

**Primal**

$$\max_{\mathbf{X} \in \mathbb{R}^{L \times L}} \text{Tr}\{\mathbf{R}_{s/s}^{-1} \mathbf{X}\}$$

$$\text{subject to } \text{Tr}\{\mathbf{B}_i \mathbf{X}\} \leq \beta_i, \quad i = 1, 2, \dots, K,$$

$$\text{Tr}\{\mathbf{X}\} \leq E_{max}, \quad \mathbf{X} \succeq \mathbf{0}$$

**Dual**

$$\min_{\mathbf{v} \in \mathbb{R}^{K+1}, \mathbf{Z} \in \mathbb{R}^{L \times L}} \mathbf{b}^T \mathbf{v}$$

$$\text{subject to } \sum_{i=1}^K v_i \mathbf{B}_i + v_{K+1} \mathbf{I} = \mathbf{R}_{s/s}^{-1} + \mathbf{Z}$$

$$\mathbf{Z} \succeq \mathbf{0}, \quad v_i \geq 0, \quad i = 1, 2, \dots, K+1$$

where  $\mathbf{b} \triangleq [\beta_1, \beta_2, \dots, \beta_K, E_{max}]$  and  $v_i$  is the  $i$ th element of  $\mathbf{v}$ .

(i) Initialize  $(\mathbf{X}, \mathbf{v}, \mathbf{Z}) \leftarrow (\mathbf{I}, \mathbf{0}, \mathbf{I})$ .

(ii) Calculate  $\Delta \mathbf{X}, \Delta \mathbf{v}, \Delta \mathbf{Z}$  by method in Appendix.

(iii) Replace  $\Delta \mathbf{X} \leftarrow \frac{1}{2}(\Delta \mathbf{X} + \Delta \mathbf{X}^T)$ .

(iv) Choose  $0 < \tau < 1$  and select steplengths  $n_1, n_2$

$$n_1 = \min(1, \tau \cdot \hat{n}_1), \quad \hat{n}_1 = \sup\{\ell_1 \in \mathbb{R} : \mathbf{X} + \ell_1 \Delta \mathbf{X} \succeq \mathbf{0}\},$$

$$n_2 = \min(1, \tau \cdot \hat{n}_2), \quad \hat{n}_2 = \sup\{\ell_2 \in \mathbb{R} : \mathbf{Z} + \ell_2 \Delta \mathbf{Z} \succeq \mathbf{0}\}.$$

(v) Update

$$\mathbf{X} \leftarrow \mathbf{X} + n_1 \Delta \mathbf{X},$$

$$\mathbf{v} \leftarrow \mathbf{v} + n_2 \Delta \mathbf{v},$$

$$\mathbf{Z} \leftarrow \mathbf{Z} + n_2 \Delta \mathbf{Z}.$$

(vi) Repeat (ii)-(v) until  $\mathbf{X}$  feasible solution for primal problem,  $(\mathbf{v}, \mathbf{Z})$  feasible solution for dual problem,

and the difference of primal and dual objective values lies within  $(-\epsilon, \epsilon)$ .

(vii) Return  $\mathbf{X}'' \leftarrow \mathbf{X}$ .

Figure 35: Proposed interior-point algorithm for solving (225).

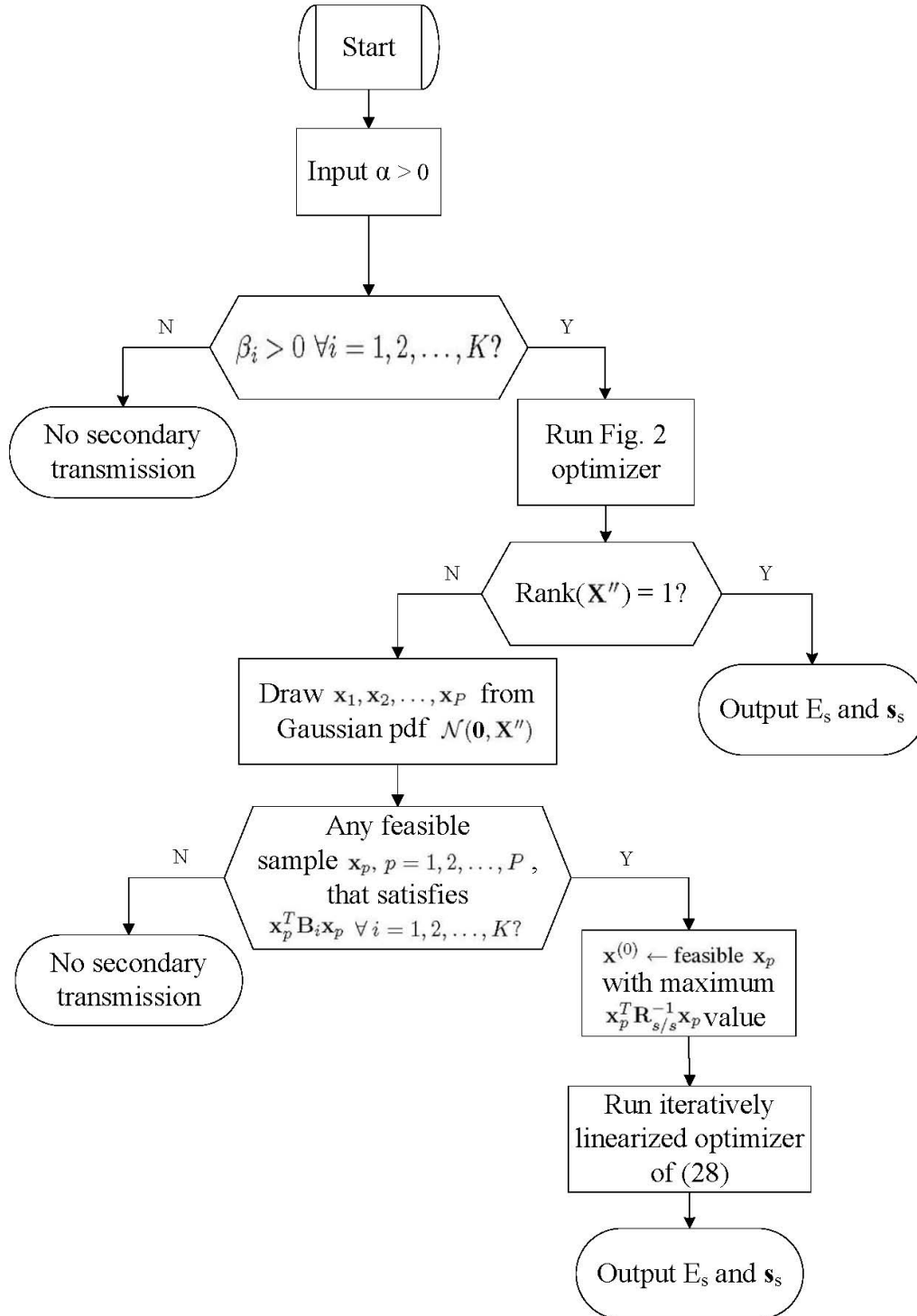


Figure 36: Flow-chart of proposed power and code allocation algorithm for secondary link.

initialization point to an iterative procedure that will lead to a much improved link design vector. The iterative procedure is developed below and its performance is evaluated by simulation studies in the next section.

First we express  $\mathbf{R}_{s/s}$  as

$$\mathbf{R}_{s/s} = \mathbf{S}\Sigma\mathbf{S}^T + \sigma^2\mathbf{I} \quad (228)$$

where  $\mathbf{S} \triangleq [\mathbf{s}_1, \mathbf{s}_2, \dots, \mathbf{s}_K]$  denotes the matrix with columns the signatures of the primary users, and  $\Sigma = \text{diag}(E_1q_1^2, E_2q_2^2, \dots, E_Kq_K^2)$ . Using the matrix inversion lemma,

$$\mathbf{R}_{s/s}^{-1} = \frac{1}{\sigma^2}\mathbf{I} - \frac{1}{\sigma^4}\mathbf{S}(\Sigma^{-1} + \frac{1}{\sigma^2}\mathbf{S}^T\mathbf{S})^{-1}\mathbf{S}^T. \quad (229)$$

Substitution of (229) in the objective function of (222) leads to

$$\mathbf{x}^T\mathbf{R}_{s/s}^{-1}\mathbf{x} = \frac{1}{\sigma^2}\mathbf{x}^T\mathbf{x} - \frac{1}{\sigma^4}\mathbf{x}^T\mathbf{Q}\mathbf{x} \quad (230)$$

where  $\mathbf{Q} \triangleq \mathbf{S}(\Sigma^{-1} + \frac{1}{\sigma^2}\mathbf{S}^T\mathbf{S})^{-1}\mathbf{S}^T$ . In (230), the first term  $\frac{1}{\sigma^2}\mathbf{x}^T\mathbf{x}$  is a convex function while the second term  $-\frac{1}{\sigma^4}\mathbf{x}^T\mathbf{Q}\mathbf{x}$  is a concave function (which implies that  $\frac{1}{\sigma^4}\mathbf{x}^T\mathbf{Q}\mathbf{x}$  is convex). Based on the first-order conditions of convex functions [96], we have

$$\mathbf{x}^T\mathbf{x} \geq 2\mathbf{x}^{(0)T}\mathbf{x} - \mathbf{x}^{(0)T}\mathbf{x}^{(0)} \quad (231)$$

where  $\mathbf{x}^{(0)}$  denotes an initial feasible vector. Then, we combine (230) and (231) and form an optimization problem that maximizes the following concave function

$$\frac{2}{\sigma^2}\mathbf{x}^{(0)T}\mathbf{x} - \frac{1}{\sigma^4}\mathbf{x}^T\mathbf{Q}\mathbf{x} - \frac{1}{\sigma^2}\mathbf{x}^{(0)T}\mathbf{x}^{(0)} \quad (232)$$

that leads to a *suboptimum* solution for our original problem in (222). To maximize (232) in view of our constraints in (222), we restrict all non-convex constraints into convex sets (linearization). In particular, we consider the non-convex constraints

$$\mathbf{x}^T\mathbf{B}_i\mathbf{x} - \beta_i \leq 0, \quad i \in \mathcal{I}_{nc}, \quad (233)$$

where  $\mathcal{I}_{nc}$  denotes the set of all indices  $i \in \{1, 2, \dots, K\}$  for which  $\mathbf{x}^T\mathbf{B}_i\mathbf{x}$  is a non-convex function. Then, we decompose the matrix  $\mathbf{B}_i$  into its positive and negative parts

$$\mathbf{B}_i = \mathbf{B}_i^+ - \mathbf{B}_i^- \quad (234)$$

where  $\mathbf{B}_i^+ = h_s^2\mathbf{R}_{p/s}^{-1}\mathbf{s}_i\mathbf{s}_i^T\mathbf{R}_{p/s}^{-1}$  and  $\mathbf{B}_i^- = \beta_i h_s^2\mathbf{R}_{p/s}^{-1}$  are all positive semidefinite. Therefore, the original constraints (233) can be written as

$$\mathbf{x}^T\mathbf{B}_i^+\mathbf{x} - \beta_i \leq \mathbf{x}^T\mathbf{B}_i^-\mathbf{x}, \quad i \in \mathcal{I}_{nc}, \quad (235)$$

where both sides of the inequality are convex quadratic functions. Linearization of the right-hand side of (235) around the vector  $\mathbf{x}^{(0)}$  leads to

$$\mathbf{x}^T\mathbf{B}_i^+\mathbf{x} - \beta_i \leq \mathbf{x}^{(0)T}\mathbf{B}_i^-\mathbf{x}^{(0)} + 2\mathbf{x}^{(0)T}\mathbf{B}_i^-(\mathbf{x} - \mathbf{x}^{(0)}), \quad i \in \mathcal{I}_{nc}. \quad (236)$$

In (236), the right-hand side is an affine lower bound on the original function  $\mathbf{x}^T\mathbf{B}_i^-\mathbf{x}$ . It is thus implied that the resulting constraints are convex and more conservative than the original ones, hence the feasible set of the linearized problem is a convex subset of the original feasible set. Thus, by linearizing the concave parts of all constraints, we obtain a set of convex constraints that are tighter than the original non-convex ones. Now, the original optimization problem takes the form

$$\begin{aligned} \mathbf{x}^{(1)} &= \arg \max_{\mathbf{x}} \frac{2}{\sigma^2}\mathbf{x}^{(0)T}\mathbf{x} - \frac{1}{\sigma^4}\mathbf{x}^T\mathbf{Q}\mathbf{x} - \frac{1}{\sigma^2}\mathbf{x}^{(0)T}\mathbf{x}^{(0)} \\ &\text{subject to } \mathbf{x}^T\mathbf{B}_i^+\mathbf{x} - \mathbf{x}^{(0)T}\mathbf{B}_i^-(2\mathbf{x} - \mathbf{x}^{(0)}) - \beta_i \leq 0, \quad i \in \mathcal{I}_{nc}, \\ &\mathbf{x}^T\mathbf{B}_i\mathbf{x} - \beta_i \leq 0, \quad i \in \bar{\mathcal{I}}_{nc}, \\ &\mathbf{x}^T\mathbf{x} \leq E_{max} \end{aligned} \quad (237)$$

where  $\bar{\mathcal{I}}_{nc} = \{1, 2, \dots, K\} - \mathcal{I}_{nc}$ . The problem in (237) is a convex QCQP problem and can be solved efficiently by standard convex system solvers [97] to produce a new feasible vector  $\mathbf{x}^{(1)}$ . The objective function  $\mathbf{x}^T \mathbf{R}_{s/s}^{-1} \mathbf{x}$  in (222) evaluated at  $\mathbf{x}^{(1)}$  takes a value that is larger than or equal to its value at  $\mathbf{x}^{(0)}$ . Repeating iteratively the linearization procedure, we can obtain a sequence of feasible vectors  $\mathbf{x}^{(0)}, \mathbf{x}^{(1)}, \mathbf{x}^{(2)}, \dots, \mathbf{x}^{(T)}$  with non-decreasing values of the objective function in (222). This procedure converges after very few (eight or nine) iterations as demonstrated experimentally in the following section.

### 3.5.3 Simulation Studies and Discussions

We consider a primary CDMA system with signature length (system processing gain)  $L = 16$  and  $K$  synchronous users. We are interested in establishing a secondary code-division transmitter/receiver pair when the primary system is fully loaded to overloaded, say  $K$  varies from 16 to 20. All signatures for primary users are generated from a minimum total-squared-correlation optimal binary signature set which achieves the Karystinos-Pados (KP) bound for each  $(K, L)$  pair of values<sup>4</sup> [98]-[100]. The transmission SNRs of the  $K$  primary users are all set equal to  $\frac{E_i}{\sigma^2} = 15dB, i = 1, 2, \dots, K$ ; the maximum allowable transmission SNR for the secondary link is set to  $\frac{E_{max}}{\sigma^2} = 12dB$ . The channel coefficients  $h_i$  and  $q_i, i = 1, 2, \dots, K$ , (see Fig. 34) are taken to be the magnitude of independent complex Gaussian random variables with mean 0 and variance 4; the same holds true for  $h_s$  and  $q_s$ . The receiver SINR threshold for primary users is set to  $\alpha = 2dB$  which corresponds to an average raw bit-error-rate (BER) at the output of the maximum SINR linear filter receiver of about  $10^{-1}$ . Ten thousand (10,000) system/secondary-line optimization experiments are run under the described (quasi-static) flat fading conditions. When random vector drawing is necessitated by the flow-chart in Fig. 36,  $P = 50$  test vector points are generated.

In Fig. 37, we plot as a function of the number of primary system users  $K$  the percentage of time that secondary transmission is enabled directly under the case  $rank(\mathbf{X}'') = 1$  or by the iterative linearized optimizer as well as the ‘‘Interference-Minimizing-Code-Assignment’’ (IMCA) scheme in [86]. We observe that significant opportunity exists for cognitive secondary transmission when the primary system is fully loaded ( $K = L = 16$ ). As we expect, Fig. 37 shows that the frequency of secondary transmissions reduces as the primary system load increases. We observe also that our proposed scheme offers more opportunities for cognitive secondary transmission than [86].

In Fig. 38, we test the quality of the secondary transmission line (the pre-set SINR-QoS of the primary system is -of course- guaranteed by the algorithmic procedure) and the significance of the iterative linearized optimizer in (237) (see flow-chart in Fig. 36). We fix the primary system load  $K = 16$  (fully loaded) and plot the secondary receiver *average* SINR for the experimental instants of  $rank(\mathbf{X}'') > 1$  as a function of the iteration of the optimizer initialized at the point/design  $\mathbf{x}^{(0)}$  that is the best out of  $P = 50$  samples drawn from the  $\mathcal{N}(\mathbf{0}, \mathbf{X}'')$  pdf. It is pleasing to observe that eight or nine iterations are enough for effective convergence.

Finally, in Fig. 39, to gain visual insight into the operation of the primary/secondary system we plot the *instantaneous* receiver SINR of a primary signal and the secondary signal for the case  $K = 17$  over an experimental data record sequence of 1000 Rayleigh fading channel realizations. Missing secondary signal SINR values indicate the instances when no secondary transmission was allowed. The proposed scheme almost doubled the occurrences of secondary transmission compared to [86]. When secondary transmissions do occur for both schemes, the joint power and sequence optimization executed by the proposed scheme results in superior SINR performance for the secondary receiver over [86].

### Appendix: Calculation of $\Delta\mathbf{X}, \Delta\mathbf{v}, \Delta\mathbf{Z}$ of Fig. 35

Let  $vec\{\cdot\}$  denote column-by-column matrix vectorization and  $mat\{\cdot\}$  the exact inverse operation. Choose  $0 \leq \delta < 1$  and define  $\mu \triangleq \delta \frac{Tr\{\mathbf{X}\mathbf{Z}\}}{L}$ .

<sup>4</sup>For  $L = 16$ , when  $K \leq L$  the KP-optimal sequences coincide with the familiar Walsh-Hadamard signature codes.

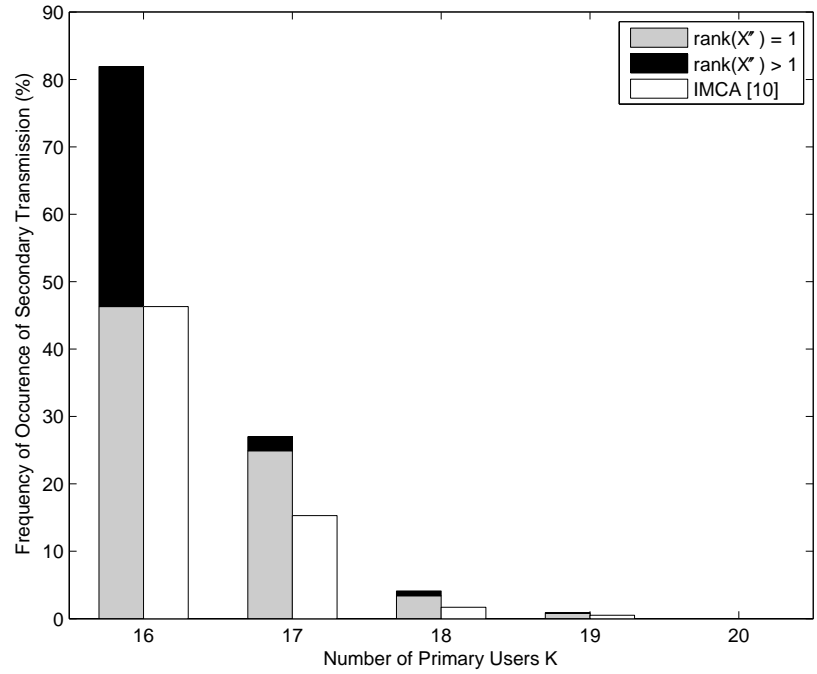


Figure 37: Secondary transmission percentage as a function of the number of primary users under Cases  $\text{rank}(\mathbf{X}'') = 1$  and  $> 1$  (the study includes also the code assignment scheme in [86]).

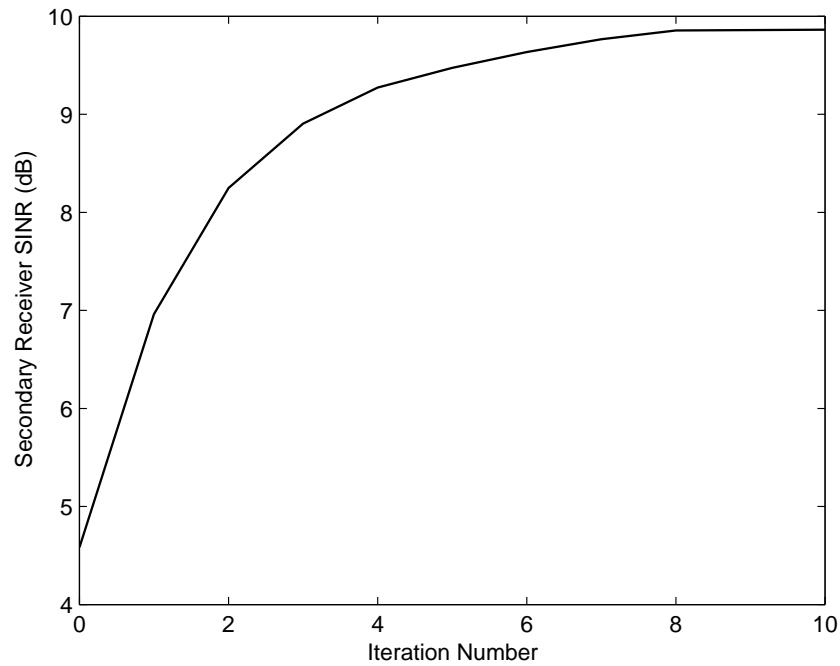


Figure 38: Secondary receiver SINR as a function of the iteration step of the linearized optimizer in (237) initialized at the best feasible sample out of  $P = 50$  drawings from the  $\mathcal{N}(\mathbf{0}, \mathbf{X}'')$  pdf.

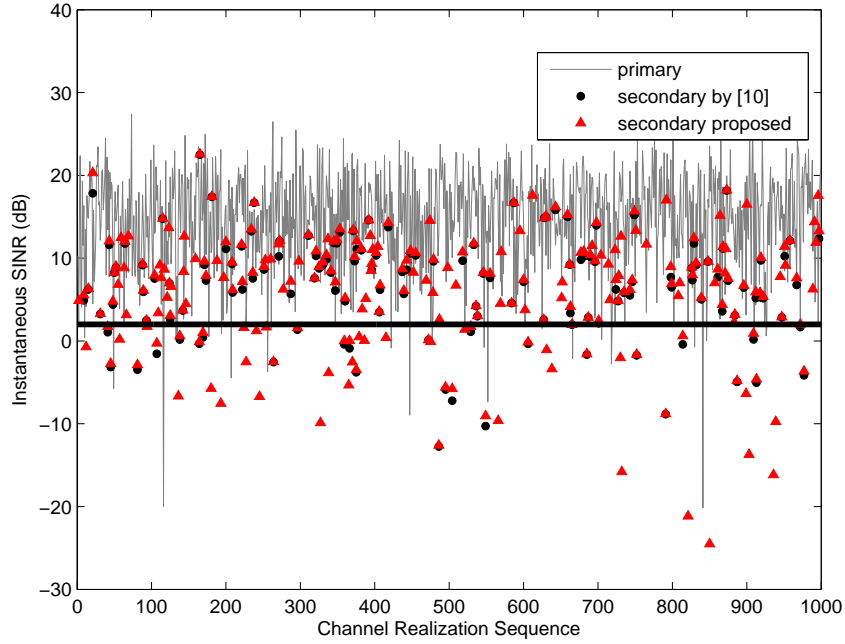


Figure 39: Instantaneous output SINR of a primary signal against SINR-QoS threshold  $\alpha$  (thick line) and instantaneous output SINR of secondary signal.

In Fig. 35,  $\Delta\mathbf{X}$ ,  $\Delta\mathbf{v}$ ,  $\Delta\mathbf{Z}$  are obtained by solving the following linear system

$$\begin{bmatrix} \mathbf{0} & \mathbf{B}^T & \mathbf{I} \\ \mathbf{B} & \mathbf{0} & \mathbf{0} \\ \mathbf{E} & \mathbf{0} & \mathbf{F} \end{bmatrix} \begin{bmatrix} \text{vec}\{\Delta\mathbf{X}\} \\ \Delta\mathbf{v} \\ \text{vec}\{\Delta\mathbf{Z}\} \end{bmatrix} = \begin{bmatrix} \text{vec}\{\mathbf{T}_1\} \\ \mathbf{t}_2 \\ \text{vec}\{\mathbf{T}_3\} \end{bmatrix} \quad (238)$$

where

$$\mathbf{B}_{(K+1) \times L^2} \triangleq \begin{bmatrix} (\text{vec}\{\mathbf{B}_1\})^T \\ \vdots \\ (\text{vec}\{\mathbf{B}_K\})^T \\ (\text{vec}\{\mathbf{I}\})^T \end{bmatrix},$$

$\mathbf{T}_1_{L \times L} \triangleq \mathbf{R}_{s/s}^{-1} + \mathbf{Z} - \text{mat}\{\mathbf{B}^T \mathbf{v}\}$ ,  $\mathbf{t}_2_{(K+1) \times 1} \triangleq \mathbf{b} - \mathbf{B} \text{vec}\{\mathbf{X}\}$ ,  $\mathbf{T}_3_{L \times L} \triangleq \mu \mathbf{I} - \mathbf{XZ}$ ,  $\mathbf{E}_{L^2 \times L^2} \triangleq \mathbf{Z} \otimes \mathbf{I}$ , and  $\mathbf{F}_{L^2 \times L^2} \triangleq \mathbf{I} \otimes \mathbf{X}$  ( $\otimes$  denotes the standard Kronecker product). Applying Gauss elimination, the solution is

$$\Delta\mathbf{v} = (\mathbf{B}\mathbf{E}^{-1}\mathbf{F}\mathbf{B})^{-1}(\mathbf{t}_2 + \mathbf{B}\mathbf{E}^{-1}(\mathbf{F}\text{vec}\{\mathbf{T}_1\} - \text{vec}\{\mathbf{T}_3\})), \quad (239)$$

$$\text{vec}\{\Delta\mathbf{X}\} = -\mathbf{E}^{-1}(\mathbf{F}(\text{vec}\{\mathbf{T}_1\} - \mathbf{B}^T \Delta\mathbf{v}) - \text{vec}\{\mathbf{T}_3\}), \quad (240)$$

$$\text{vec}\{\Delta\mathbf{Z}\} = \text{vec}\{\mathbf{T}_1\} - \mathbf{B}^T \Delta\mathbf{v}. \quad (241)$$

## 4 Conclusions

In this report, we summarized our findings resulting from the project and described in details the system models and the proposed methods and procedures. First, we developed, for the first time, a closed-form asymptotically tight (as  $\text{SNR} \rightarrow \infty$ ) approximation of the outage probability for the DF cooperative ARQ relay scheme under fast fading conditions. The analytical approach relies on two lemmas that we established in this project. The closed-form expression provides significant insight on the benefits of the DF cooperative ARQ relaying relative

to direct ARQ scheme in fast fading scenarios and shows that the cooperative scheme achieves diversity order equal to  $2L - 1$  while the diversity order of the direct scheme is only  $L$ . Simulation and numerical results show that the closed-form approximation of the outage probability is tight at high SNR. Based on the asymptotically tight approximation of the outage analysis, we were able to determine an optimum power allocation for the DF cooperative ARQ relay scheme. It turns out that the equal power allocation is not optimum in general and the optimum power allocation depends on the link quality of the channels related to the relay. It shows that we should allocate more power at the source and less at the relay. Simulation results show that the DF cooperative ARQ relay scheme with the optimum power allocation has a performance improvement of more than 1dB compared to the scheme with the equal power allocation.

Second, we determined an optimal transmission power assignment strategy for the H-ARQ protocol in quasi-static Rayleigh fading channels to minimize the average total transmission power. A locally optimal power sequence was found first by the Lagrangian multiplier and then it was shown optimal globally. The optimal transmission power sequence is described by a set of equations which allow an exact recursive calculation of the optimal power sequence. To reduce calculation complexity, we also developed an approximation to the optimal power sequence that is close to the numerically calculated exact result. It is interesting to observe that the optimal transmission power sequence is neither increasing nor decreasing; its form depends on given total power budget and targeted outage performance levels. The optimal power assignment sequence reveals that conventional equal-power assignment is far from optimal. For example, for a targeted outage performance of  $10^{-5}$  and maximum number of transmissions  $L = 5$ , the average total transmission power by the optimum assignment is about 27 dB less than that of using the equal-power assignment. We also observe that with the same targeted outage performance, the larger the number of retransmission rounds allowed in the H-ARQ protocol, the larger the performance gain between the optimal power assignment scheme and the equal-power assignment scheme. Moreover, the lower the required outage probability, the more performance gain of the optimal power assignment strategy compared to the equal-power strategy.

Third, we analyzed the outage probability performance of the differential amplify-and-forward (DAF) relaying and obtained an exact formula that involves only a single integral and is much more practical than the only previously known result that involves a triple integral. To gain further insight in the process of the DAF relaying, we also developed a simple closed-form approximation for the outage probability which is tight at high SNR. Based on the tight outage probability approximation, we finally determined an asymptotically optimum power allocation scheme for the DAF relaying. We have carried out extensive numerical calculations and simulations to validate and illustrate our analysis.

Fourth, we designed and optimized a multi-source multi-destination relay network where a relay amplifies and forwards simultaneously the signals received from all sources. We developed two optimum power assignment schemes. The first scheme minimizes the total power consumption of all sources and the relay under the constraint that the SINR requirement of each source-destination pair is satisfied, while the second scheme maximizes the minimum SINR of all source-destination pairs. Clearly, both optimization problems as stated above involve  $K$  power variables, where  $K$  is the number of source-destination pairs in the network, which implies that an exhaustive search approach is prohibitive for large  $K$ . In this paper, we derived an asymptotically tight approximation of the SINR that allows us to reformulate the original optimization problems, and eventually reduce them to single-parameter optimization problems, which can be easily solved by numerical search of the single parameter. Then, the corresponding optimal transmission power at each source and at the relay can be calculated directly. The proposed optimization scheme is scalable and the power assignment algorithm has the same optimization complexity for any number of source-destination pairs in the network. Moreover, we also applied the developed methodology to solve a related max-min SINR based optimization problem, where for any given total power budget, we are able to determine the optimum power assignment for the sources and the relay to maximize the minimum SINR of all source-destination pairs.

Finally, we considered the problem of cognitive code-division channelization for cognitive airborne networks. The goal is to improve the efficiency of spectrum utilization and coexisting of primary and secondary users in heterogeneous cognitive airborne networks, by jointly assigning power and code-channel allocation for a secondary transmitter/receiver pair coexisting with a primary CDMA system. Unfortunately, in a common Rayleigh fading wireless environment, the formulated constrained optimization problem is non-convex

and NP-hard in the code vector dimension. Nevertheless, in pursuit of a computationally manageable and performance-wise appealing suboptimal solution, we first converted the amplitude/code-vector optimization problem to an equivalent matrix optimization problem under a rank-1 constraint. Disregarding (relaxing in formal language) the rank-1 constraint makes the problem amenable to an easy polynomial-cost semidefinite programming solution. When luckily, a rank-1 matrix happens to be returned, optimal secondary-line design is achieved. For the common case of a higher rank, we developed an iterative linearized polynomial-cost convex optimizer with much appealing (yet suboptimal) amplitude/code-vector design solutions after a few iterations. Extensive numerical studies have validated our theoretical developments and the proposed iterative algorithm. The proposed scheme almost doubled the occurrences of secondary transmission compared to some early work. The joint power and sequence optimization executed by the proposed scheme results in superior SINR performance for the secondary receiver compared to prior work. The proposed scheme has great potential to improve the efficiency of coexisting of primary and secondary users in heterogeneous cognitive airborne networks.

## References

- [1] A. Sendonaris, E. Erkip, and B. Aazhang, "User cooperation diversity-Part I: system description," *IEEE Trans. Comm.*, vol. 51, pp.1927-1938, Nov. 2003.
- [2] A. Sendonaris, E. Erkip, and B. Aazhang, "User cooperation diversity-Part II: implementation aspects and performance analysis," *IEEE Trans. Comm.*, vol. 51, pp.1939-1948, Nov. 2003.
- [3] J. N. Laneman, D. N. C. Tse, and G. W. Wornell, "Cooperative diversity in wireless networks: efficient protocols and outage behavior," *IEEE Trans. Inform. Theory*. vol. 50, pp.3062-3080, Dec. 2004.
- [4] J. N. Laneman and G. W. Wornell, "Distributed space-time coded protocols for exploiting cooperative diversity in wireless networks," *IEEE Trans. Inform. Theory*, vol. 49, pp.2415-2425, Oct. 2003.
- [5] A. Nosratinia, T. E. Hunter and A. Hedayat, "Cooperative communication in wireless networks," *IEEE Communications Magazine*, vol. 42, pp.74-80, Oct. 2004.
- [6] T. E. Hunter and A. Nosratinia, "Diversity through coded cooperation," *IEEE Trans. Wireless Comm.*, vol. 5, pp.283-289, Feb. 2006.
- [7] W. Su, A. K. Sadek, and K. J. R. Liu, "Cooperative communication protocols in wireless networks: performance analysis and optimum power allocation," *Wireless Personal Communications (Springer)*, vol. 44, no. 2, pp.181-217, January 2008.
- [8] K. J. R. Liu, A. Sadek, W. Su, and A. Kwasinski, *Cooperative Communications and Networking*, New York, NY: Cambridge University Press, 2009.
- [9] E. C. van der Meulen, "A survey of multi-way channels in information theory: 1961-1976," *IEEE Trans. Inform. Theory*, vol. 23, no. 1, pp.1-37, Jan. 1977.
- [10] T. M. Cover and A. A. El Gamal, "Capacity theorems for the relay channel," *IEEE Trans. Inform. Theory*, vol. 25, no. 5, pp.572-584, Sep. 1979.
- [11] A. Høst-Madsen and J. Zhang, "Capacity bounds and power allocation for wireless relay channels," *IEEE Trans. Inform. Theory*, vol. 51, pp.2020-2040, Jun. 2005.
- [12] G. Kramer, M. Gastpar and P. Gupta, "Cooperative strategies and capacity theorems for relay networks," *IEEE Trans. Inform. Theory*, vol. 51, pp.3037-3063, Sep. 2005.
- [13] T. Himsoon, W. P. Siriwongpairat, W. Su, and K. J. R. Liu, "Differential modulation with threshold-based decision combining for cooperative communications," *IEEE Trans. on Signal Processing*, vol. 55, no. 7, pp.3905-3923, July 2007.
- [14] W. Su and X. Liu, "On optimum selection relaying protocols in cooperative wireless networks," *IEEE Trans. on Communications*, vol. 58, no. 1, pp.52-57, January 2010.
- [15] S. Lin and D. J. Costello, Jr., *Error Control Coding: Fundamentals and Applications*. Englewood Cliffs, NJ: Prentice-Hall, 2004.
- [16] A. Goldsmith, *Wireless Communications*. New York, NY: Cambridge University Press, 2005.
- [17] D. Chase, "A combined coding and modulation approach for communication over dispersive channels," *IEEE Trans. Comm.*, vol. 21, pp. 159-174, Mar. 1973.
- [18] S. Lin and P. Yu, "A hybrid ARQ scheme with parity retransmission for error control of satellite channels," *IEEE Trans. Comm.*, vol. 30, pp. 1701-1719, Jul. 1982.

- [19] G. Benelli, "An ARQ scheme with memory and soft error detectors," *IEEE Trans. Comm.*, vol. 33, pp. 285-288, Mar. 1985.
- [20] R. Comroe and D. J. Costello, Jr., "ARQ schemes for data transmission in mobile radio systems," *IEEE J. Select. Areas Commun.*, vol. 2, pp. 472-481, Jul. 1984.
- [21] G. Caire and D. Tuninetti, "The throughput of hybrid-ARQ protocols for the Gaussian collision channel," *IEEE Trans. Inform. Theory*, vol. 47, pp. 1971-1988, July 2001.
- [22] B. Zhao and M. C. Valenti, "Practical relay networks: a generalization of hybrid-ARQ," *IEEE J. Select. Areas Commun.*, vol. 23, no. 1, pp.7-18, Jan. 2005.
- [23] T. Tabet, S. Dusad and R. Knopp, "Diversity-multiplexing-delay tradeoff in half-duplex ARQ relay channels," *IEEE Trans. Inform. Theory*, vol. 53, pp.3797-3805, Oct. 2007.
- [24] L. Weng and R. D. Murch, "Achievable diversity-multiplexing-delay tradeoff for ARQ cooperative broadcast channels," *IEEE Trans. Wireless Communications*, vol. 7, no. 5, pp.1828-1832, May 2008.
- [25] S. Tomasin, M. Levorato, and M. Zorzi, "Analysis of outage probability for cooperative networks with HARQ," in *Proc. IEEE Int. Symp. Infor. Theory (ISIT)*, Nice, France, June 2007.
- [26] S. Tomasin, M. Levorato, and M. Zorzi, "Steady state analysis of coded cooperative networks with HARQ protocol," *IEEE Trans. Communications*, vol. 57, no. 8, pp.2391-2401, Aug. 2009.
- [27] H. Boujemaa, "Delay analysis of cooperative truncated HARQ with opportunistic relaying," *IEEE Trans. Vehicular Technology*, vol. 58, no. 9, pp.4795-4804, Nov. 2009.
- [28] S. M. Alamouti, "A simple transmit diversity technique for wireless communications," *IEEE J. Select. Areas Commun.*, vol. 16, no. 8, pp.1451-1458, Oct. 1998.
- [29] J. N. Laneman, "Limiting analysis of outage probabilities for diversity schemes in fading channels," in *Proc. IEEE Global Comm. Conf. (GLOBECOM)*, vol. 3, pp.1242-1246, Dec. 2003.
- [30] I. S. Gradshteyn and I. M. Ryzhik, *Table of Integrals, Series, and Products*, San Diego, CA: Academic Press, 1994.
- [31] M. Chang, C. Kim, and C. C. J. Kuo, "Power control for packet-based wireless communication systems," in *Proc. IEEE Wireless Comm. Networks Conf. (WCNC)*, New Orleans, LA, Mar. 2003, vol. 1, pp. 542-546.
- [32] I. Stanojev, O. Simeone, Y. Bar-Ness, and D. Kim, "On the energy efficiency of hybrid-ARQ protocols in fading channels," in *Proc. IEEE ICC.*, Glasgow, UK, Jun. 2007, pp. 3173-3177.
- [33] N. Arulselvan and R. Berry, "Efficient power allocations in wireless ARQ protocols," in *Proc. IEEE 5th Symp. on Wireless Personal Multimedia Commun.*, Honolulu, Hawaii, Oct. 2002, vol. 3, pp. 976-980.
- [34] A. K. Karmokar, D. V. Djonin, and V. K. Bhargava, "Delay constrained rate and power adaptation over correlated fading channels," in *Proc. IEEE GLOBECOM*, Dallas, Texas, Nov. 2004, vol. 6, pp. 3448-3453.
- [35] H. Seo and B. G. Lee, "Optimal transmission power for single- and multi-hop links in wireless packet networks with ARQ capability," *IEEE Trans. Comm.*, vol. 55, pp. 996-1006, May 2007.
- [36] C. Shen, T. Liu, and M. P. Fitz, "On the average rate performance of hybrid-ARQ in quasi-static fading channels," *IEEE Trans. Comm.*, vol. 57, no. 11, pp. 3339-3352, Nov. 2009.
- [37] D. G. Brennan, "Linear diversity combining techniques," *Proceedings of IEEE*. vol. 91, pp. 331-356, Feb. 2003.

- [38] M. K. Simon and M.-S. Alouini, *Digital Communications over Fading Channels: A Unified Approach to Performance Analysis*, John Wiley & Sons, New York, NY, 2000.
- [39] J. N. Laneman, D. N. C. Tse, and G. W. Wornell, "Cooperative diversity in wireless networks: Efficient protocols and outage behavior," *IEEE Transaction on Information Theory*, vol. 50, pp. 3062-3080, Dec. 2004.
- [40] G. Kramer, M. Gastpar, and P. Gupta, "Cooperative strategies and capacity theorems for relay networks," *IEEE Trans. Inform. Theory*, vol. 51, no. 9, pp.3037-3063, September 2005.
- [41] T. Himsoon, W. P. Siriwongpairat, W. Su, and K. J. R. Liu, "Differential modulation with threshold-based decision combining for cooperative communications," *IEEE Trans. on Signal Processing*, vol. 55, no. 7, pp.3905-3923, July 2007.
- [42] T. Himsoon, W. Su, and K. J. R. Liu, "Differential Transmission for Amplify-and-Forward Cooperative Communications," *IEEE Signal Processing Letters*, vol. 12, pp. 597-600, Sep. 2005.
- [43] Q. Zhao and H. Li, "Differential Modulation for Cooperative Wireless Systems," *IEEE Trans. on Signal Processing*, vol. 55, pp. 2273-2283, May. 2007.
- [44] B. L. Hughes, "Differential space-time modulation," *IEEE Trans. Inform. Theory*, vol. 46, pp. 2567-2578, Nov. 2000.
- [45] B. M. Hochwald and W. Sweldens, "Differential unitary space-time modulation," *IEEE Trans. Commun.*, vol. 48, pp. 2041-2052, Dec. 2000.
- [46] J. G. Proakis, *Digital Communications*, 4th ed. New York: McGraw-Hill, 2000.
- [47] M. K. Simson and M. S. Alouini, *Digital Communications Over Fading Channels: A Unified Approach to Performance Analysis*, New York: Wiley, 2000
- [48] I. S. Gradshteyn and I. M. Ryzhik, *Table of integrals, series, and products*, 4th Edition, New York: Academic Press, 1980.
- [49] M. Abramowitz and I. A. Ryzhik, *Handbook of Mathematical Functions With Formulas, Groups, and Mathematical Tables*, New York: Dover, 1972.
- [50] A. Sendonaris, E. Erkip, and B. Aazhang, "User cooperation diversity-Part I: system description," *IEEE Transactions on Communications*, vol. 51, no. 11, pp.1927-1938, Nov. 2003.
- [51] A. Sendonaris, E. Erkip, and B. Aazhang, "User cooperation diversity-Part II: implementation aspects and performance analysis," *IEEE Transactions on Communications*, vol. 51, no. 11, pp.1939-1948, Nov. 2003.
- [52] J. N. Laneman and G. W. Wornell, "Distributed space-time-coded protocols for exploiting cooperative diversity in wireless networks," *IEEE Transactions on Information Theory*, vol. 49, no. 10, pp.2415-2425, Oct. 2003.
- [53] G. Kramer, M. Gastpar, and P. Gupta, "Cooperative strategies and capacity theorems for relay networks," *IEEE Transactions on Information Theory*, vol. 51, no. 9, pp.3037-3063, September 2005.
- [54] A. Reznik, S. R. Kulkarni, and S. Verdu, "Degraded Gaussian multirelay channel: capacity and optimal power allocation," *IEEE Transactions on Information Theory*, vol. 50, pp.3037-3046, Dec. 2004.
- [55] W. Su, A. K. Sadek, and K. J. R. Liu, "Cooperative communication protocols in wireless networks: performance analysis and optimum power allocation," *Wireless Personal Communications (Springer)*, vol. 44, no. 2, pp.181-217, January 2008.

- [56] A. K. Sadek, W. Su, and K. J. R. Liu, "Multi-node cooperative communications in wireless networks," *IEEE Transactions on Signal Processing*, vol. 55, no. 1, pp.341-355, January 2007.
- [57] K. J. R. Liu, A. Sadek, W. Su, and A. Kwasinski, *Cooperative Communications and Networking*, New York, NY: Cambridge University Press, 2009.
- [58] O. Sahin and E. Erkip, "Achievable rates for the Gaussian interference relay channel," in *Proc. IEEE Global Telecommunications Conference*, pp.1627-1631, Washington, DC, Nov. 2007.
- [59] O. Sahin, O. Simeone, and E. Erkip, "Interference channel aided by an infrastructure relay," in *Proc. IEEE International Symposium on Information Theory*, pp.2023-2027, Seoul, Korea, Jun. 2009.
- [60] O. Sahin, E. Erkip, and O. Simeone, "Interference channel with a relay: Models, relaying strategies, bounds," in *Information Theory and Application Workshop*, pp.90-95, San Diego, CA, Feb. 2009.
- [61] A. Carleial, "Interference channels," *IEEE Transactions on Information Theory*, vol. 24, no. 1, pp.60-70, Jan. 1978.
- [62] I. Maric, R. Dabora and A. Goldsmith, "On the capacity of the interference channel with a relay," in *Proc. IEEE International Symposium on Information Theory*, pp.554-558, Jul. 2008.
- [63] R. Dabora, I. Maric, and A. Goldsmith, "Interference forwarding in multiuser networks," in *Proc. IEEE Global Telecommunications Conference*, pp.1-5, New Orleans, LO, Nov. 2008.
- [64] O. Sahin and E. Erkip, "On achievable rates for interference relay channel with interference cancellation," in *Proc. Asilomar Conference on Signals, Systems and Computers*, pp.805-809, Pacific Grove, CA, Nov. 2007.
- [65] S. Sridharan, S. Vishwanath, S. A. Jafar, and S. Shamaï "On the capacity of cognitive relay assisted Gaussian interference channel," in *Proc. IEEE International Symposium on Information Theory*, pp.549-553, Jul. 2008.
- [66] L. Le and E. Hossain, "Multihop cellular networks: potential gains, research challenges, and a resource allocation framework," *IEEE Communications Magazine*, vol. 45, no. 9, pp.66-73, Sep. 2007.
- [67] J. Tang and X. Zhang, "Cross-layer resource allocation over wireless relay networks for quality of service provisioning," *IEEE Journal on Selected Areas in Communications*, vol. 25, no. 4, pp.645-655, May 2007.
- [68] K. G. Seddik, A. K. Sadek, W. Su, and K. J. R. Liu, "Outage analysis and optimal power allocation for multi-node relay networks," *IEEE Signal Processing Letters*, vol. 14, no. 6, pp.377-380, Jun. 2007.
- [69] Y. Liang, V. V. Veeravalli, and H. V. Poor, "Resource allocation for wireless fading relay channels: Max-min solution," *IEEE Transactions on Information Theory*, vol. 53, no. 10, pp.3432-3453, Oct. 2007.
- [70] D. S. Michalopoulos and G. K. Karagiannidis, "Physical-layer Fairness in amplify and forward cooperative diversity systems," *IEEE Transactions on Wireless Communications*, vol. 7, no. 3, pp.1073-1083, Mar. 2008.
- [71] O. Sahin and E. Erkip, "Dynamic resource allocation for multi source-destination relay networks," in *Proc. 41st Annual Conference on Information Sciences and Systems*, pp.19-24, Baltimore, MD, Mar. 2007.
- [72] T. K. Phan, T. Le-Ngoc, S. A. Vorobyov, and C. Tellambura, "Power allocation in wireless relay networks: A geometric programming based approach," in *Proc. IEEE Global Telecommunications Conference*, pp.1-5, New Orleans, LO, USA, Nov. 2008.
- [73] T. K. Phan, L. B. Le, S. A. Vorobyov, and T. Le-Ngoc, "Centralized and distributed power allocation in multi-user wireless relay networks," in *Proc. IEEE International Conference on Communications*, pp.1-5, Dresden, Germany, Jun. 2009.

- [74] M.O. Hasna and M.S. Alouini, "Performance analysis of two-hop relayed transmissions over Rayleigh fading channels," in *Proc. IEEE 56th Vehicular Technology Conference*, vol.4, pp. 1992-1996, Sep. 2002.
- [75] R. A. Horn and C. R. Johnson, *Matrix Analysis*, New York: Cambridge Univ. Press, 1990.
- [76] D. Tse and P. Viswanath, *Fundamentals of Wireless Communication*, Cambridge University Press, 2005
- [77] Federal Comm. Commission, Spectrum Policy Task Force, Report ET Docket no. 02-135, Nov. 2002.
- [78] J. Mitola and G. Q. Maguire, "Cognitive radios: Making software radios more personal," *IEEE Pers. Commun.*, vol. 6, pp. 13-18, Aug. 1999.
- [79] S. Haykin, "Cognitive radio: Brain-empowered wireless communications," *IEEE J. Select. Areas Commun.*, vol. 23, pp. 201-220, Feb. 2005.
- [80] A. Ghasemi and E. S. Sousa, "Fundamental limits of spectrum-sharing in fading environments," *IEEE Trans. Wireless Commun.*, vol. 6, pp. 649-658, Feb. 2007.
- [81] S. Srinivasa and S. A. Jafar, "The throughput potential of cognitive radio: A theoretical perspective," *IEEE Commun. Magazine*, vol. 45, pp. 73-79, May. 2007.
- [82] G. Ganesan and Y. Li, "Cooperative spectrum sensing in cognitive radio, Part I: Two-user networks," *IEEE Trans. Wireless Commun.*, vol. 6, pp. 2204-2213, Jun. 2007.
- [83] Q. Qu, L. B. Milstein, and D. R. Vaman, "Cognitive radio based multi-user resource allocation in mobile ad hoc networks using multi-carrier CDMA modulation," *IEEE J. Select. Areas Commun.*, vol. 26, pp. 70-82, Jan. 2008.
- [84] F. Granelli, P. Pawelczak, R. V. Prasad, K. P. Subbalakshmi, R. Chandramouli, J. A. Hoffmeyer, and H. S. Berger, "Standardization and research in cognitive and dynamic spectrum access networks: IEEE SCC41 efforts and other activities," *IEEE Commun. Magazine*, vol. 48, pp. 71-79, Jan. 2010.
- [85] Y. Xing, C. Mathur, M. A. Haleem, R. Chandramouli, and K. P. Subbalakshmi, "Dynamic spectrum access with QoS and interference temperature constraints," *IEEE Trans. Mobile Computing*, vol. 6, pp. 423-433, Apr. 2007.
- [86] A. Elezabi, M. Kashef, M. Abdallah, M. Khairy, "CDMA underlay network with cognitive interference-minimizing code assignment and semi-blind interference suppression," in *Journ. Wireless Commun. Mob. Comput.*, vol. 9, pp. 1460-1471, 2009.
- [87] M. Kashef, M. Abdallah, A. Elezabi, M. Khairy, "System parameter selection for asymmetric underlay CDMA networks with interference-minimizing code assignment," in *Proc. IEEE 10th Workshop on Signal Proc. Advances in Wireless Comm.*, Perugia, Italy, Jun. 2009, pp. 722-726.
- [88] L. Zhang, Y. C. Liang, and Y. Xin, "Joint beamforming and power allocation for multiple access channels in cognitive radio networks," *IEEE J. Select. Areas Commun.*, vol. 26, pp. 38-51, Jan. 2008.
- [89] M. Islam, Y. Liang, and A. Hoang, "Joint power control and beamforming for cognitive radio networks," *IEEE Trans. Wireless Commun.*, vol. 7, pp. 2415-2419, Jul. 2008.
- [90] J. Huang, R. Berry, and M. L. Honig, "Auction-based spectrum sharing," *ACM/Springer Mobile Networks and Applications J. (MONET)*, vol. 11, no. 3, Jun. 2006.
- [91] D. G. Manolakis, V. K. Ingle, S. M. Kogon, *Statistical and adaptive signal processing: Spectral estimation, signal modeling, adaptive filtering, and array processing*. New York, NY: McGraw-Hill, 2000.
- [92] P. M. Pardalos and S. A. Vavasis, "Quadratic programming with one negative eigenvalue is NP-hard," *J. Global Optim.*, vol. 1, pp. 15-22, 1991.

- [93] S. Haykin, *Adaptive Filter Theory, 4th edition*. Upper Saddle River, NJ: Prentice Hall, 2002.
- [94] M. Goemans and D. P. Williamson, "Improved approximation algorithms for maximum cut and satisfiability problems using semidefinite programming," *J. Assoc. Comput. Mach.*, vol. 42, no. 6, pp. 1115-1145, Nov. 1995.
- [95] F. Alizadeh, J. Haeberly, and M. Overton, "Primal-dual interior point methods for semidefinite programming: Convergence rates, stability and numerical results," *SIAM J. Optimiz.*, vol. 8, no. 3, pp. 746-768, Aug. 1998.
- [96] S. Boyd and L. Vandenberghe, *Convex Optimization*. Cambridge, UK: Cambridge University Press, 2004.
- [97] M. Grant and S. Boyd, CVX Version 1.2—A MATLAB software, Feb. 2009.
- [98] G. N. Karystinos and D. A. Pados, "New bounds on the total squared correlation and optimum design of DS-CDMA binary signature sets," *IEEE Trans. Commun.*, vol. 51, pp. 48-51, Jan. 2003.
- [99] C. Ding, M. Golin, and T. Kløve, "Meeting the Welch and Karystinos-Pados bounds on DS-CDMA binary signature sets," *Designs, Codes and Cryptography*, vol. 30, pp. 73-84, Aug. 2003.
- [100] V. P. Ipatov, "On the Karystinos-Pados bounds and optimal binary DS-CDMA signature ensembles," *IEEE Commun. Lett.*, vol. 8, pp. 81-83, Feb. 2004.

## ACRONYMS

ACK	ACKnowledgement
AF	Amplify-and-Forward
ARQ	Automatic-Repeat-reQuest
CDMA	Code-Division Multiple-Access
CR	Cognitive Radio
CSI	Channel State Information
DAF	Differential Amplify-and-Forward
DDF	Differential Decode-and-Forward
DF	Decode-and-Forward
H-ARQ	Hybrid Automatic-Repeat-reQuest
IRC	Interference Relay Channel
MIMO	Multiple-Input-Multiple-Output
MRC	Maximal-Ratio-Combining
NACK	Negative-ACKnowledgement
QoS	Quality-of-Service
SINR	Signal-to-Interference-plus-Noise Ratio
SNR	Signal-to-Noise Ratio